UNIVERSITÀ DEGLI STUDI DI GENOVA

Department of Chemistry and Industrial Chemistry

Doctorate in Sciences and Technologies of Chemistry and Materials

XXXVI Cycle

Curriculum: Chemical Sciences and Technologies

PhD Coordinator: Renata Riva

Detection of emerging contaminants in remote and anthropized environments using passive sampling techniques

Candidate: Chiara Scapuzzi

PhD Tutor: Prof.ssa Marina Di Carro

Homme libre, toujours tu chériras la mer!

La mer est ton miroir; tu contemples ton âme

Dans le déroulement infini de sa lame,

Et ton esprit n'est pas un gouffre moins amer.

C. Baudelaire

Table of contents

Abstract

The PhD project was focused on the development of passive sampling techniques for the detection of Emerging organic Contaminants (ECs) in water matrices.

In 2004, the Polar Organic Chemical Integrative Sampler (POCIS) was introduced and became one of the most powerful devices for the detection of mid-polar and polar ECs in water. POCIS consists of a receiving phase sandwiched between two protective polyethersulfone membranes (PES). Although the accumulation of several ECs onto the PES layer has been observed, a comprehensive assessment of the relationship between the sorption and the physico-chemical properties of organic compounds is missing.

Initially, the research focused on the use of PES membranes as single-phase passive samplers for ECs that showed previously a good retention by the PES membrane of POCIS. Laboratory calibration experiments were carried out to assess the affinity of the ECs for the sampler, the impact of the flow rate on the accumulation and the linearity of the uptake during the exposure time. A field application in S. Margherita Ligure harbour was also performed to test the sampler under environmental conditions. To deeply understand the sorption mechanism, the influence of the manufacturing of PES on the sorption capacity and the affinity for PES of a larger number of compounds with different polarities were evaluated.

The effect of the presence of PES in the POCIS uptake of different ECs was studied under several environmental conditions through the deployment in different sites (harbour and offshore waters, seawater and wastewater, anthropized or remote environments).

Considering the growing awareness on the use of greener approaches in analytical chemistry, the ability of PES membrane to sorb ECs was also compared to the sorption performance of a home-made biobased porous polymeric film.

Finally, different sorbents were tested to assess their ability to adsorb nitramines for the future development of a hydrogel based passive sampler for the detection of these contaminants in freshwater.

Aim of the thesis

The monitoring of ECs in the aquatic environment is of utmost importance due to their possible detrimental effects on aquatic organisms and ecosystems. Nevertheless, the detection of these contaminants is challenging since they present different physico-chemical properties and since ECs can be found in surface waters at low concentration levels. Moreover, to obtain a representative overview of the occurrence of emerging contaminants in water bodies, frequent samplings are needed. In this context, the classical spot sampling is not enough and the acquisition of composite samples by repetitive spot sampling or using autosamplers is required. Another solution is the employment of passive sampling, a better alternative compared to active sampling in term of costs and energy consumption.

Nonetheless, the use of passive sampling is not always reliable for the quantification of contaminants in water, as the uptake in passive sampling devices is strictly related to the environmental conditions (flow rate, temperature, pH, fouling, etc.). For this reason, an in-depth knowledge of the sampler-analyte sorption kinetics and sorption mechanism is necessary.

In this PhD project the aim was to develop passive sampling techniques for the detection of several emerging contaminants in water and to investigate comprehensively the ECs accumulation in the compartments of one of the most employed passive samplers, the Polar Organic Chemical Integrative Sampler (POCIS). In particular, the focus was on the comprehension of the sorption interaction established between polyethersulfone membranes (employed as receiving phase or as protective layer in passive samplers) and the analytes.

Chapter 1. Emerging Contaminants in water

1.1 Water policy

The Directive 2000/60/EC of the European Parliament (Water Framework Directive, WFD) established a framework for the action of the EU Community in the field of water policy. The WFD defined criteria and actions for the evaluation and the classification of the ecological status of the European water bodies and their management. This Directive has been implemented in the Italian D.Lgs 152/2006.

Afterwards, the Directive 2008/105/EC introduced the Environmental Quality Standards (EQS) for priority substances and eight other pollutants (33 substances or groups of substances) [1]. Thresholds for 1-year average concentrations (long-term exposure) and for maximum concentrations of each measurement (short-term exposure) were proposed for the compounds concerned. The number of priority substances and the threshold values are continuously revised.

With the aim to support the selection of priority substances in surface waters, in 2013 the EU Directive 2013/39/EU introduced the Watch List mechanism. The Watch List includes a limited number of chemicals, usually considered Emerging Contaminants (ECs), that must be monitored up to four years; the compounds that during this monitoring period do not pose a significant risk for the aquatic environment are discarded from the list, while the others may be included in the Priority Substances List. The last published list on the EU Official Journal dates back to the 6th of July 2022. Among the nine new entries in the Watch List, the sunscreen agents benzophenome-3 and octocrylene, the anti-diabetic drug metformin and the antibiotic ofloxacin were introduced. Furthermore, on the 19th of January 2022, the first Watch List was adopted for drinking water.

1.2 Definition of Emerging Contaminants

The term Emerging Contaminants was introduced to indicate chemicals not monitored in routine programs, for which further research is requested to assess their occurrence, ecotoxicity and potential health effects before their possible introduction in regulations. Many of them are not new chemicals and may have been present in waters for years; thus,

the term Contaminants of Emerging Concern (CEC) can also be used to underline this aspect [2].

ECs include pharmaceuticals, personal care products (PCPs), flame retardants, industrial additives, surfactants, pesticides, food additives and their metabolites/degradation products. The NORMAN Substance Database (SusDat) is a continuously revised database that lists the most frequently studied ECs (https://www.norman-network.com/nds/susdat/).

Considering the broad range of substances involved, several sources of ECs can be identified such as plastic containers, skin care products, human excretion and industrial/ agricultural activities. Furthermore, the ubiquitous usage of products containing these substances and intense anthropogenic activities cause the continuous release of ECs into the environment, making them pseudo-persistent. ECs reach the aquatic environment principally through wastewaters (domestic, hospital, industries, etc.) and have been identified in several aqueous media (groundwater, rivers, lakes and seawater) [3].

Concerns about the presence of ECs are fairly recent [4]. This is mainly related to the presence of these substances at low concentrations in the environment. The advancement in analytical chemistry has permitted the detection of compounds even at trace and ultra-trace levels (μg L^{-1} and ng L^{-1}). The development of hyphenated instrumental analytical techniques such as chromatography coupled to mass spectrometry has allowed to obtain methods characterized by high sensitivity and selectivity. These advantages were increased by the progress made in the field of sample preparation.

Despite the low concentrations of these compounds in the aquatic environment, their effects on aquatic organisms were observed. Several ECs are pharmaceuticals or classified as endocrine disruptive compounds: toxic effects on biota, impacts on community structure and the interaction with other species in the ecosystem were studied [5]. These investigations were mainly carried out in laboratory exposures under controlled conditions, however synergistic/antagonistic effects with other substances present in the environment and the impact on different trophic levels need more research [6,7].

Chapter 2. Analytical Techniques

2.1 Sample preparation

The analytical process includes several steps: sampling, sample treatment, separation, detection and data analysis [8]. The first two steps are the principal sources of errors and affect accuracy and the reliability of the final result.

Sampling consists in collection, preservation and transport of a portion of material; the key point of this step is the representativeness of the samples, as well as correct storage conditions. Instead, sample preparation is often a multiple-step procedure and the more time-consuming stage; as consequence it is susceptible to contamination and to the loss of compounds. The aim of this step of the analytical process is to convert the analytes in a proper form for the subsequent instrumental analysis (e.g., derivatization), to clean-up, isolate and pre-concentrate the target compounds from the matrix in order to minimize the presence of interferents and obtain an adequate concentration of the analytes in the final sample (over the limit of quantification of the instrumental method). Considering the low concentrations of ECs in the environment, the complexity of matrices and the presence of interferences, the use of powerful instrumental techniques as those described in chapter 2.2 and the simple "dilute and shoot" approach are not sufficient. Thus, the sample preparation steps remain indispensable most frequently. Usually, the sample treatment consists in an extraction, although other techniques (e.g., precipitation of the interferents) are also available. The extraction step involves a sorbent (solid or liquid) in contact with the sample matrix (or a multiphase sample matrix) and the partition of the analytes between the two phases [9]. Furthermore, the extraction could be exhaustive or non-exhaustive, depending on the removal capacity of the sorbent. Several techniques were developed, and sample preparation has become one of the most significant topics in analytical chemistry. Different configurations and different materials were tested to improve the selectivity and the sensitivity of the analytical methods, and more recently to make the sample preparation step more sustainable [10]. Some of the most popular techniques are solid-phase extraction (SPE), dispersive solid-phase extraction (d-SPE), stir-bar sorptive extraction (SBSE), dispersive liquid-liquid microextraction (DLLME), solid-phase microextraction (SPME),

molecular imprinted polymers (MIPs), ionic liquids (ILs), metal organic frameworks (MOFs) and passive sampling.

2.1.1 SPE

Solid-phase extraction (SPE) is the most employed technique for the selective extraction, preconcentration and clean-up of different liquid samples or extracts of solid samples (environmental, food, biological, etc.) before instrumental analysis. The main configuration consists of a plastic or glass cartridge filled with a solid sorbent of a defined particle size. The mechanism involved in this technique is the sorption on the sorbent of the target compounds (if the aim is the enrichment or the change of solvent) or of the interferents (if the aim is purification) present in the sample/extract. The amount and the nature of the receiving phase should be carefully selected to obtain a reliable method of extraction/purification. The selection of the amount of sorbent depends on the expected concentrations in the samples of the species of interest. Breakthrough can occur when the capacity of the sorbent is overloaded or if the retention capacity of the sorbent for the analyte is insufficient. In general, the maximum loading capacity of the receiving phase is usually considered 5% of its weight (e.g., considering 200 mg of sorbent the maximum amount of analyte in the liquid sample should be 10 mg). The selection of the type of sorbent is based on the physico-chemical properties of the investigated chemicals in order to obtain good retention ability. More details regarding the available sorbents are reported in section 2.1.4.1.

Once the type and the amount of sorbent, the solvent of the washing step, the eluent and flux of loading and elution have all been selected, four steps are involved in the SPE procedure:

1- Column conditioning: the aim of this step is to remove interferents potentially present in the stationary phase and to solvate the functional groups of the sorbent. Different solvents can be employed for these purposes, in general during the solvation step mid-polar solvent are employed (methanol, isopropanol, etc.). Solvation is followed by an equilibration step where a solvent similar to the sample matrix is employed.

2- Sample loading: the sample could be pretreated to maximize the interaction with the sorbent and filtered to remove particulate matter. Then it is accurately transferred into the cartridge and filtered. The loading flux needs to be carefully selected to avoid the loss of the analyte caused by too short interaction times (max 2 mL min^{-1}).

Moreover, in this step the overloading due to a large volume of sample and due to high concentration of analytes must be avoided.

3- Washing: during this phase a solvent is selected in order to remove the interferent species of the sample weakly sorbed on the cartridge stationary phase. For this reason, the washing solvent must have an intermediate strength between the sample (weak) and the eluent (strong), and miscible with both.

4- Elution: the aim is to desorb the target compounds retained on the sorbent, but no other species that may be present on the SPE bed and not eluted during the washing. The eluent selected could be a pure sorbent or a mixture of different solvents. The pH can be adjusted to permit the desorption of charged compounds. Furthermore, the eluent should be compatible with the instrumental technique selected for the detection of the target compounds or easily evaporated to reconstruct the sample with a compatible solvent. The volume employed should be minimum to permit the analyte's preconcentration. Also, in this step the flux must be minimum.

2.1.2 Solid Phase Microextraction

Solid phase microextraction (SPME) is an economical and easily automatable technique, introduced in the 1990 by Arthur and Pawliszyn [11]. This device is now employed for the extraction, pre-concentration and purification of organic compounds from different samples (environmental, food, biological, etc.). One of the most recent and suggestive employments is the application of *in vivo* SPME using biocompatible extracting phases [12,13]. SPME consists of a fused silica fibre coated with a thin layer of liquid or solid sorbents. The selection of the sorbent is based on the volatility and the polarity of the analytes, and on the sample matrix. The accumulation of the analytes in the extracting phase of SPME devices depends on the nature of the sorbent: absorption with liquid coatings or adsorption with solid coatings. In contrast to SPE, SPME is a non-exhaustive extraction technique. The uptake capacity of the device is determined by the distribution coefficient of the analyte between the polymer and the sampled media, and by the thickness of the coating. In general, due to the device configuration, equilibrium is achieved in few minutes/hours. The use of SPME in the linear or pseudo-linear regime of the uptake is limited. The SPME fibre can be exposed in the headspace or directly to the sample media (direct immersion). Afterwards, SPME is

usually coupled to chromatographic techniques for the quantification of the target analytes. When SPME is employed for the extraction of volatile compounds, it can be coupled to gas chromatography and the analytes can be thermally desorbed. In this way the technique became completely solvent free. However, thanks to the thin layer of sorbent, small volume of solvents is employed during the step of desorption, making this technique a good choice in the development of green sample preparation strategies.

During the PhD project, SPME was employed for the solvent-free determination of polycyclic aromatic hydrocarbons in plant buds coming from different areas of the city of Turin, characterized by different pollution levels (data not reported in the Thesis) [14].

2.1.3 Passive sampling

Passive sampling is a technique that exploits the spontaneous flux of a chemical from the sampled medium to a receiving medium, merging the sampling to the pre-concentration/purification step directly in-situ.

This process is due to the differences in the chemical potentials between the matrix (higher potential) and the sorbent (lower potential). The uptake into/onto the receiving phase involves several steps. First, in the bulk phase (water) the analytes are transported by convection; however, close to the sampler its extent decreases and molecular diffusion gains more influence until a point (δ) in which the flux of analytes is mainly controlled by diffusion. The zone between the sampler and δ is called "water boundary layer" (WBL), whose thickness depends on the analytes' diffusion coefficients in water and the rate of convection in the sample/matrix. Once the sampler is reached, the chemicals diffuse into the protective layer, if present, and then are sorbed onto/in the receiving phase. Sometimes, the presence of biofouling on the sampler implies the diffusion even through this layer.

Compared to spot sampling, passive sampling permits to obtain data more representative of the status of contamination of water bodies, in particular when the concentrations of contaminants are subject to fluctuations or in presence of episodic events of pollution (see next sections). Moreover, the preconcentration of the analytes in the sorbent during the sampler deployment allows to avoid the sampling of large volumes of water to obtain enough sensitivity. Compared to continuous active sampling, the use of passive samplers is less laborious and expensive both in terms of work and energy.

2.1.3.1 Sampler configuration

As mentioned above, the protective layer may or may not be present in the device (Fig.2.1). Single-phase passive samplers are devices where only the sorbent is present, while dual-phase passive samplers present a layer covering the sorbent with the aim both to protect the sorbent and to slow down the sorption, to avoid a fast achievement of equilibrium.
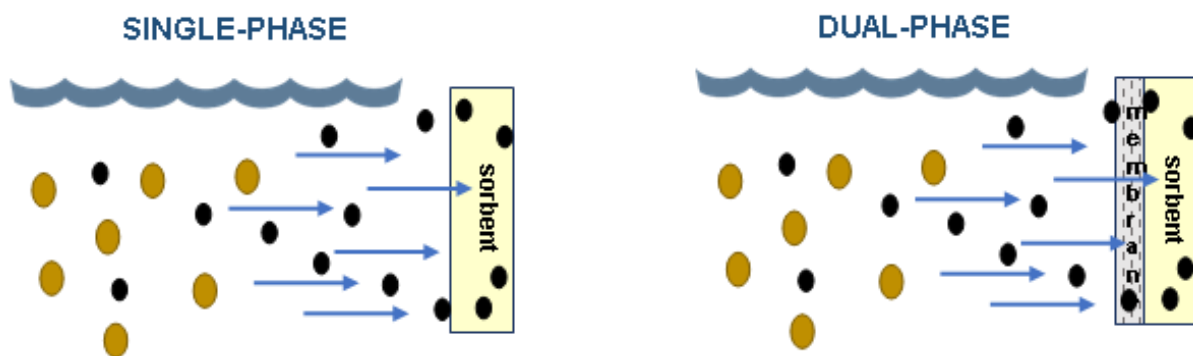
Fig. 2.1 Schematic representation of passive samplers' configuration: single-phase (left) and dual-phase (right). The black circles represent the analytes in the aqueous matrix and the yellow circles other compounds present in the media.

Passive sampling devices (PSDs) were initially developed for the monitoring of air pollutants [15]. However, in 1980 the first PSD for water applications, consisting in an organic solvent contained by a polymeric membrane, was developed by Byrne and Aylott [16]. In 1987, Södergren presented a PSD and its application for waterborne hydrophobic organic contaminants (HOCs) [16]. This PSD was made of hexane as a receiving phase and a hydrophilic regenerated cellulose dialysis bag as holder. The presence of this membrane also serves as a molecular-weight cutoff, permitting the passage only of the HOCs dissolved fraction. Afterwards, several configurations were developed to improve the performance of the device, different solvents as receiving phase (dichloromethane, ethyl acetate, etc.) and different membranes (low-density polyethylene, silicon, polypropylene, etc.) were tested. Huckins et al. (1990) presented the Semi-Permeable Membrane Device (SPMD) polyethylene tubing containing thin films of triolein, one of the most employed PSDs for HOCs [17]. In 2000, Kingstone at al. presented two sampling devices, both using the solid-phase C18 Empore^{TM} disk as sorbent but two different membranes for the sampling of more polar (2 < LogKow < 4) and non-polar (LogKow > 4) organic contaminants:

polyethersulfone and polyethylene, respectively. The device for polar compounds, named Polar Chemcatcher®, was then employed in several configurations [18].

Another sampler for polar organic compounds is the Polar Organic Chemical Integrative Sampler (POCIS). This device, introduced in 2004 by Alvarez et al., consists of a polymeric receiving phase, typically HLB, enclosed between two PES membranes [19]. Different configurations of POCIS have been tested to improve the performance of the devices for specific groups of compounds.

Finally, the Diffusive Gradients in Thin films (DGTs) passive sampler, first developed for inorganic species [20], was adapted by Chen et al. (2012) for polar organic contaminants (o-DGT) [21]. The device consists of a protective membrane (optional but often present), a diffusive gel layer and a binding gel which is the receiving phase of the target compounds. The presence of a diffusive hydrogel (typically agarose) allows to control the analyte uptake, in particular limiting the influence of the WBL on sampling rates. The binding gel is usually of the same nature as the diffusive gel and the sorbent is selected on the basis of the target compounds [22,23].

Among the samplers employed for the detection of polar ECs, the POCIS is the most employed both in freshwater and seawater [24,25]. However, the presence of a diffusive layer in o-DGTs limits the influence of the flow rate on the uptake making this device a powerful tool for field applications. Furthermore, the o-DGT sampler was principally used for the detection of strongly polar compounds showing promising performance ($LogK_{ow} < 1$) [26].
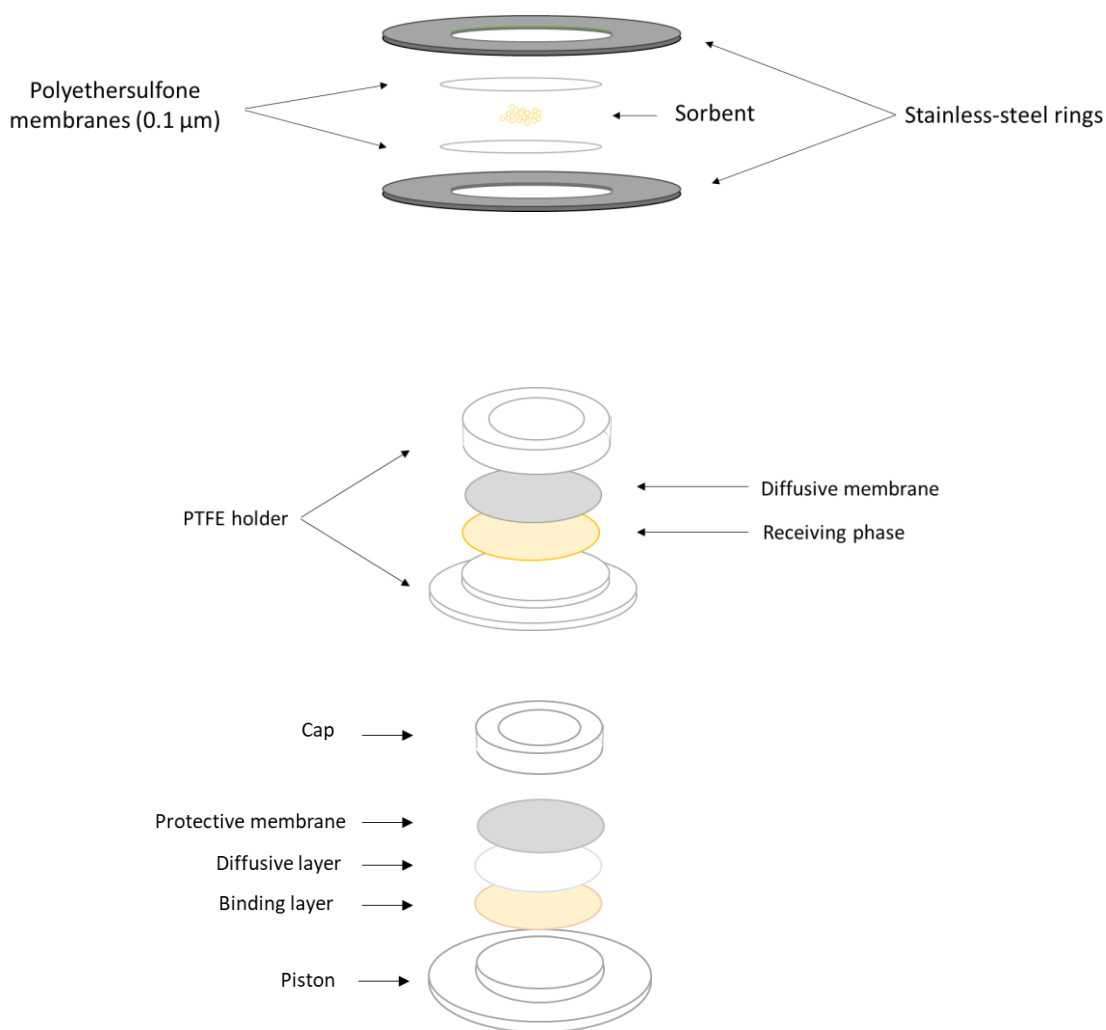
Fig. 2.2 Schematic representation of the principal dual-phase passive samplers for hydrophilic contaminants: POCIS, Chemcatcher® and o-DGTs.

Regarding single-phase PSDs, the first device without a protective membrane was tested for the first time by Huckins in 1989. Low-density polyethylene (LDPE) strips were employed for the detection of ^{14}C-2,2',5,5'-tetrachlorobiphenyl [27]. Afterwards, other polymers have been employed as single-phase passive samplers, such as silicon rubber (SR), polyurethane (PU), nylon, polyethersulfone (PES) and polyoxymethylene (POM) [28].

2.1.3.2 Uptake kinetics

As mentioned before, passive sampling exploits the free flow of chemicals by molecular diffusion from the bulk phase to the receiving phase. This flux continues until the

equilibrium is reached, or in other words when the chemical potential between the two phases is equal or when the uptake coefficient is equal to the elimination coefficient.

Molecular diffusion can be described using Fick's first law (Eq. 2.1)

$$\boldsymbol{J}_i = -D_i \boldsymbol{\nabla} C_i \qquad\qquad Eq.\,2.1$$

Where $\boldsymbol{J}$ is the flux of a chemical through the considered phase [M L^{-2} T], D_i its diffusion coefficient and C_i its concentration. Considering a one-dimensional concentration gradient and a specific phase of thickness δ, Eq. 2.1 can be written as follow (Eq. 2.2):

$$J = \frac{D_i}{\delta} \Delta Ci = k_i\,\Delta C_i \qquad\qquad Eq.\,2.2$$

Where k_i is the mass transfer coefficient and ΔC_i the difference of concentration across the phase.

Considering PSDs in which equilibrium is reached in all the interfaces, fluxes through the phases are equal, Eq. 2.2 can be written as Eq.2.3

$$J = k_0 \left(C_w - \frac{C_s}{K_{sw}} \right) \qquad\qquad Eq.\,2.3$$

Where k_0 is the overall mass transfer coefficient, C_s the concentration in the sorbent and K_{sw} the sorbent-water partition coefficient. The overall mass transfer coefficient can be written as the sum of the mass transfer coefficients of the single phases, considering a single-phase PSD:

$$k_0 = k_w + K_{sw} k_s = \frac{D_w}{\delta_w} + K_{sw}\frac{D_s}{\delta_s} \qquad\qquad Eq.\,2.4$$

This relationship is of utmost importance to understand the limiting step of the uptake and for the selection of the correct model to describe the accumulation in the sorbent.

During sampling, the concentration of chemicals in the sorbent changes over time. The rate of change of the target compound concentration in the sorbent can be expressed considering the area A and the volume V_s of the sampler by Eq. 2.3 as follows:

$$\frac{dC_s}{dt} = J\frac{A}{V_s} = \frac{A}{V_s}k_0\left(C_w - \frac{C_s}{K_{sw}}\right) \qquad\qquad Eq.\,2.5$$

Integrating the equation [29] and considering a constant C_w, $C_s = 0$ at $t = 0$ and C_s the concentration at time t, the obtained Equation is the following:

$$C_s = K_{sw}C_w\left(1 - e^{-\frac{Ak_0}{V_sK_{sw}}t}\right) \qquad\qquad Eq.\,2.6$$

The product Ak_0/V_sK_{sw} is usually indicated as k_e and represents the exchange rate constant. The model described above is named Mass-Transfer Coefficient (MTC) model and may be used to describe the transfer of a chemical through distinct phases in contact with each other (Fig. 2.3).
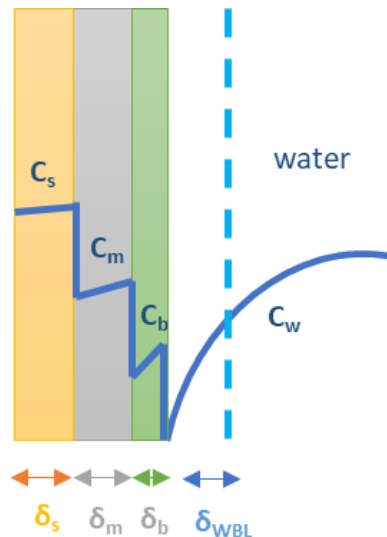
Fig. 2.3 Schematic representation of the concentration profile (blue lines) in a dual-phase passive sampler, in the biofilm layer and in the WBL. The orange layer represents the sorbent of thickness δ_s, the gray layer the membrane, the green layer the biofilm.

The exchange constant can be rewritten defining the sampling rate R_s as described in Eq.2.7

$$R_s = A\,k_0 \qquad\qquad Eq.\,2.7$$

Eq. 2.7 clearly demonstrates the linear relationship between the sampling rate and the area of the sampler. Finally, Eq. 2.6 can be written as:

$$C_s = K_{sw} C_w \left(1 - e^{-\frac{R_s}{V_s K_{sw}} t} \right) \qquad\qquad Eq.\,2.8$$

A similar result can be obtained using models based on the analogy with Chemical Reaction Kinetics (CRK), which have been employed to describe bioconcentration. In MTC models the exchange constant is described by fundamental processes, while the uptake (k_u) and release (k_e) constant in CRK models are only empirical.

$$\frac{dC_s}{dt} = k_u C_w - k_e C_s \qquad\qquad Eq.\,2.9$$

$$C_s = \frac{k_u}{k_e} C_w (1 - e^{-k_e t}) \qquad\qquad Eq.\,2.10$$

The mentioned models clearly describe the uptake as a process flowing first-order kinetics. Thus, the accumulation in the sorbent of a PSD can be described by an initial linear uptake, followed by a curvilinear regime and a final attainment of equilibrium Fig. 2.4.
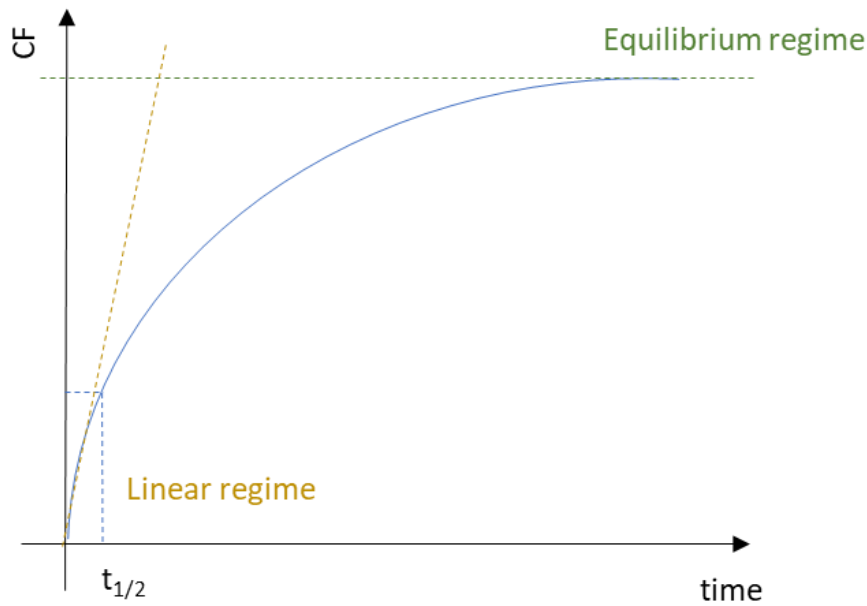
Fig. 2.4 Graphical representation of uptake in a passive sampler. The Concentration Factor (CF) represent the ratio between the amount of analyte accumulated in the sorbent and the concentration of the analyte in water. The linear regime is represented by the dotted line in gold while the green line marks the equilibrium regime.

In the linear regime, the rate of release of a chemical from the sampler is negligible compared to uptake, meaning the concentration in the sampler is sufficiently lower than the equilibrium concentration ($C_s \ll C_w K_{PESw}$). The mathematical description of the linear regime (Eq. 2.11) can be obtained by Eq. 2.5 under the integration condition stated above.

$$C_s = \frac{R_s}{V_s} C_w t \qquad\qquad Eq. 2.11$$

The volume of the sampler can be substituted by the mass of the sampler because mass is easily measured, and all the terms expressed as consequence with the appropriate units.

This relation is applicable if the exposure time is lower than the time needed to achieve half of the equilibrium ($t_{1/2}$):

$$t_{\frac{1}{2}} = \frac{ln2}{k_e} = \frac{ln2\ K_{PESw} V_s}{R_s} \qquad\qquad Eq. 2.12$$

Regarding equilibrium, no changes in the analyte's concentration is observed in the sorbent because the uptake rate is equal to the release rate. As consequence, Eq. 2.5 reduce to Eq. 2.13.

$$C_w = K_{sw} C_s \qquad\qquad Eq. 2.13$$

Nevertheless, the use of these models is correct only when the mass transfer coefficients are not time-dependent, or if the time-dependent coefficients can be neglected. Otherwise, more complex diffusion models are needed based on the time-dependent Fick's second law [30,31]. In particular, the WBL mass transfer coefficients are considered time independent as the achievement of a steady-state concentration in this phase occurs in few seconds/minutes, and the deployment time scale of passive samplers is much higher [30]. On the contrary, the presence of a gradient of concentrations in the sorbent causes a time-dependence of the mass transfer coefficient k_s. In this case, its value is no longer described by Eq. 2.4, but rather by a sum of exponential characterized by different mass transfer coefficients [31].

The inverse of mass transfer coefficients is named mass transfer resistance and is used to evaluate the time-dependence of the sorption. The sorption of hydrophobic compounds is usually limited by the WBL due to their lower affinity for water. Instead, for polar compounds the sorption might be governed by the sorbent considering their higher diffusivity in water. Furthermore, the hydrodynamic conditions impact the mass transfer resistance being k_w influenced by the WBL thickness. In the presence of a protective layer, a further consideration must be done. In fact, if the protective membrane does not interact with the chemical and the transport occurs only through the water filled pores, the transfer coefficient of the membrane is not time dependent. On the contrary, if the membrane presents significative sorption, this layer also possesses a time-dependent coefficient.

In conclusion, the nature of the chemicals and the sorbent as well as the hydrodynamic conditions affect the mass transfer. The understanding of this mechanism is crucial to select the appropriated model to describe the uptake of chemicals into PSDs as it affects the reliability of the passive sampling method.

2.1.3.3 Classification based on the uptake regime

Passive samplers are employed as equilibrium PSDs or integrative PSDs. Using PSDs as equilibrium devices requires an exposure time long enough to achieve the thermodynamic equilibrium between the medium sampled and the receiving phase. The equilibrium regime starts when reaching 95% of the equilibrium concentrations [32]. The evaluation of the time requested for equilibrium for a specific analyte can be evaluated using Eq. 2.14:

$$t_{95} = \frac{ln20}{k_e} = \frac{ln20 \; K_{PESw}V_s}{R_s} \qquad\qquad Eq. \, 2.14$$

Once at equilibrium, the unknown water concentration is estimated by Eq. 2.13. This implies that the value of the sorbent-water partition coefficient must be carefully evaluated for an accurate estimation of C_w. The evaluation of this parameter can be performed using different designs, described in Chapter 4. Nevertheless, the use of PSDs in equilibrium regime provides only the equilibrium concentration between the water medium and the sampler and is not useful in environments characterized by significant variability of chemical's concentration as in a WWTP. More powerful is their employment in the integrative regime.

The integrative regime is characterized by a negligible release rate and permits the evaluation of the Time Weighted Average (TWA) concentration of the target compound in the environmental matrix considered. The TWA concentration can be estimated if the sampler is able to respond to small variation over time and if reliable sampling rates are available. The determination of sampling rates can be carried out in laboratory calibrations or in situ. For calibration purposes, Eq. 2.11 is employed. However, the sampling rate depends on several environmental factors (flow, temperature, fouling, pH). Thus, to obtain accurate R_s values the laboratory calibrations must be carried out trying to mimic the environmental conditions. It is worth noting that in the absence of robust sampling rates, passive sampling can be considered only semi-quantitative [33].

Different configurations can be employed in laboratory to assess the sampling rates or to evaluate the linearity of the uptake. The simplest is the static depletion method, which consists in a sole spike of the target compounds in a small volume of exposed water followed by the monitoring of their decrease in water concentration [32,34–36]. Using this procedure, other losses must be monitored to obtain dissipation factors useful to correct the estimated sampling rates [36].

More consistent is the static renewal design. In this experiment the sampled media is refreshed at fixed times in order to limit the decrease of the compounds (usually less than 10% is suggested). Water concentrations must be monitored at the beginning and at the end of each renewal, at least. Moreover, the accumulation of the target compound is evaluated through the extraction of the analytes from the sorbent. This design requires much more effort compared to the static depletion design but is necessary to avoid overestimation of the sampling rates when dissipation of the analyte from water is not only due to the sorption in the receiving phase (e.g, sorption onto the glass walls of the beakers or sorption into the protective membrane). Finally, flow-through systems were also employed for the estimation of R_s to maintain a constant concentration of the target chemicals and to assess the impact of the flow rate on the uptake [37,38].

In situ calibrations are more costly and time consuming compared to laboratory calibrations. For this reason, Performance Reference Compounds (PRCs) can be used to correct the lab-derived R_s and to reduce the inaccuracy linked to the estimation of the analyte's concentrations in water [39–41]. Unfortunately, unlike hydrophobic passive samplers based

on partitioning, the application of PRCs is no longer possible with adsorption-based sorbents where the release of this compounds is anisotropic [42,43]. To overcome to this problem, other methods were developed to take into account the effect of hydrodynamic conditions in environmental deployments: the co-deployment of alabaster plates or PRCs-spiked silicone [44–46]. In fact, the employment of SR makes the use of PRCs possible, as the uptake of a contaminant is a partitioning between the SR sampler and the aqueous media.

2.1.4 Interactions between sorptive materials and ECs

Several commercial sorbents, polymeric or not, are available for preparative methods [47]. A large number of sorbents has been developed to improve the performance and reliability of the analytical methods. Sorption of analytes with a wide range of polarities and different physico-chemical properties, compatibility with water or organic sorbent and higher sorption capacity, are some examples of the improved parameters. Thus, sorption-phases selection is of utmost importance to guarantee selectivity and effectiveness of the sample pre-treatment, especially in complex matrices. In this context, the comprehension of sorbent, analyte and matrix interactions is crucial. Several retention mechanisms are possible depending on the nature of the sorbent and of the analytes, and the mutual interactions (hydrophobic, dipole-dipole, electrostatic, H-bonding and π-π interaction).
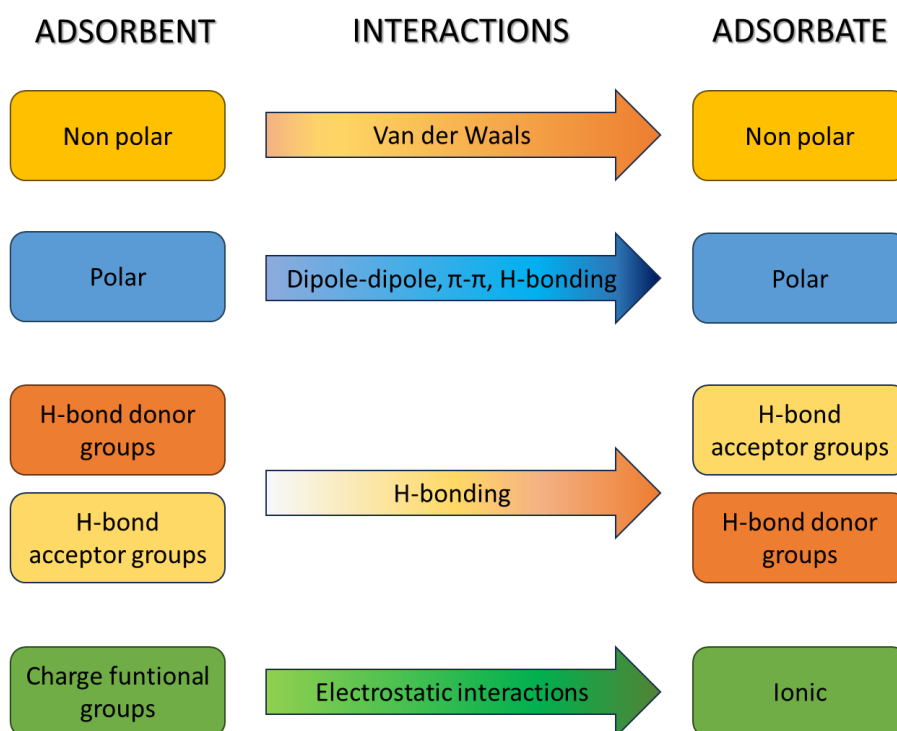
Fig. 2.5 Representation of the principal interactions between the sorbent and the sorbed molecules.

22

More details on the sorbent and the interaction involved are exemplified in the next sections.

2.1.4.1 SPE sorbents

The most diffused sorbents in SPE are reversed phase; however ion-exchange, normal phase, adsorption base or mixed-mode are also employed [48].

In reversed phase retention, hydrophobic interactions (Van der Waals forces) are dominant. Usually, the presence of hydrophobic alkyl or aryl functional groups (e.g., octyl, octadecyl or phenyl endcapped) causes the sorption of mid- and nonpolar analytes present in a polar or moderately polar matrix (e.g., water). Nevertheless, considering the increasing interest towards polar compounds [49], more polar sorbents have been developed through the introduction of polar functional groups in the polymeric structure. For instance, the Oasis Hydrophilic-Lipophilic-Balanced (HLB) is a co-polymer made of divinylbenzene (DVB), a lipophilic monomer, and the hydrophilic monomer N-vinylpyrrolidone. This sorbent provides hydrophobic interactions thanks to the DVB moieties and dipole-dipole interaction and H-bonding with O and N atoms present in pyrrolidone. Furthermore, the presence of aromatic rings in the polymer structure enables to enhance the adsorption capabilities through π-π interaction.

The use of ion-exchange sorption phases permits the retention of analytes by electrostatic interactions. The target compounds with basic or acidic groups, present in solution in the ionized form, are attracted by the complementary charged functional groups of the sorbent. Specifically, acidic analytes, such as acidic drugs, can be sorbed using quaternary amine functional groups (strong bases); on the contrary, basic analytes can be retained using cation exchange sorbent with sulfonic functionalities. The cited functional groups are strong ion-exchanger. The use of weaker ion-exchanger (i.e., carboxylic-cation exchanger or piperazine-anion exchanger) is also possible. Moreover, mixed-mode sorptive phases have been developed to combine reverse-phase and ion-exchange interactions. Using this type of sorbent, the pH of the solution plays a key role in the retention.

Other useful sorptive materials in environmental analysis are the adsorption-based sorbents [48]. Among them, carbonaceous adsorption media such as graphitized carbon-based packing (i.e., ENVI-Carb, Supelco) are suitable for polar and nonpolar compounds in

environmental matrices. Nonetheless, the nonspecific sorption abilities of these materials may cause the loss of selectivity.

To improve the selectivity for specific compounds other materials have been introduced, such as molecular imprinted polymers (MIPs). MIPs are polymeric materials in which the selectivity for the target compounds is improved through shape-functional groups recognition in specific cavities [50]. In fact, during the polymerization the presence of a template (generally the target compound, later removed) permits the formation of specific binding (covalent or noncovalent) sites.

2.1.4.2 Sorptive material in SPME

The selection of the appropriate coating in SPME is crucial for the selectivity of the extraction method. The extracting phases mainly employed in SPME applications are polydimethylsiloxane (PDMS), polyacrylate (PA) and divinylbenzene (DVB) and their combinations as DVB/PDMS or DVB/Car/PDMS. The use of the liquid coating PDMS is advantageous for its resistance to fouling compared to the other solid sorbents, however the selectivity for mid-polar and polar analytes is poor. Other sorbents have been proposed to improve the selectivity and sensitivity of the methods or to ameliorate the biocompatibility of the coatings for *in vivo* or *ex vivo* studies: HLB, ionic liquids, MIPs, MOFs or carbon nanomaterials [12].

2.1.4.3 Sorptive materials in passive sampling

In dual-phase PSDs several commercially available sorbents in the form of particles or disks are typically employed. Many of them are those employed in SPE procedures. The above mentioned POCIS are typically made of HLB as sorbent phase, however other sorbents as carbon-based and mixed-mode ionic-exchange sorbents, ionic liquids, MIPs, etc. have been employed [51,52]. The same considerations presented above were then extended to sorption in the receiving phase of passive samplers.

In single-phase PS, polymer such as LDPE, SR, PES and POM are employed. These polymers can be classified as rubbery polymers, SR and LDPE, or glassy, like PES. Two sorption mechanisms can be involved in sorption: absorption and adsorption. While adsorption is a surface process absorption implies the partitioning of the analytes between

the polymer matrix and the aqueous media. Considering the nature of rubbery polymers, absorption is the main mechanism of sorption of HOCs into these polymers. On the other hand, considering glassy polymers both adsorption and adsorption are involved. In particular, adsorption is the main mechanism in the crystalline regions and the degree of crystallinity in the polymer influences the extent of adsorption.

2.2 Instrumental analysis

The development of an analytical method necessitates reliable instrumental detection for the evaluation of the presence of the target compounds in the samples. The sample preparation step is functional to the following instrumental technique employed. Among instrumental analytical techniques, Mass Spectrometry (MS) and chromatography are the most powerful for the detection of target molecules in different samples. The hyphenation of chromatography to MS was of utmost importance considering complex samples such as biological and environmental ones.

Mass spectrometry is based on the ionization and further fragmentation of molecules (organics and inorganics) in the gas phase. The generated ions are then separated in the analysers based on their mass to charge ratio (m/z) and detected. Tandem mass spectrometry can be performed in space coupling two different analysers (MS/MS), or in time involving only one spectrometer but multiple separation steps over time (MS^n). The cheapest and most diffuse device among tandem mass spectrometers is the QqQ. Four scan modes are possible: product scan, precursor scan, neutral loss scan and selected reaction monitoring or multiple reaction monitoring (MRM). The latter mode involves the selection of the precursor ion in the first quadrupole, its fragmentation in the collision cell by means of an inert gas and finally the selection of the generated product ions in the second quadrupole. Usually, the most abundant product ion is selected for quantification (named quantifier) and several others for confirmation (qualifiers).

At the end of the 1950s, the first coupling of gas chromatography to mass spectrometry was reported by McLafferty and Gohlke. The development of the so-called *hyphenated* techniques has been fundamental for the modern instrumental analytical chemistry. The aim was to exploit the separative abilities of chromatography and to enhance the selectivity and sensitivity of the separative methods using a MS as detector. Furthermore, the development

of LC-MS in the 1980s led to significant improvement in the development of analytical methods: considering that GC-MS was applicable only to volatile and thermally stable species, the range of analytes detectable using LC-MS increased considerably.

The instrumental analytical technique employed during the PhD project was the high-performance liquid chromatography (HPLC) coupled to triple quadrupole tandem mass spectrometry (QqQ) using an ESI source. The quantification of the target compounds was performed using the MRM mode.

2.3 Principal Component Analysis

Along with the instrumental techniques, during the thesis some basic chemometric tools were employed to help the data interpretation.

An object (sample, molecule or individual) can usually be described by several variables (chemical and physical parameters). Considering one variable at a time to describe objects, the information linked to intercorrelation between variables could be lost, offering only a partial understanding of a complex phenomenon. The use of a multivariate approach permits to maximize the information extractable from data. In particular, the variability associated to the case study can be used as a source of information.

The Principal Component Analysis (PCA) is a multivariate exploratory technique that exploits the variance associated with the data to obtain a visual representation of them. PCA was introduced by Karl Pearson in 1901 and then developed in 1933 by Harold Hotelling. PCA is an unsupervised method (no a priori information regarding classes) that allows to investigate and reveal relationship among the objects and the variables that describe the objects. This exploratory analysis allows to recognize the importance and the correlations among variables, permits to understand the relationship between objects and to reduce the dimensions of data, removing non-significant variability.

PCA consists of a conversion of the experimental variables in new variables called Principal Components (PCs). These new variables are linear combination of the original ones, and their main characteristic is that they are orthogonal (not correlated). This means that the variance explained by a PC is not explained by any other one. The number of new variables correspond to the number of original variables; however, the total variance of the

system is distributed differently from the original variables and the first PCs explain the majority of this variance. In such a way, the dimension reduction became possible when significant correlation occurs. In this case, the information lost selecting only the significant PCs (generally the first PCs) is not statistically relevant, since principally linked to the noise.

Geometrically, PCA correspond to a rotation of the original axis in the direction of the maximum variation of the data (highest variance). Whereas the position of the original axis change (without changes of angles between them), the position of the objects remains constant. The cosines of the angles between the directions described by the original variables and those of the new PCs are called **loadings**. The coordinates given by the projection of the objects in the new space defined by the PCs are called **scores**.

Algebrically, the PCs are a linear combination of the original variables. Starting from the matrix of the original data $[X]_{oxv}$ the variance and covariance matrix $[Cov]_{vxv}$ is calculated. Through the diagonalization of the $[Cov]_{vxv}$ a matrix containing values different from zero only along the diagonal is obtained (diagonal matrix). The diagonal values correspond to the **eigenvalues** which give the amount of variance explained by each principal component. From the $[Cov]_{vxv}$ the **eigenvectors** can also be estimated knowing the eigenvalues. The eigenvectors are orthogonal since the covariance matrix is symmetric. The number of eigenvalues and eigenvectors is equal to the number of original variables. Furthermore, the eigenvectors represent the columns of the **loading matrix** $[L]_{vxv}$ while the rows represent the original variables. The loading matrix allows to observe the load of each original variable on the new PCs. If the data were subjected to pretreatment before the PCA, the correlation matrix would be used instead of the $[Cov]_{vxv}$. In fact, to maximize the comparison between data with different measurement units, some column pretreatments are needed [53].

Finally, to obtain a representation of the object in the new space defined by the PCs, the score matrix $[S]_{oxv}$ can be calculated as follows:

$$[S]_{oxv} = [X]_{oxv} \cdot [L]_{vxv} \qquad\qquad Eq. 2.15$$

Once the PCs are obtained, the selection of the most significant PCs need to be carried out. The selection is based on the principle that variability of information is greater than the variability associated to the noise. For the selection of the number of significant PCs, the **scree plot** is usually employed (Fig. 2.6) and the PCs considered correspond to the components with the highest variation of the % of explained variance.
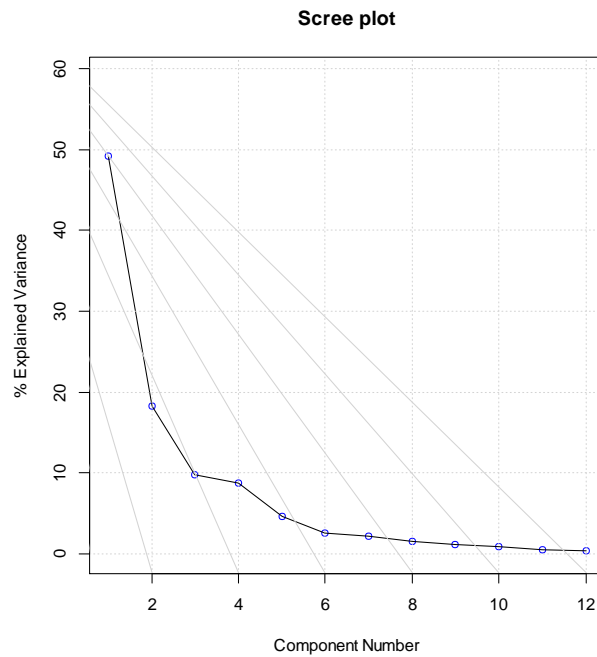
Fig. 2.6 Example of scree plot for the selection of the significant PCs. The greatest changes in the variance explained correspond to the first two principal components.

When the variables are selected, different graphs can be employed to visualize the data in the new space defined by PCs. The **score plot** permits to observe the position of the object in the space described by the selected PCs; thanks to this graph the presence of outliers, of groups and trends can be observed. Another important graph is the **loading plot,** which allows to observe the importance of each original variable in building the components and the correlation among them. The **biplot** is a simultaneous representation of the object and the original variables in the new space and is informative regarding the relationship between objects and variables. Normally, if a variable is close/overlapped to an object in the biplot, it means that the object is characterized by a high value of this original variable.
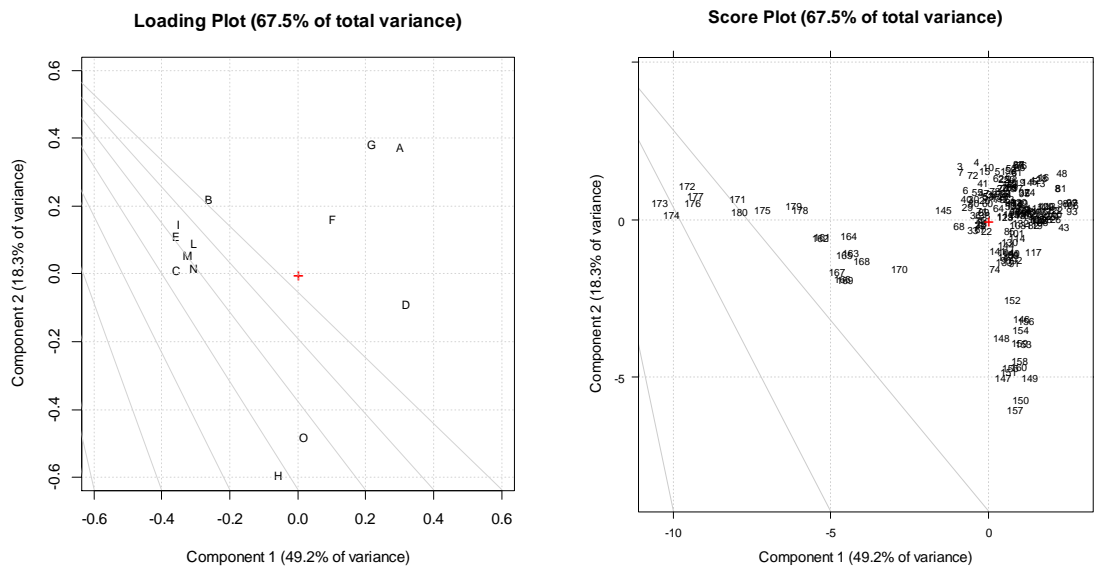
Fig. 2.7 Example of a loading plots (left) and a score plot (right). The letters represent the original variables and the numbers the object. The first two components described the 67.5% of the total variance, in particular 49.2% PC1 and 18.3% PC2.

To better interpret the influence of the variables on the components, the Varimax rotation can be applied [54]. The rotated components are named factors and are as much as possible collinear with distinct clusters of vectors. In fact, factors maximize the separation of groups of intercorrelated variables [55].

Chapter 3: Polyethersulfone membrane as single-phase passive sampler

3.1 Introduction

Passive sampling devices (PSDs) can be divided into two main groups based on their configuration: single-phase and two-phase samplers [51]. Among single-phase polymeric PSDs (the simplest and cheapest devices), the most popular are silicone rubber (SR) and low-density polyethylene (LDPE) [28]. These two types of samplers have low affinities for the more polar and ionic contaminants. Hence the necessity to find devices more suited for chemicals such as pharmaceuticals, hormones and pesticides [56].

Regarding dual-phase PSDs, the Polar Organic Chemical Integrative Sampler (POCIS) has become one of the most used devices for the monitoring of emerging contaminants (ECs) [25]. POCIS consists in a sorbent phase, typically hydrophilic-lipophilic-balanced (HLB), sandwiched between two polyethersulfone (PES) membranes held together by stainless steel rings. This device was developed for slightly polar substances ($0 < LogK_{ow} < 4$), however the range of polarity of the investigated analytes has been recently extended to compounds such as octocrylene ($LogK_{ow} = 6.8$) [57]. Several works have demonstrated the accumulation of analytes onto the PES membrane of POCIS [58–61] and in some applications the amount accumulated in the membranes may exceed that in the sorbent phase [62].

Polyethersulfone (PES) was first proposed as a sorptive material for microextraction of Ecs from water samples [63]. Afterwards, several works presented its use for sorptive microextraction in aqueous matrices of polar and non-polar chemicals, permitting an improvement in the extraction efficiency of the less hydrophobic compounds compared to other polymeric materials [64–70]. The PES polymer was recently tested as a single-phase passive sampler in the form of tube/hollow fiber [71–73] and flat sheet membrane [72,74]. The tested analytes covered a broad range of $LogK_{ow}$ (from -0.9 to 8.54).

In the first part of the PhD, the performance of the PES membrane as a single-phase passive sampler for short-term exposures was tested. The uptake kinetics of ten Ecs that showed the highest affinity for PES in a previous work [75] were studied. The sorption of five UV filters, three estrogens, bisphenol-A and triclosan ($LogK_{ow}$ between 3.59 and 6.78) were investigated in several laboratory experiments to evaluate the sampler capacity, the uptake

kinetics and the influence of factors such as salinity and flow rate on the accumulation. Furthermore, a field exposure was carried out deploying PES membranes in Santa Margherita Ligure harbor (Genoa, Italy) to assess the application of the sampler in a real environment. The results obtained using passive sampling were also compared to those of spot sampling.

3.2 Materials and methods

3.2.1 Chemicals (standards and reagents)

High-Performance Liquid Chromatography (HPLC) grade methanol (MeOH), acetonitrile and acetic acid were obtained from Merck (Darmstadt, Germany). Water was purified by a Milli-Q system (Millipore, Watford, Hertfordshire, UK).

Standards of benzophenone-3 (BP-3), bisphenol-A (BPA), estrone (E1), β-estradiol (E2), 17α-ethinyl estradiol (EE2), ethyl hexyl methoxy cinnamate (EHMC), octyl dimethyl *p*-aminobenzoate (OD-PABA), octocrylene (OC) and triclosan (TCS) were obtained from Sigma-Aldrich (Milan, Italy). All standards were of high purity grade (> 98%). Stock solutions of the considered analytes were prepared at a concentration of 2000-5000 mg L^{-1} in MeOH. A mix standard was prepared at 50 mg L^{-1} in 50:50 (v/v) milli-Q/MeOH. Working solutions of all analytes were prepared in the 0.2-200 µg L^{-1} range by subsequent dilution of the stock solution in 50:50 (v/v) milli-Q/MeOH. The stock solutions were stored at -20°C and working solutions were freshly prepared for every run. The chemical structures and physico-chemical properties of the target compounds were reported in the Appendix (Tab. 1A-2A).

Salts employed in the preparation of a simple version of Synthetic SeaWater (SSW) were sodium chloride (NaCl, ≥ 99%) from Sigma Aldrich (Milan, Italy), sodium sulfate (Na$_2$SO$_4$, 99%) and potassium chloride (KCl, 99.5%) from Carlo Erba Reagenti (Rodano, MI, Italy). SSW was prepared by adding NaCl, KCl and Na$_2$SO$_4$, to tap water at a concentration of 22.64 g L^{-1}, 0.78 g L^{-1} and 4.15 g L^{-1} respectively [76].

A buffer solution was prepared using sodium hydroxide (> 98%) from Sigma Aldrich (Milan, Italy) and ammonium acetate (> 98%) from Merck (Darmstadt, Germany): 0.044 g L^{-1} and 1.928 g L^{-1}, respectively [56].

3.2.2 PES membrane characteristics

Microporous PES membranes of 0.1 μm pore size were obtained from Pall Italia (Buccinasco, Italy). PES membranes were washed for 24 h in a ultrapure water/MeOH solution (80:20 v/v), then with MeOH for 24 h. Afterwards, the membranes were dried under a laminar hood [75].

PES was cut into pieces of different dimensions for the different experiments. The membrane pieces were weighted and those that differed by more than 10% from the standard sampler (34.1 mg for 14 cm^2) were excluded.

3.2.3 Analyte extraction from PES membrane

The extraction procedure was developed comparing two different methods: ultrasound (US) assisted extraction (USC600D by VWR, Leuven, Belgium) and extraction with a rotator drive (STR4/4, Stuart, UK) (AR). In both the procedures the membranes were wetted with ultrapure water and spiked with 50 μL of a standard solution in MeOH containing the target analytes at 1 mg L^{-1}. The PES membranes were left to dry for almost an hour, then they were rinsed with ultrapure water and left to dry again. The extraction was then performed in 20-mL-vials containing 12 mL of MeOH. The extraction procedure was repeated twice. Using US, the extraction was performed for 10 min (cycle I) and 5 min (cycle II), while using AR the rotation was set at 24 rpm and extraction time was 20 min for the first cycle and 10 min for the second. These procedures were called US1 and AR1, respectively. After the final extraction, the vial was further rinsed with 2 mL of MeOH, thus leading to a total volume of 26 mL. The eluate was then reduced to dryness on a rotary evaporator (Rotavapor® R-100, BUCHI, Switzerland) and reconstituted in 1 mL of methanol; this solution was filtered through a regenerated cellulose (RC) 0.2 μm filter. The extraction methods were evaluated in terms of recovery, matrix effect and precision.

Afterwards, to improve the recoveries, the procedure was modified using longer extractions: two cycles of 30 min were performed using both US and AR (procedure US2 and AR2). The speed of rotation in the AR was increased to 36 rpm to enhance the repeatability.

Based on the recoveries obtained, the final procedure was AR2 which involved the use of AR and extraction of 30 min.

In particular, for the evaluation of recoveries the final extracts were diluted 1:5 (spike before extraction: sample B). Blank membranes were extracted using the same procedure and the

extracts were diluted 1:5 or 1:50. Then, both the diluted extracts were spiked to obtain a final concentration of 10 µg L^{-1}, which corresponded to a 100% theoretical recovery (spike after extraction: sample A). The two different dilutions served to evaluate matrix effect.

Recovery (R%) was calculated by using the following formula:

$$R\% = 100 \; \frac{A_B - A_{NS}}{A_A - A_{NS}} \qquad\qquad Eq.\,3.1$$

Where A$_B$ and A$_A$ are the LC-MS peak areas obtained by analyzing samples B and A, respectively. A$_{NS}$ corresponded to the blank signal.

The matrix effect was evaluated both on the extracts obtained in the recovery tests and on real samples, by using the following expression:

$$ME\% = 100 \; \frac{A_A - A_{NS}}{A_{std}} \qquad\qquad Eq.\,3.2$$

Where A$_A$ is the LC-MS peak areas obtained by analyzing sample A (at different dilutions), while A$_{NS}$ and A$_{std}$ are the peak areas obtained by analyzing a membrane extract without any spike and a neat standard at 10 µg L^{-1}, respectively.

The precision of the extraction methods was evaluated in terms of repeatability and of inter-day precision (2 days); the results were expressed as coefficients of variation (CV%).

This method was performed for each lab-experiment of the work described below; on the contrary the procedure was slightly changed for the extraction of field PES pieces (section 3.2.8) containing the sorbed analytes. The membranes were carefully rinsed with ultrapure water to remove the fouling present on the exposed surface, then they were left to dry under the fume hood on acetone-rinsed aluminum foil for several hours. When dry, they were placed in 20-mL vials and extraction was performed with 20 mL of MeOH, on the rotator drive at 36 rpm for 30 minutes. The eluate was transferred to a flask and the procedure was performed twice. After the final extraction, the vial was further rinsed with 4 mL of MeOH, thus leading to a total volume of 44 mL. The following steps were the same as described above.

In general, a proper final dilution with a milli-Q/MeOH mixture (50:50, v/v) was performed before injection in the HPLC-MS/MS system.

3.2.4 HPLC-MS/MS analysis

Analyses were carried out on a 1200 SL Liquid Chromatograph by Agilent technologies (Santa Clara, CA, USA) by using a Kinetex® C18 Polar column (100 mm × 2.1 mm i.d.; 2.6 μm particle size, Phenomenex, Torrance, CA, USA), coupled to an Agilent 6430 Triple Quadrupole mass spectrometer (MS), equipped with an ESI interface. The MassHunter 10.0 software was used for data acquisition and processing. Mass detection was performed using dynamic-multiple reaction monitoring (d-MRM), to enhance sensitivity. The most abundant fragment transition was used for quantification and the others for confirmation purposes. The optimized MS conditions and the selected MRM transitions are reported in Tab. 3A.

For the detection of BPA, estrogens and TCS a chromatographic method was developed using the Kinetex® C18 Polar column. The chromatographic conditions involved a temperature of 40 °C, a flow rate of 0.3 mL min^{-1} and a gradient of ultrapure water and acetonitrile (Tab. 3.1). The MS detection was performed in negative ESI mode.

At the beginning of the work, a previously developed method for UV filters was adapted to the Kinetex® C18 Polar column. Column temperature was fixed at 30 °C, the flow rate employed was of 0.3 mL min^{-1} and an isocratic elution was performed using 30% of ultrapure water and 70% of acetonitrile, both phases containing the 0.1% of acetic acid (v/v). The MS detection was performed in positive ESI mode. The isocratic elution was then replaced by a gradient of eluent and of flux to reduce problems of carry over for the more hydrophobic UV filters [76]. The acid concentration in both the eluents was reduced to 0.01% of acetic acid. Due to the lower content of acid, the sensitivity of the method for EHS resulted very low and the analyte was not studied since the introduction of the new method. The conditions of the final method are reported in Tab. 3.2.

Tab. 3.1 Gradient conditions of the method employed for the detection of the 5 target analytes detected in negative ESI.

Time (min)	H$_2$O (%)	ACN (%)	Flow (mL min^{-1})
BPA, estrogens and TCS			
0	60	40	0.3
0.2	60	40	0.3
5	10	90	0.3
6	10	90	0.3
7	60	40	0.3

Tab. 3.2 Gradient conditions of the method employed for the detection of the 4 target analytes detected in positive ESI.

Time (min)	H$_2$O (%)	ACN (%)	Flow (mL min^{-1})
UV filters			
0	60	40	0.3
2	30	70	0.3
6	30	70	0.3
7	30	70	0.4
9	30	70	0.4
10	60	40	0.3

3.2.5 Quality assurance

UV filters are tricky analytes. Some of them are photosensitive and degradation can occur if dark conditions are not maintained. Furthermore, their tendency to sorb on plastic materials can cause problems of contamination and loss on the experimental equipment. For these reasons, stability tests and blanks were performed for each analysis.

The EC stability in water was assessed under calibration condition (see section 3.2.7). The ambient temperature was fixed at 25°C using a thermostat.

Beakers filled with water were spiked with a standard solution of the target compounds, the analytes' concentration in water was then checked after 20 and 168 hours. The sorption of the target chemicals in the presence of polymers competing with PES membranes was evaluated monitoring the water concentration in presence of a magnetic stirrer [77]. The sampled waters were diluted 1:1 (v/v) with MeOH and filtered through a 0.2 μm RC filter prior to HPLC-MS/MS analysis.

Procedural blanks were performed, exposing the membranes to the matrix without any spiked analyte and following the extraction protocol.

The stability of the analytes sampled by PES membrane was also evaluated after 60 and 180 days in storage conditions (-20 °C).

The multivariate statistical analysis (PCA) was performed using the software CAT (Chemometric Agile Tool) [78]; for the other statistical evaluations Excel (Microsoft) was employed.

3.2.6 PES-water partition coefficients

PES-water partition coefficients (K_{PESw}) were estimated using the single dose design [77] as the ratio of the analyte's concentration in the membrane ($C_{PES,eq}$) and the analyte's concentration in water ($C_{w,eq}$) at the equilibrium (Eq. 3.3).

$$K_{PESw} = \frac{C_{PES,eq}}{C_{w,eq}} \qquad\qquad Eq.\,3.3$$

Initially, K_{PESw} were evaluated using ultrapure water as matrix (pH 5.5). Beakers containing 1.8 L of water were spiked with a standard solution of the analytes to obtain a final concentration of 5 µg L^{-1} (EXP1). An equilibration time of 30 minutes at a stirring rate of 1,000 rpm using F30 magnetic stirrers (Falc Instruments, Italy) was applied. Two membranes of 7 cm^2 were deployed in each beaker, fixed onto a brass grid (Fig. 3.1). After 7 days, membranes were collected and extracted as described above. The attainment of the equilibrium was assessed monitoring the analyte concentrations in water. These results were compared to those obtained in a longer experiment (EXP2) of 12 days performed in the same conditions but using a more concentrated solution (10 µg L^{-1}). The same conditions of EXP2 were applied to assess the K_{PESw} of PES membranes purchased by a different supplier (Hangzhou Anow Microfiltration Co., Ltd). This was only a first attempt, a more in depth-study is presented in Chapter 4.
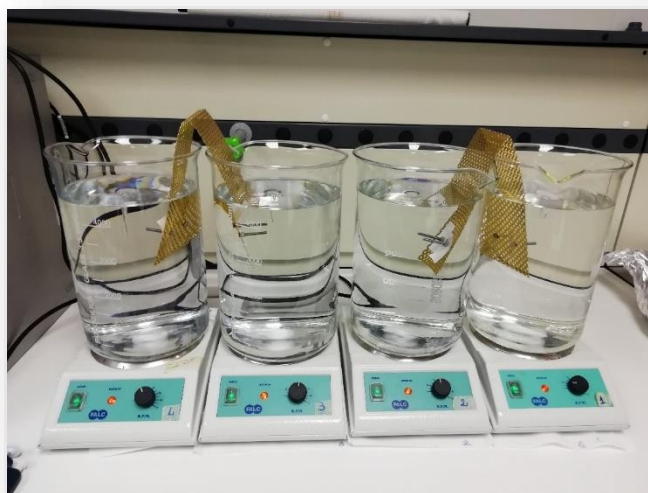
Fig. 3.1 Experimental setup of calibration experiments.

Afterwards, different conditions were employed to assess the influence of pH and ionic strength in sorption. Beakers were filled with 1.8 L of ultrapure water (EXP3) or SSW (EXP4) maintained at pH 7.5 and pH 7.8 using the buffer solution prepared as described above. A standard mix containing all analytes was added to obtain a final concentration of 5 μg L^{-1} of each compound. The experimental configuration was the same of the evaluation in ultrapure water at pH 5.5.

The experimental setup is summarized in Tab.3.3.

Tab. 3.3 Membranes with an exposed surface area of 7 cm^2 were deployed in 1.8 L of water spiked with the target analytes, without water renewal and under stirring conditions (1000 rpm). The experimental parameters employed which vary among the tests for the evaluation of K_{PESw} were reported in this table.

	MATRIX	pH	CONCENTRATION (μg L^{-1})	TIME OF EXPOSUR (d)
EXP 1	Ultrapure water	5.5	5	7
EXP 2	Ultrapure water	5.5	10	14
EXP 3	Ultrapure water	7.5	5	7
EXP 4	SSW	7.8	5	7

3.2.7 Uptake and calibration experiments

A preliminary static depletion experiment was performed for 24 h using membranes of 28 cm^2 (total surface area considering both sides) with the aim of evaluating how quickly analyte water concentrations were reduced in the beakers. Beakers filled with 4.5 L of tap water were spiked with the 10 target compounds to obtain a final concentration of 10 µg L^{-1}. After 30 min of equilibration (stirring rate of 1000 rpm) two membranes fixed onto a brass grid were deployed in each beaker. Duplicates were withdrawn at 1, 2, 3, 4, 5, 15 and 24 h. After the deployment, the PES membranes were extracted as described above and different final dilutions were used depending on the expected analyte concentrations. For each withdrawal of membranes, water was sampled, diluted 1:1 (v/v) with MeOH and analysed.

Afterwards, calibration experiments were carried out using the static renewal method [43].

Based on the preliminary results, a 96-h calibration in tap water was carried out. Beakers containing 4.5 L of tap water were spiked with a standard mix to reach a final concentration of 1 µg L^{-1}. After the equilibration time, two membranes of 14 cm^2 were deployed in each beaker (total of 7 beakers). Water was renewed every 12 hours, membranes were removed from each beaker at 10, 24, 38, 48, 58, 72 and 96 h in duplicates. The concentration in water was monitored at the beginning and at the end of each renewal to avoid a depletion higher than 20% [79]. The solution was stirred at roughly 1000 rpm.

A 96-h calibration was also performed using SSW for the evaluation of the sampling rates in this different matrix. 4.5L of SSW prepared as described above were spiked with a standard solution of the analytes to obtain a final concentration of 1 µg L^{-1}. Water was renewed every 24 h, thus smaller membranes were employed. Two PES sheets of 7 cm^2 fixed onto a brass grid were deployed in each beaker and membrane pairs were removed at 24, 48, 72 and 96 h. The stirring rate was roughly 1000 rpm.

Furthermore, two uptake experiments were performed to compare the effect of different flow conditions on the analytes' accumulation onto the PES membranes. Beakers filled with 4.5 L of tap water were spiked with a standard mix to get a final concentration of 5 µg L^{-1}. Two membranes of 14 cm^2 fixed onto a brass grid were deployed in each beaker. During the calibration, two beakers were subjected to agitation at 1000 rpm and two beakers were kept in static conditions. PES membranes were removed after 2, 4, 6 and 8 h in duplicates for each experiment.

The experimental setup is summarized in Tab. 3.4.

Tab. 3.4 Experimental conditions of the calibration experiments. The volume of water employed for all the setup was 4.5 L.

	Matrix	Conc. (µg L^{-1})	Renewal (h)	Agitation (rpm)	Sampler Area (cm^2)	Exposure Time (h)
PRELIMINARY CAL	tap water	10	no	1000	29	24
CALIBRATION 1	tap water	1	12	1000	14	96
CALIBRATION 2	SSW	1	24	1000	7	96
STATIC UPTAKE	tap water	5	no	0	14	8
STIRRED UPTAKE	tap water	5	no	1000	14	8

3.2.8 Field deployment

PES membranes of 90 cm^2 fixed onto a stainless-steel grid were employed for the field sampling. This larger surface area was selected to increase the amount of target compound accumulated into the sampler during the exposure in seawater, considering the expected ultra-trace concentrations.

The deployment was performed in Santa Margherita Ligure Harbor (Genoa, Italy) in September 2022 (44.330 N, 9.214 E). To assess the linearity of the uptake, two samplings of two days each were performed in series (2d-S1 and 2d-S2 from the 5th to the 7th and from the 7th to the 9th of September, respectively), and a parallel four-day deployment (4d-S from the 5th to the 9th of September) was carried out. A pair of PES membranes were exposed for each sampling. Besides, spot sampling was performed at the beginning, in the middle and at the end of the four-day deployment (SPE-1, SPE-2 and SPE-3, respectively) to compare the results of passive sampling with a standardized method. A volume of 500 mL of seawater was filtered (MF-Millipore mixed cellulose esters, 0.45 µm) to consider only the dissolved fraction of the target compounds. Then the sampled marine water was subjected to SPE, by using 200 mg-HLB cartridges (Supelco, Bellefonte, PA, USA). The analytes were eluted using a method optimized in a previous work for the chemicals of interest [76].

3.3 Results and discussion

3.3.1 Quality assurance

On the one hand, the results obtained during the stability test after 20 h under stirring conditions did not show significant losses for all the target compounds, excluding OD-PABA (loss of 69%). On the other hand, the degradation of this UV-filter appears negligible after 20 h in static conditions. The degradation of the target compound after 168 h with agitation was higher for most of the compounds; as expected OD-PABA showed the highest loss, 84%. Thus, the results of the partition coefficients obtained for this UV filter can be affected by higher uncertainty.

The presence of a magnetic stirrer did not affect the analytes' concentration in water through sorption.

The storage conditions at -20°C resulted adequate for 6 months, although the evaluation of the stability of OC was affected by errors in the instrumental detection.

To keep the same membrane properties throughout the study (porosity, tortuosity, total surface area and thickness) membranes purchased from the same supplier were employed.

3.3.2 Selection of the extraction method

To obtain a reliable sampling method, the trueness and the precision of the extraction protocol were investigated. The trueness of the method was estimated using Recovery (Eq. 3.1) and Matrix Effect (Eq. 3.2). The inter-day and intra-day precision were assessed in terms of Relative Standard Deviation (RSD%).

Initially, two extraction procedures were evaluated as described above: US1 and AR1. The degradation of the analytes in the extraction conditions was assessed, showing a good stability with both the tested procedures (86%-100%). Moderate ME% was observed considering dilutions 1:5 and 1:50. The recoveries obtained using US1 resulted between 57% and 94%; recoveries lower than 70% were obtained for the more hydrophobic UV filters (OC, OD-PABA, EHS and EHMC). Slightly higher recoveries were obtained using AR1, however a greater RSD% was observed (13-60%) compared to US1 (2-13%). For these reasons the procedures US2 and AR2 were tested. The time of extraction was extended and a higher rotation speed was employed to enhance the repeatability of AR extraction.

The highest recoveries were observed using AR2 procedure. The results obtained are showed in Fig. 3.2. Furthermore, the repeatability of the method AR2 resulted improved, showing RSD% between 3% and 14%.
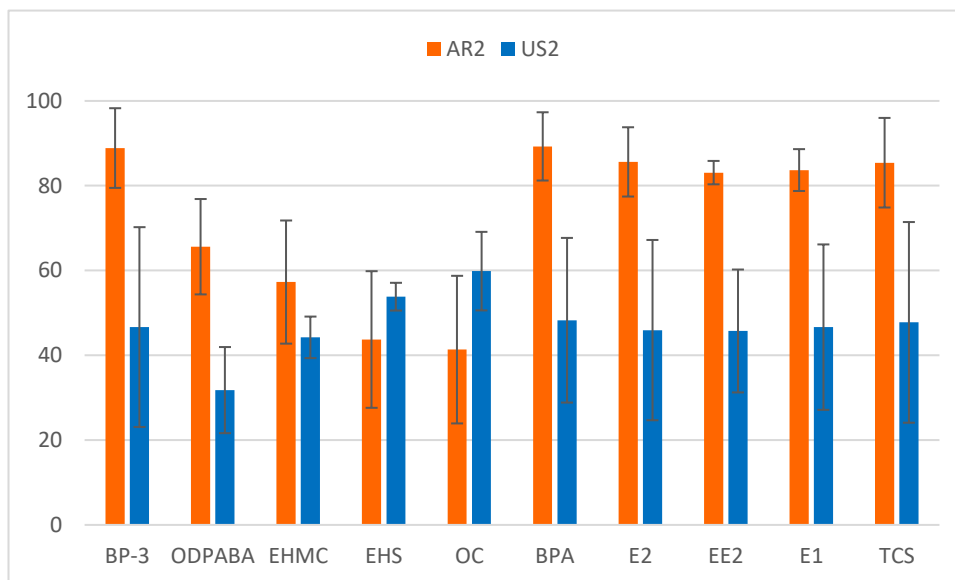
Fig. 3.2 Recoveries obtained using the AR2 and US2 methods.

Besides recovery, the reliability of an analytical method can be affected by matrix effect. This phenomenon is due to an alteration of the ionization efficiency that causes an enhancement (ME > 100%) or suppression (ME < 100%) of the analyte signal and occurs when other substances in the sample co-elute with the analytes during chromatographic separation [30]. ME is preeminent using ESI [31] compared to other ion sources. The two extraction methodologies were also compared in terms of matrix effect at two different dilutions, 1:5 and 1:50. The resulting ME% were reported in Fig. 3.3. In both cases, the ME% resulted soft for most compounds; only OC showed a high signal suppression.
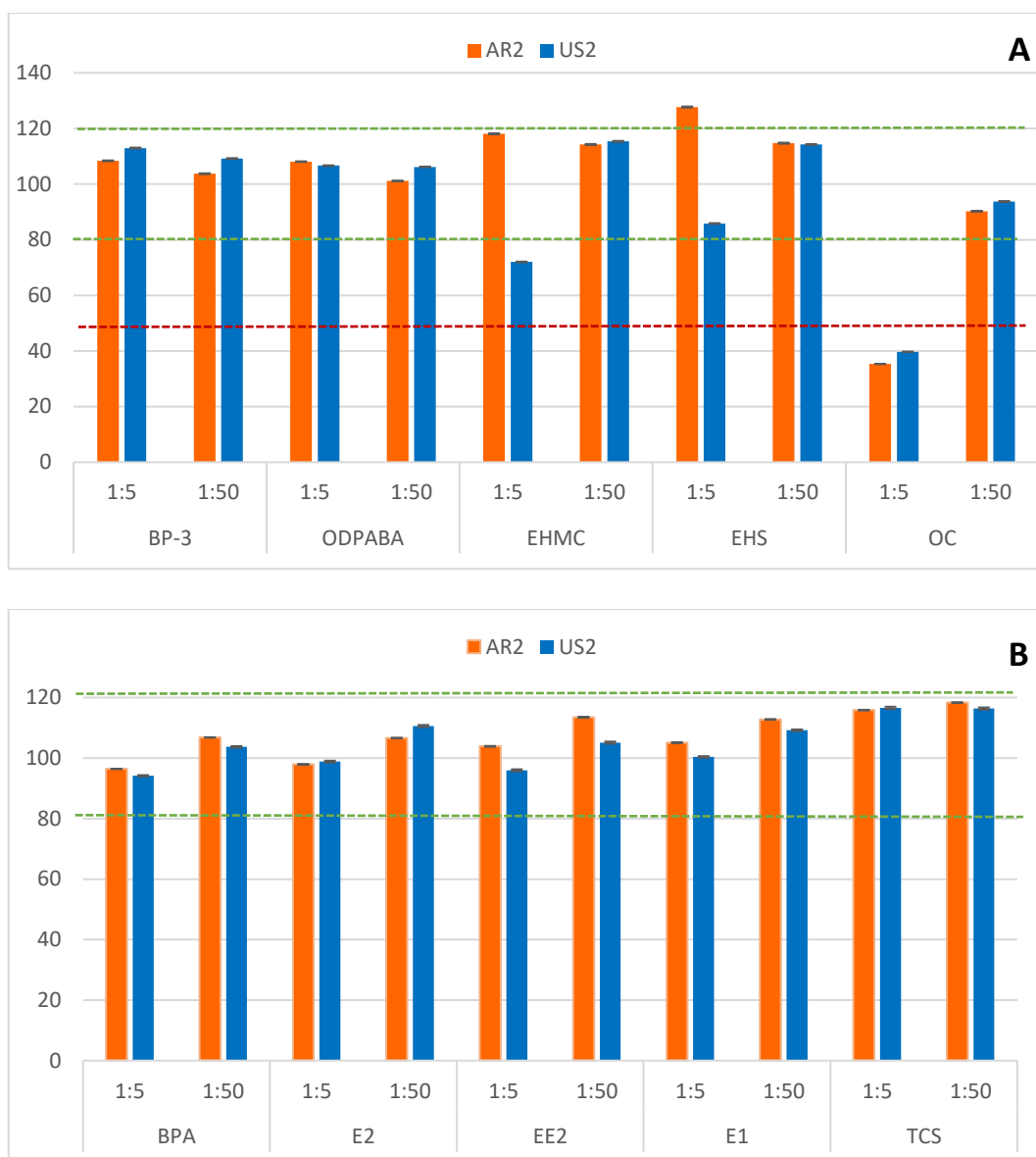
Fig 3.3 Results of ME% (± err.st) obtained for the extraction procedure AR2 (orange) and US2 (blue) considering two different dilutions (1:5 and 1:50) for UV filters (A) and BPA, three estrogens and TCS (B).

3.3.3 Evaluation of method accuracy

Based on the result presented in section 3.3.2, the protocol selected was AR2. In synthesis, the highest recoveries were obtained for BP-3, BPA, estrogens and TCS, between 78 and 85%, while the more hydrophobic UV filters had 66% < R% < 69%. An attempt to improve R% using a less polar solvent (DCM) was done but due to the solubility of the membrane in the solvent, this tentative was discarded [74].

In the applied extraction conditions (MeOH), a correlation ($R^2 = 0.66$) between recovery and hydrophobicity (expressed as logD at pH=5.5) was observed for the four UV filters (Fig. 3.4).
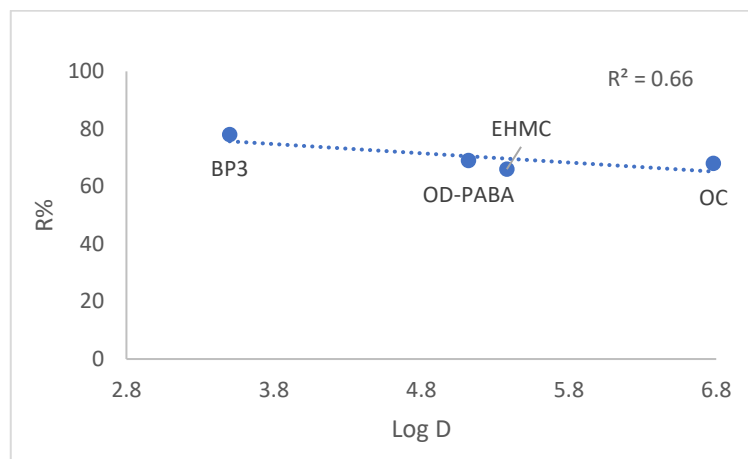
Fig. 3.4 Recovery (R%) of the extraction procedure from PES: linear regression of the R% obtained for the target UV filters vs. logD (pH 5.5).

These results could suggest a different sorption mechanism linked to compounds' hydrophobicity. In particular, sorption is a combination of adsorption and absorption. Adsorption is a surface process which involves interactions by several forces (e.g. H-bonding, van der Waals, ionic and π-π interactions), while absorption is a partitioning process where only the weaker forces are involved (van der Waals) [80]. The latter implies the dissolution and the diffusion into the polymer [81] and is mainly related to the compound hydrophobicity. Usually, the sorption of chemicals takes place in the non-crystalline domains of polymers [82]. Considering the glass transition temperature (T_g), amorphous polymers are also divided into rubbery and glassy. Rubbery polymers (with T_g lower than the environmental temperature) are characterized by the presence of mobile and flexible polymer segments, and sorption of organic molecules occurs principally by absorption [83]. This sorption mechanism is exploited by some passive samplers such as SR and LDPE. Instead, glassy polymers (T_g higher than the environmental temperature) are more condensed and present internal nanovoids, regions where the sorbed chemicals can interact with the internal surface through adsorption-like interactions, which make the compound release more difficult [82,84,85]. PES is an amorphous and glassy polymer. The less hydrophobic compounds (LogD < 5), interact with the polymer/pores surface through adsorption. On the other hand, the more hydrophobic compounds (UV filters with LogD > 5) can interact both

through adsorption and absorption. Therefore, the diffusion into the matrix allows them to reach internal nanovoids, leading to the possible formation of stronger interactions. The linear relationship between recovery and LogD was not followed by TCS, this compound presents a different behaviour due to the presence of electron-withdrawing groups on the aromatic rings.

As mentioned above, the matrix effect was investigated in order to verify if the membrane itself could release any interferent compound during the methanol extraction. The ME values of the AR2 method are presented here more in detail. For the target compounds, ME were between 96-118% for two different dilutions (1:5 and 1:50) indicating no significant signal suppression or enhancement. The only exception was OC, whose ionization was suppressed at the lowest dilution (ME=35%). This suppression could be due to the presence of some residuals of the manufacturing process released from the membranes [62], although membranes were pre-washed. Still, at the highest dilution, matrix suppression was greatly reduced and a completely acceptable ME was obtained (ME=90%).

The ME was also evaluated using the extracts of the SSW calibration (see section 3.2.7 and 3.3.5) to observe the influence of salts. The results obtained in 50-fold diluted extracts ranged from 90 to 126%. Considering the higher dilution, ME could be defined as rather soft with the AR2 extraction [86].

The same evaluation was performed on the field deployment extracts. To guarantee sensitivity, these samples were subjected to a rather lower dilution. The ME observed in a 1:1 diluted extract resulted between 53-131% for the detected compounds, except for OC, which was strongly suppressed (average ME= 9%). A higher dilution factor was also tested to limit the matrix effect; however, the advantage was not high enough to compensate for the loss in sensitivity. The presence of salts as well as other interferents sorbed onto the PES might enhance the ME of OC which was sensitive to suppression also in lab-conditions. Thus, the ionization efficiency must be carefully evaluated in each field deployment, since different sampling conditions may alter the sample composition.

Finally, the repeatability and the inter-day precision were evaluated for the extraction procedure AR2. The RSD% obtained ranging between 3-14% and 4-18%, respectively.

The analyte-specific results obtained for the R%, RSD% and ME% were reported in Tab. 3.5.

Tab.3.5 Recovery (R%) and precision (repeatability and inter-day precision in terms of coefficient of variation CV%) of the extraction procedure, and matrix effect (ME%) at different dilutions and conditions.

	R%	Repeatability RSD% (n = 3)	Inter-day RSD% (n = 6)	ME% 1:50	ME% 1:5	ME% (1:50 SSW)	ME% (1:1 field)
BP-3	78	7	14	104	108	126	65
OD-PABA	69	7	9	101	108	125	65
EHMC	66	8	13	114	118	106	58
OC	68	8	18	90	35	90	9
BPA	85	9	10	107	96	107	60
E2	82	12	11	107	98	107	137
EE2	81	14	10	114	104	96	67
E1	83	4	4	113	105	101	123
TCS	85	3	7	118	116	115	64

3.3.4 PES-water partition coefficients

The PES-water partition coefficient can be employed as an indication of the affinity of a target compound for the sampler. As described in section 2.1.3.3, K_{PESw} is a fundamental parameter in the case of equilibrium samplers because it links the amount of analyte in the sorbent to the equilibrium concentration in water.

Initially, the partition coefficients were evaluated using ultrapure water at pH 5.5 and the attainment of the equilibrium was assessed monitoring the analytes concentration in water. The first measurements (EXP 1) were obtained using a 7-day exposure, and a total of 4 PES membranes were deployed. The second experiment (EXP 2) was carried out for a longer period of 14 days and a pair of samplers were exposed. The results of K_{PESw} for the two set of experiments are reported in Fig. 3.5 in [L kg^{-1}], unless otherwise specified. The mass balances resulted acceptable in both cases (66% - 128%), except for OD-PABA (37% and 17 %, respectively). The poor mass balance of OD-PABA was due to the established degradation in presence of the magnetic stirrer (section 3.3.1).
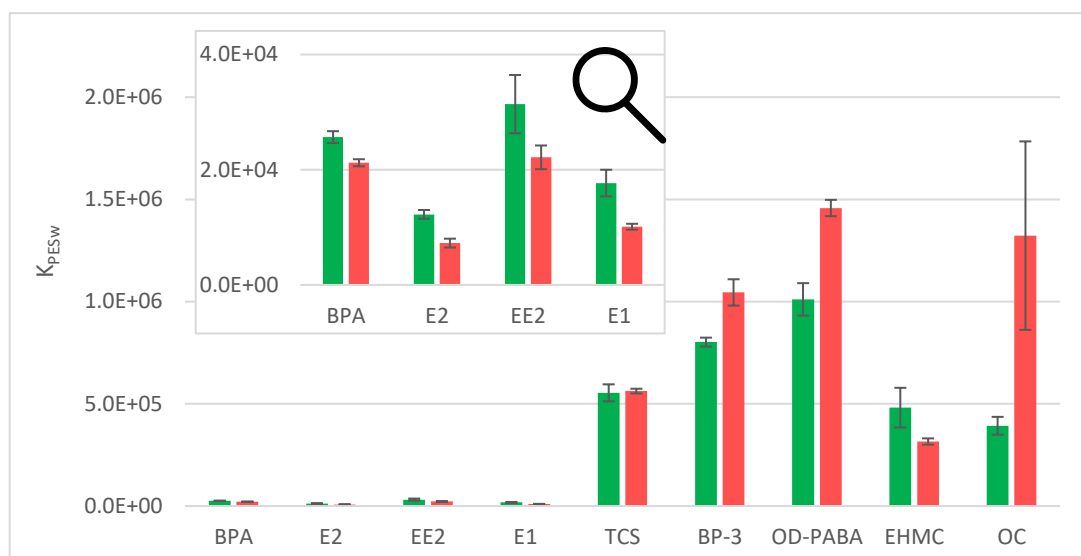
Fig. 3.5 Data of K_{PESw} obtained by the EXP 1 (n = 4) (green bars) and EXP 2 (n = 2) (pink bars).

Differences higher than 30% were observed for E2, E1, OD-PABA, EHMC and OC. In general, the results were higher for EXP 2 (BP-3, OD-PABA and OC). The results of OC were clearly affected by a great error for EXP 2 and a conclusion cannot be drawn. Regarding OD-PABA, the compound with the highest difference after OC, the greater value of K_{PESw} in EXP 2 can be due to the longer exposure and the further degradation of the compound in water. Another reason could be the apparent equilibrium reached in EXP 1 revealed by the longer deployment in EXP 2. Indeed, some compounds showed a slower accumulation after a certain period, giving the impression of the achievement of equilibrium. This behavior was related to different sorption mechanisms involved considering a PES sampling material. The sorption can occur on the total surface of PES membranes (adsorption), which involves also the surface of the narrow pores, and in the PES matrix (absorption in the amorphous regions); as the diffusion through the water-filled pores is usually the limiting step for the more hydrophobic compounds, due to their low diffusion coefficients in water, the sorption resulted slowed down [74].

During EXP 2, a first attempt to evaluate the impact of the manufacturing (different suppliers) on ECs sorption onto PES membranes was carried out. The highest differences were observed for the compounds with lower values of LogD (pH 5.5): BPA, estrogens and BP-3 (LogK_{PESw} > 0.5). These results suggested a relationship between sorption and analyte's hydrophobicity. Further investigations were carried out and are presented in Chapter 4.

To observe the influence of ionic strength and pH on sorption affinity, two different conditions were studied: ultrapure water (EXP 3) and SSW (EXP 4), both maintained at a pH of 7.5. The results of mass balance for the experiments were between 67-135% and 59-111% respectively, excluding OD-PABA (18% and 24%, respectively).

The results were reported in Fig. 3.6 and showed an enhancement of the partition coefficients as the ionic strength was increased for three UV filters (increase in K_{PESw} > 30%). In fact, the enhancement of ionic strength may favour the sorption of the more hydrophobic compounds creating a salting-out effect [87,88]. Moreover, the presence of cationic species could reduce the repulsion among the ionized BP-3 and the negative charge of the PES membrane [62]. On the other hand, a lower influence of salinity was observed for EHMC, TCS, estrogens and BPA in SSW. Similar results were obtained for the sorption of EE2 onto polyethylene debris [88].
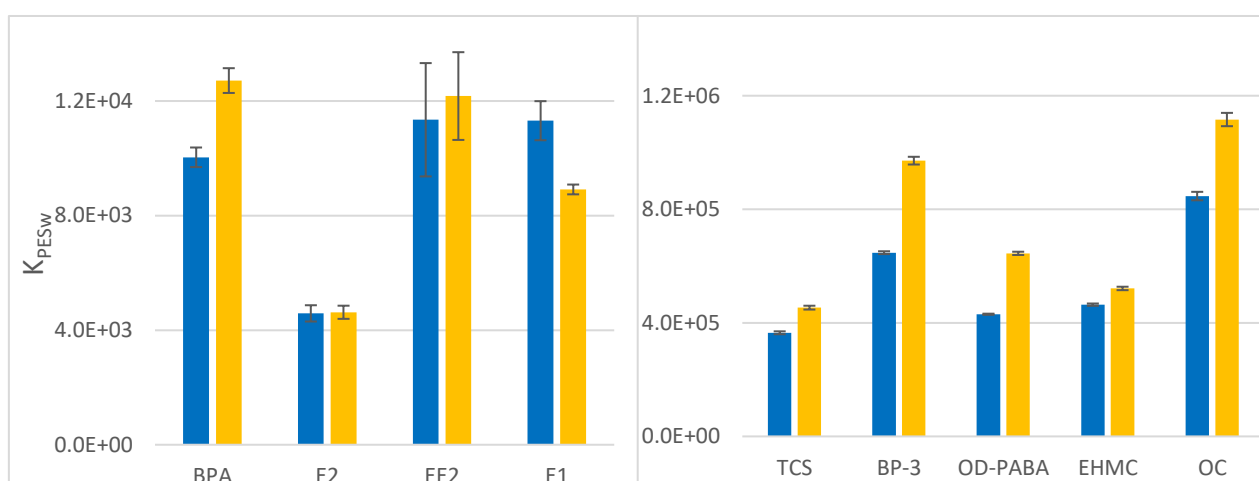
Fig. 3.6 K_{PESw} (L kg^{-1}) values obtained in milli-Q water at pH 7.5 (blue) compared to those in SSW at pH 7.8 (yellow).

The PES-water partition coefficients were then compared to the data reported in previous studies (Tab. 3.6), including one using the PES polymer and others using the hydrophobic sampler silicon rubber (SR).

Prieto et al. [63] reported partition coefficients for E2, TCS, OD-PABA and OC using in-tube PES samplers for sorptive extraction in ultrapure water:MeOH, 80:20 (*v/v*). Comparing these results with those of EXP 1 (Tab. 3.6), differences between 0.7 and 1.3 Log units were observed. This is due to the presence of an organic solvent in water. The presence of MeOH in water increases the solubility of the more hydrophobic compounds lowering the partition coefficients between the solution and the sorbent [89].

The EXP1 results were also compared with those obtained using SR as single-phase passive sampler. All the experiments were performed in ultrapure water thus, they were compared only to EXP 1. SR is the most employed passive samplers for hydrophobic contaminants, but it presented lower values of partition coefficients for the less hydrophobic compounds (TCS and BP-3). The different sorption mechanism described in section above and the presence of pores, which increase the surface area, resulted in a greater sorption capacity of PES for these compounds. The K_{PESw} of OC and EHMC fell in a the range of the reported data of silicon rubbers [90,91]. Suggests similar interaction between the two UV-filters and the considered hydrophobic polymer (SR and PES).

Tab. 3.6 Comparison of the apparent $LogK_{PESw}$ obtained in this study for EXP 1 with those obtained in literature for PES tube [60] and Silicon Rubber [89–91].

	$LogK_{PESw}$ EXP 1 (L L^{-1})	$LogK_{PESw}$ 20% MeOH (L L^{-1})	$LogK_{PESw}$ EXP 1 (L kg^{-1})	$LogK_{SRw}$ (L kg^{-1})	$LogK_{SRw}$ (L kg^{-1})	$LogK_{SRw}$ (L kg^{-1})
Ref.	*this work*	[63]	*this work*	[91]	[90]	[89]
BPA	4.01 ± 0.02	/	4.41 ± 0.02	/	/	/
E2	3.69 ± 0.03	**2.97 ± 0.08**	4.09 ± 0.03	/	/	/
EE2	4.01 ± 0.07	/	4.45 ± 0.07	/	/	/
E1	3.85 ± 0.06	/	4.25± 0.06	/	/	/
TCS	5.34 ± 0.03	**4.03 ± 0.05**	5.74 ± 0.03	/	**3.02 ± 0.13**	**3.89 ± 0.04**
BP-3	5.50 ± 0.01	/	5.90 ± 0.01	**3.69 ± 0.11**	**3.08 ± 0.02**	/
OD-PABA	5.60 ± 0.03	**4.33 ± 0.05**	6.01 ± 0.03	/	/	/
EHMC	5.28 ± 0.09	/	5.68 ± 0.09	**6.4 ± 0.04**	**4.77 ± 0**	/
OC	5.19 ± 0.05	**4.39 ± 0.05**	5.59 ± 0.05	**6.32 ± 0.06**	**4.96 ± 0.11**	/

3.3.5 Uptake experiment: flow rate influence

Flow rates affect the sampling kinetics in passive sampling. As described in section 2.1.3, the R_s is directly related to the overall mass transfer coefficient (k_0). If the resistance to mass transfer is considered, the overall resistance ($1/k_0$) can be written as the sum of the single compartment involved in the uptake (Eq. 3.4)

$$\frac{1}{k_0} = \frac{1}{k_w} + \frac{1}{K_{PESw}k_{PES}} \qquad\qquad Eq.\,3.4$$

Where k_w is the water boundary layer (WBL) mass transfer coefficient and k_{PES} the sorbent mass transfer coefficient.

If the mass transfer coefficients are time independent or if the time-dependent terms are negligible, these coefficients can be written as the ratio of the diffusion coefficient to the phase thickness [32].

$$\frac{1}{k_0} = \frac{\delta_w}{D_w} + \frac{\delta_{PES}}{K_{PESw}D_{PES}} \qquad\qquad Eq.\,3.5$$

Where δ_w the thickness of the WBL and D_w the diffusion coefficients of the analytes in water, δ_{PES} the thickness of the PES membrane and D_{PES} the diffusion coefficients in the polymer.

This assumption is correct for k_w [30], but for membrane-controlled diffusion the analytical solution is a sum of exponentials describing the establishment of concentration gradients in the PES. As consequence, the partition coefficients change over time and the second term of Eq. 3.5 is not correct [31].

Nevertheless, the uptake for the more hydrophobic compounds is generally controlled by the WBL because of their low diffusion coefficients in water [91] and the value of $k_0 \approx k_w$. In this scenario the application of the sampling rate model (Eq. 2.11 section 2.1.3) results corrected.

To evaluate the impact of the WBL, uptake experiments under static and stirring conditions were carried out. These experiments permitted to assess the impact of the thickness of the WBL on the amount of analytes sorbed onto the PES, hence on the R_s.
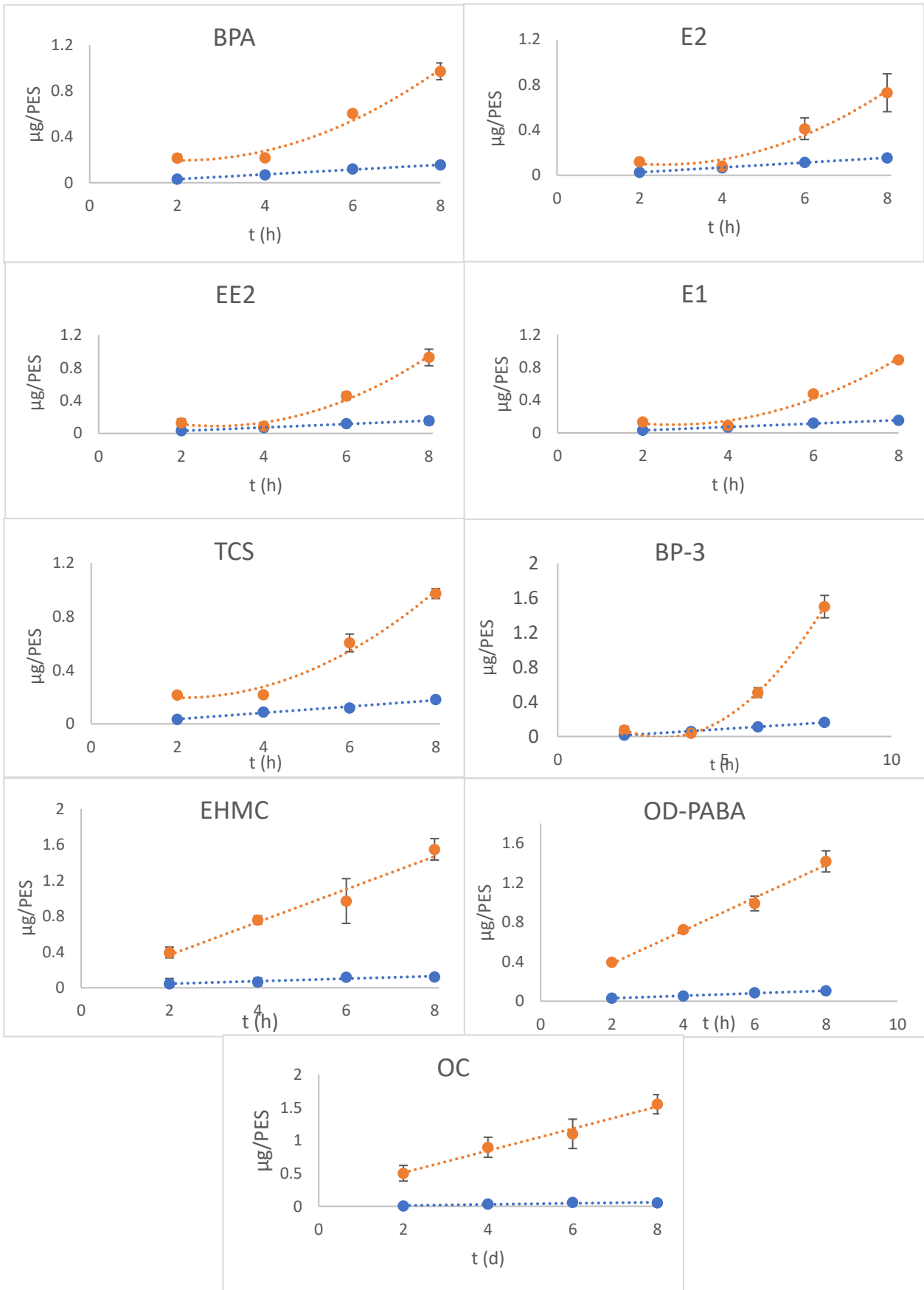
Fig. 3.7 Uptake curves obtained for the 8-h calibration under static (blue) and stirred (orange) conditions. The error bars are the confidence intervals ($\alpha = 0.05$; n=2).

On the one hand, the more hydrophobic UV-filters showed a significantly different accumulation already in the first two hours (Fig. 3.7), clearly indicating a WBL-dependent uptake. On the other hand, during the first four hours no substantial difference was observed for the less hydrophobic compounds (e.g., BP-3 and E1). For the last group of compounds poor accumulation both in stirred and static conditions was observed in the first few hours, especially for BP-3 and the estrogens. This behavior suggests that the uptake is initially under the sorbent control [35] for compounds with the lower LogD and with more affinity for water. Nonetheless, in the following hours the uptake for these compounds became more relevant under stirred conditions with a similar accumulation rate of the more hydrophobic UV filters.

Due to the expected longer time of the field deployment (2-4 days), the first lag-phase for the less hydrophobic compounds may be neglected. Therefore, the sampling rate model was considered applicable for all compounds and calibration experiments were performed to evaluate R_s.

3.3.6 Calibration experiments

A preliminary static depletion calibration was performed in tap water to monitor the decrease in concentration of the contaminants in water during the sampling. The aim was to define the frequency of water renewal during longer calibrations to maintain analytes' concentration in water almost constant (decrease lower than 20%). However, after 24 hours the concentration of most compounds significantly decreased. A water loss between 40-70% at the end of the experiment was observed for UV filters and TCS. The water concentrations for the remaining compounds had a decrease lower or equal to 30%.

During the 96-h calibration in tap water the spiked tap water was hence renewed every twelve hours. Furthermore, to slow down the uptake process, the surface area of the PES sheets was halved. These measures were needed to guarantee an analyte concentration in water as constant as possible [43].

Two different uptake trends were observed:

1. TCS and UV filters presented a linear uptake during all the 96h (Type I)

2. BPA, E2, EE2 and E1 had already reached an apparent equilibrium after 10 hours (Type II)

During the 96-h calibration in tap water also EHS was studied showing a linear uptake. This UV filters was discarded in the following experiments due to the change of the chromatographic method and the decrease of sensitivity.

To better display the accumulation trends, the results of both the 24-h and 96-h calibrations are reported in Fig. 3.8:
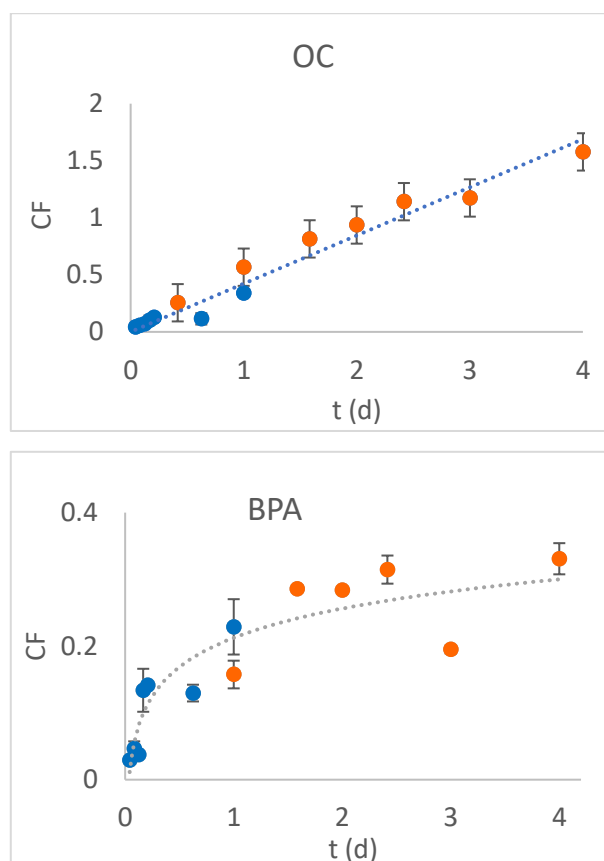

Fig. 3.7 Examples of Type I (OC) and Type II (BPA) accumulation curves. The data in blue were obtained from the 24-h calibration, while the orange data represent the results of the 96-h calibration. CF was the concentration factor estimated as the ratio between the amount of analyte in the sorbent and its concentration in water.

For confirmation of the linear accumulation, several statistical tests were performed. Only the 96-h calibration data were employed, due to the uncertainty of the results of the 24-h calibration as consequence of the decrease of concentration in water. Initially, the linear regression was performed and a Student's *t*-test (Tab. 4A) was carried out to evaluate the significance of the intercept (significance level set at α = 0.01). Based on the results obtained, the fitting was forced through the origin.

Furthermore, the determination coefficient (R^2), the Mandel's fitting test (significance level 1%) [92], the residual plot and the plot of experimental vs. predicted values were examined, confirming that a linear model was suitable for fitting the data (detailed results of the statistical analysis in the Appendix (Tab. 5A and Fig. 1A).

The resulting plots of the statistical test are exemplified in Fig. 3.8.

$$Rs = \frac{m_t}{A \cdot t \cdot C_w}$$

R_s: sampling rate
m_t: mass of the analyte in the sorbent
A: membrane area
t: exposure time
C_w: analyte concentration in water.
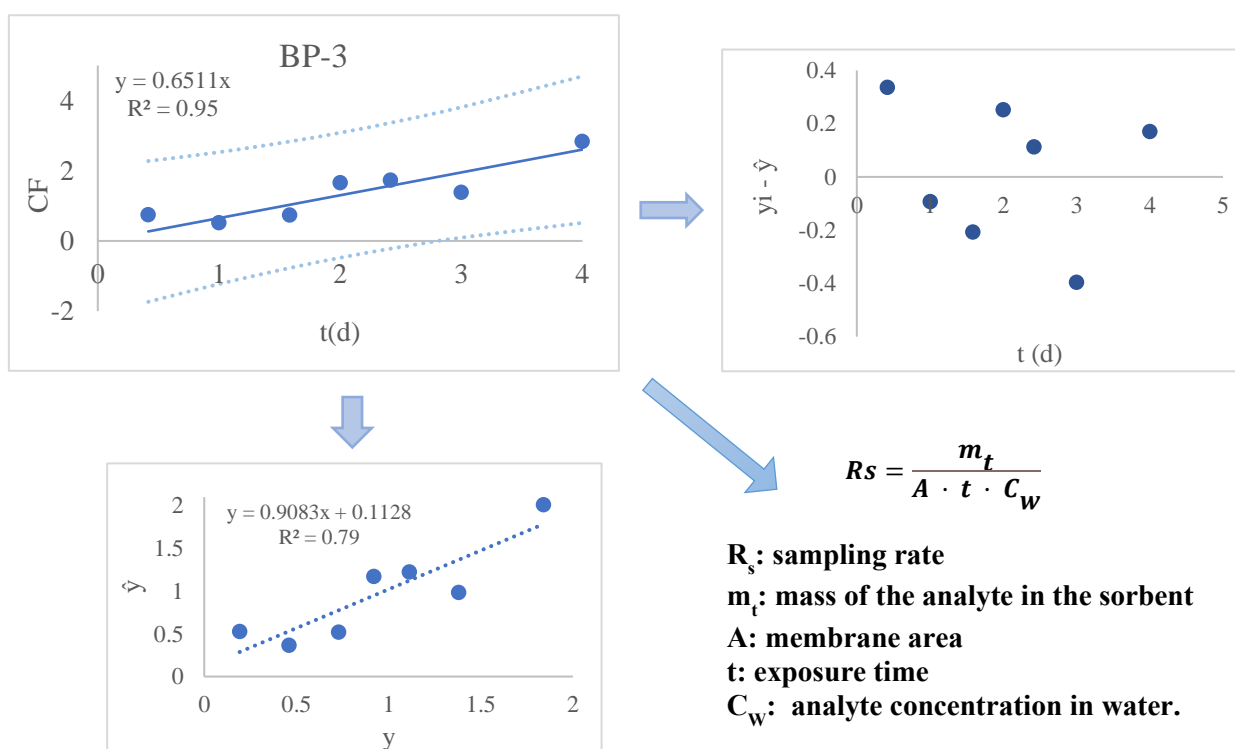
Fig. 3.8 Example of the data obtained from the linearity evaluation of Type I compounds. The linear regression reporting the correlation coefficient and the prediction intervals (α = 0.05), the residual plot (yi − ŷ) and the plot of experimental vs. predicted values were presented. CF was the concentration factor estimated as the ratio between the amount of analyte in the sorbent and its concentration in water.

Linear regressions of the Type I analytes are reported in Fig. 3.9.
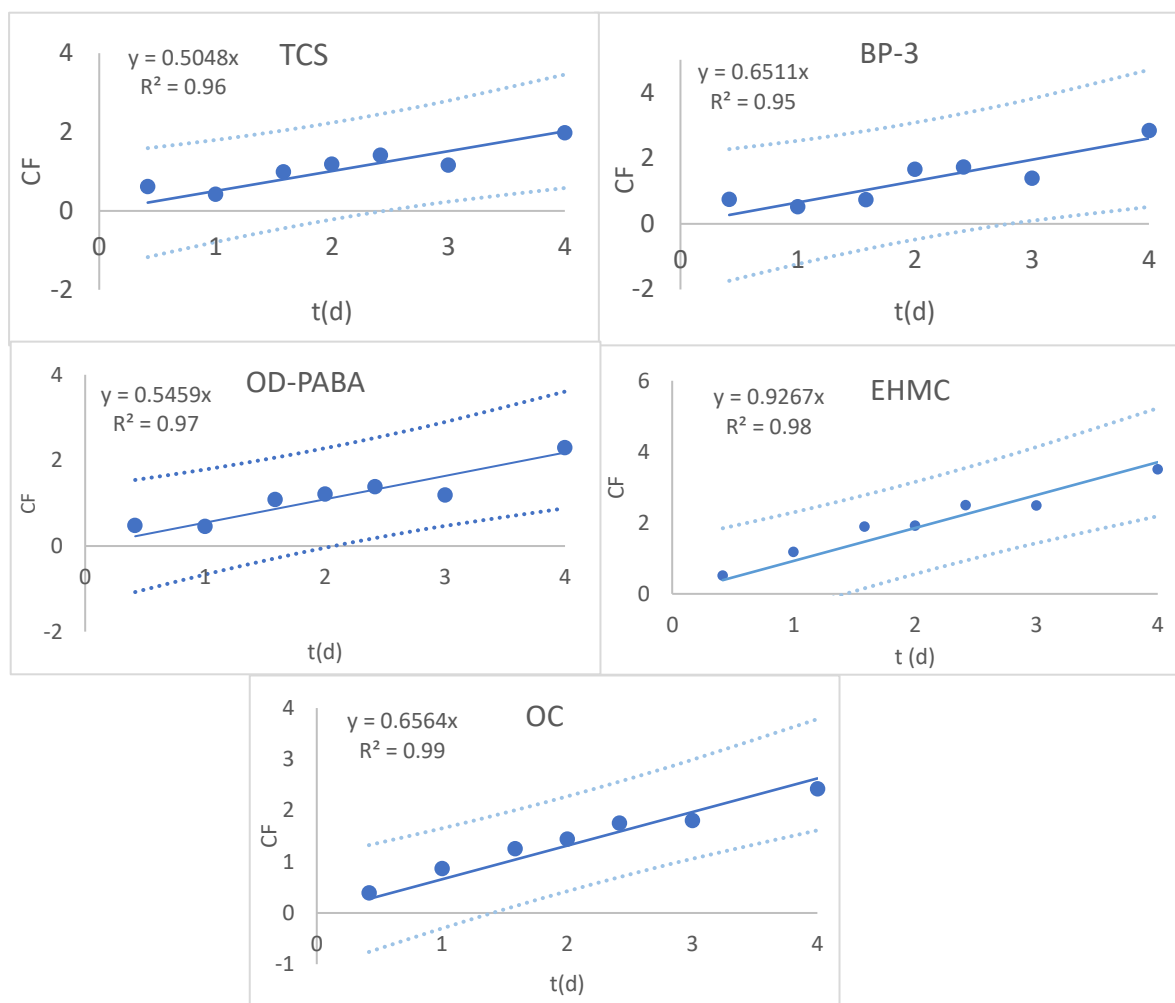
Fig. 3.9 Tap water uptake curves obtained for the Type I analytes. Dot lines represent the prediction intervals ($\alpha = 0.01$, $n = 7$). CF is the concentration factor estimated as the ratio between the amount of analyte in the sorbent and its concentration in water.

A similar 96-h calibration experiment was performed in SSW. Estrogens and BPA also achieved equilibrium during this second calibration. Instead, linear uptake was confirmed for Type I compounds (Fig. 3.10).
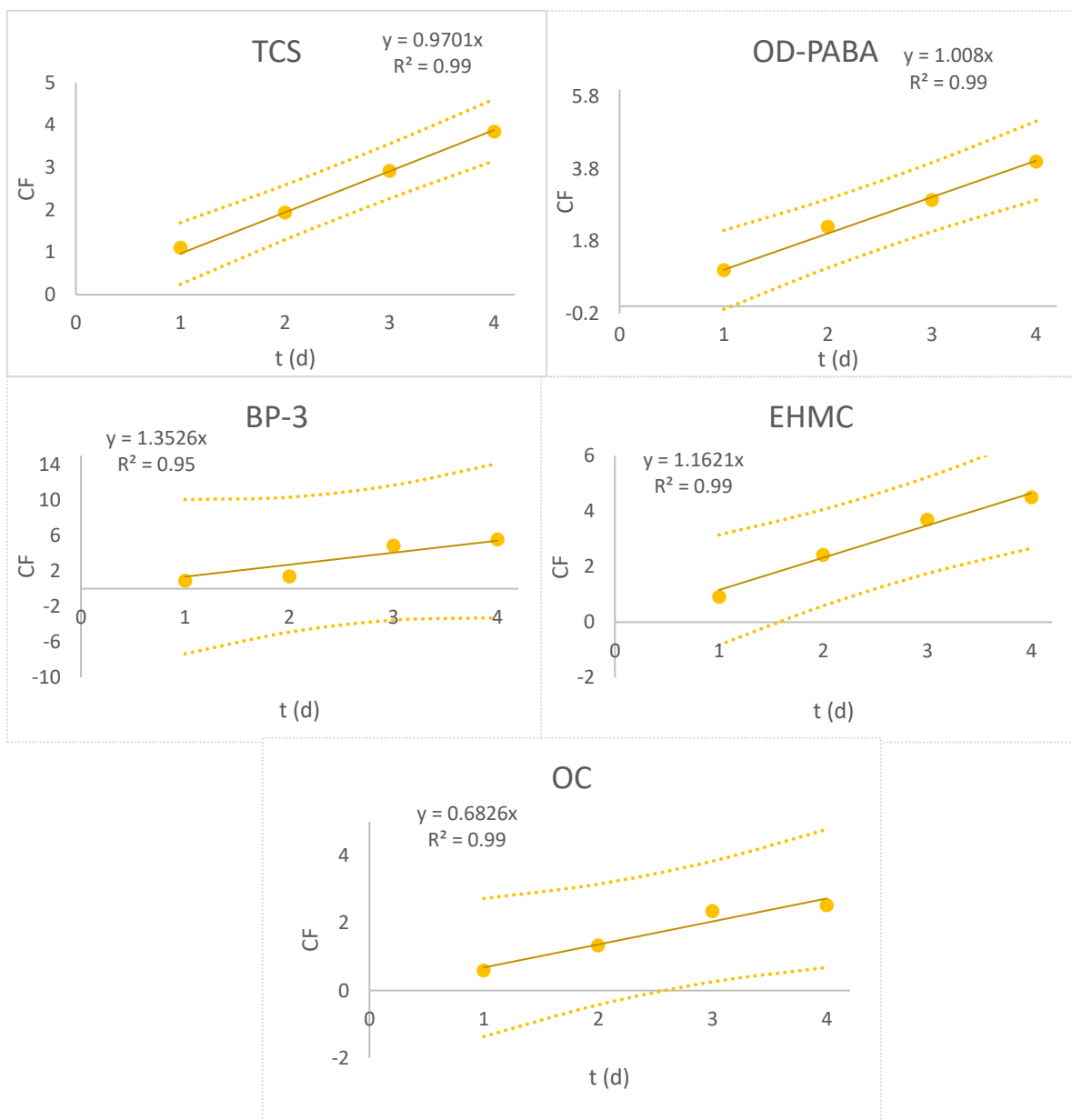
Fig. 3.10 Linear regression of the data obtained during the SSW 96-h calibration. CF is the concentration factor estimated as the ratio between the amount of analyte in the sorbent and its concentration in water. The dotted lines represent the prediction interval ($\alpha = 0.05$, n=4).

The same statistical tests applied in tap water confirmed the linear uptake in SSW (Tab. 6A-7A and Fig. 2A).

Thanks to Type I linear uptake, R_s could be estimated by using Eq. 2.11 (section 2.1.3). The results obtained for tap water and SSW from the 96-hour calibrations are reported in Tab.

3.7. The accumulation of the target compounds onto the membranes was higher in SSW compared to tap water, as shown by the sampling rates reported above.

Tab. 3.7 R_s ± standard error obtained for 96 hours calibration in tap water and SSW. The highest values were observed in SSW as stated in the text.

	R_s tap water $(L\ d^{-1}cm^{-2})$	R_s SSW $(L\ d^{-1}cm^{-2})$
BP-3	0.05 ± 0.01	0.10 ± 0.04
OD-PABA	0.039 ± 0.006	0.072 ± 0.005
EHMC	0.066 ± 0.007	0.08 ± 0.01
OC	0.047 ± 0.005	0.05 ± 0.01
TCS	0.036 ± 0.007	0.069 ± 0.003

Moreover, the high surface specific R_s and the possibility to greatly increase the surface area of the sampler enable to achieve low LOD and LOQ. Therefore, the quantification of the analytes even for short exposures is possible. This aspect is more relevant considering the possibility to shorten exposure durations and avoid biofouling in environments such as harbors, which may change the sampling performance of the PES devices.

3.3.7 Principal Component Analysis

The Principal Component Analysis (PCA) permitted to rationalize the sorption of the target analytes in the PES membranes. The analytes were considered as objects and several physico-chemical properties and sorption parameters as starting variables. The objective was to find correlations among the parameters representing the sorption mechanisms (K_{PESw}) and the sorption kinetics (the total amount of compound accumulated onto the PES polymer in the calibration experiments m_{96h}) and different physico-chemical properties of the analytes, such as LogD, polarizability and the topological polar surface area. The selected physico-chemical properties (see Tab. 1A) are usually employed to estimate the chemicals' absorption and transport through biological barriers. Some of them were previously correlated to sorption in passive sampling [59].

Since no bivariate correlation was observed between the different properties and K_{PESw} or m_{96h}, the PCA was performed with good results. A multivariate correlation of the physico-chemical characteristics with the sorption experimental data was observed.

The PCA was performed after a column pre-treatment: the autoscaling (mean centering and scaling) was necessary to make the data comparable. Afterwards, the first two Principal Components (PCs) were chosen to describe the studied system. The selection of the first two PCs is supported by the scree plot that showed a first inflection point in correspondence to the third PC. In particular, the first two PCS explain 76.1% of the total variance, indicating a good overall correlation among the starting variables.

Three groups were shown by the score plot of the first two PCs (Fig. 3.11). The first group was composed of three of the most hydrophobic UV filters (OC, EHMC and OD-PABA), the second group by TCS and BP-3, and the third group included the Type II compounds.

The loading plot (Fig. 3.11) suggested a correlation among sorption descriptors (LogK$_{PESw}$ and m_{96h}) and the properties characterizing hydrophobicity (i.e. LogD and polarizability) along PC1 and also an anticorrelation with solubility. Several works have indicated a correlation between hydrophobicity and K_{PESw} [58–61]. A high negative value of PC1 characterizes the first group, suggesting that their accumulation onto PES membrane occurs principally through hydrophobic adsorption and/or absorption. Furthermore, an anticorrelation of these physico-chemical characteristics and the recoveries was shown along PC1.

A **Score Plot (76.1% of total variance)**
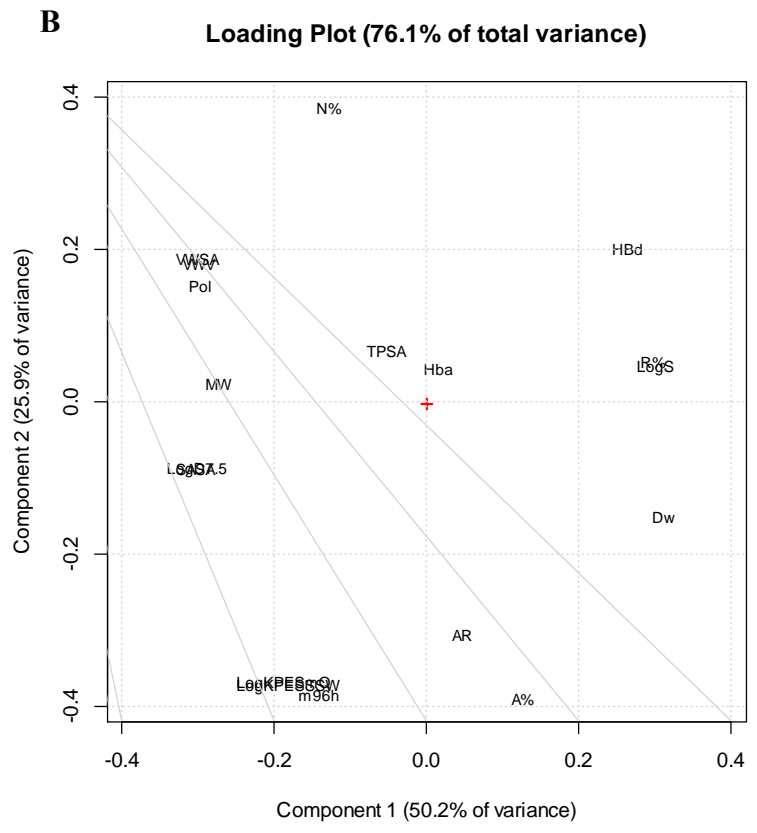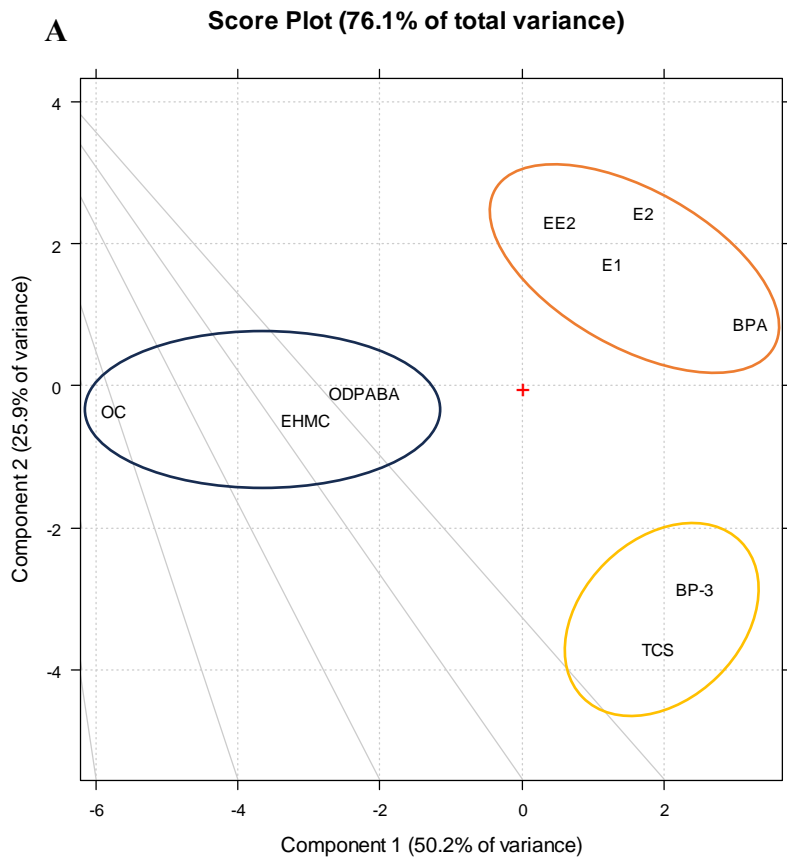
B **Loading Plot (76.1% of total variance)**

Fig. 3.11 Principal Component Analysis results: Score Plot (A) and Loading Plot (B) of PC1 and PC2.

Along PC2 the loadings of PES-water partition coefficients and the number of aromatic rings were correlated. The PC2 may describe adsorption through π–π stacking interactions and O-π interactions. The compounds more influenced by those properties were TCS and BP-3, which presented quite high and negative scores on PC2. The presence of supramolecular interaction was hypothesized to explain the uptake of some aromatic molecules. In particular, higher uptake has been observed for molecules with a higher number of aromatic rings and the presence of chlorinated and nitroaromatic compounds, thus in presence of electron withdrawing groups [58–60]. The anticorrelation of $LogK_{PESw}$ /m_{96h} and number of H-bonding donor groups (HBd) was observed along both the PCs. The position of Type II analytes in the plot indicated positive correlation with HBd. The presence of a higher number of donor groups in estrogens and BPA make the sorption less favorable [93] due to the interaction with water through H-bonding. Studies on the interaction of EE2 and PES polymers confirmed the importance of hydrogen bonding in sorption, though π–π interaction seems to have a major contribution [94–96].

In conclusion, PCA allowed to distinguish the behaviour of the different analytes as well as better understand which physico-chemical properties influence sorption the most.

3.3.8 Field application: harbor sampling

To test the performance of the sampling strategy in a real environment, a field application was performed in Santa Margherita Harbor from the 7th to the 9th of September 2022 (Fig. 3.12). This step in the development of a sample preparation procedure is of basic importance. In fact, the complexity of the environmental conditions is hard to mimic in the laboratory. In particular, several factors have an impact on the uptake in passive sampling such as flow rate, biofouling, the presence of suspended sediments and in some cases the presence of competitive species [97–99].
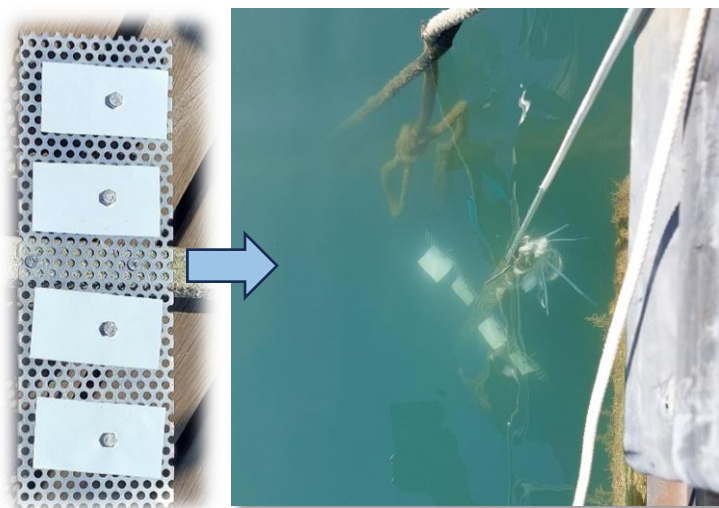
Fig. 3.12 Field deployment in Santa Margherita Harbor of PES membranes with a total exposed surface area (both sides) of 90 cm^2.

PES membranes are developed to resist fouling and are mainly use in microfiltration applications [100]. Thanks to the fouling resistance of PES during short deployments, no visible biofouling was observed onto the samplers after the field exposure, even in a heavy fouled environment such as a harbor.

The passive sampling by PES membranes of 90 cm^2 permitted to highlight the presence of five analytes above LOD in the harbor seawater in all samples: BP-3, EHMC, OC, BPA and E1. The TWA concentrations were estimated for Type I analytes, while only the amounts accumulated onto the PES is reported for Type II compounds. TWA concentrations were calculated for the detected UV filters by applying the R$_s$ previously reported for SSW (see Tab. 3.7), prior to normalization to the surface area of the exposed PES pieces (Eq. 2.7 section 2.1.3).

The results of the TWA concentration of the target compound are reported in Tab. 3.8.

Tab. 3.8 TWA concentration of detected UV-filters in the harbor waters. Concentrations in the extracts of the two deployed membranes were averaged (2d-averaged) and TWA concentrations were obtained by applying the calculated R_s in SSW (average ± standard error).

	TWAC (ng L^{-1})		
	BP-3	**EHMC**	**OC**
2d-S1	0.21 ± 0.08	0.6 ± 0.1	9 ± 5
2d-S2	0.16 ± 0.06	0.6 ± 0.2	9 ± 2
2d-averaged	0.18 ± 0.07	0.6 ± 0.2	9 ± 3
4d-S	0.13 ± 0.05	0.21 ± 0.05	6 ± 3

The averaged data of the two 2-d deployments (2d-averaged) were also compared with the 4-d exposure, to assess the linearity of the uptake. In fact, hypothesizing that the integrative uptake regime was maintained for the total duration of the sampling, the 4-day TWA concentrations (4d-S) should be comparable to the average of the two 2-day TWA concentrations (2d-S1 and 2d-S2).

Fig. 3.13 shows the sum of the analyte amounts accumulated during the 2-day exposures in comparison with those accumulated in the 4-day exposure. The results substantially agreed for BP-3 and OC, suggesting an integrative sampling in the considered period and conditions. On the contrary, EHMC showed a higher difference. Therefore, the accumulation kinetics can be considered linear for BP-3 and OC. Instead, a deviation from linearity was observed for EHMC.
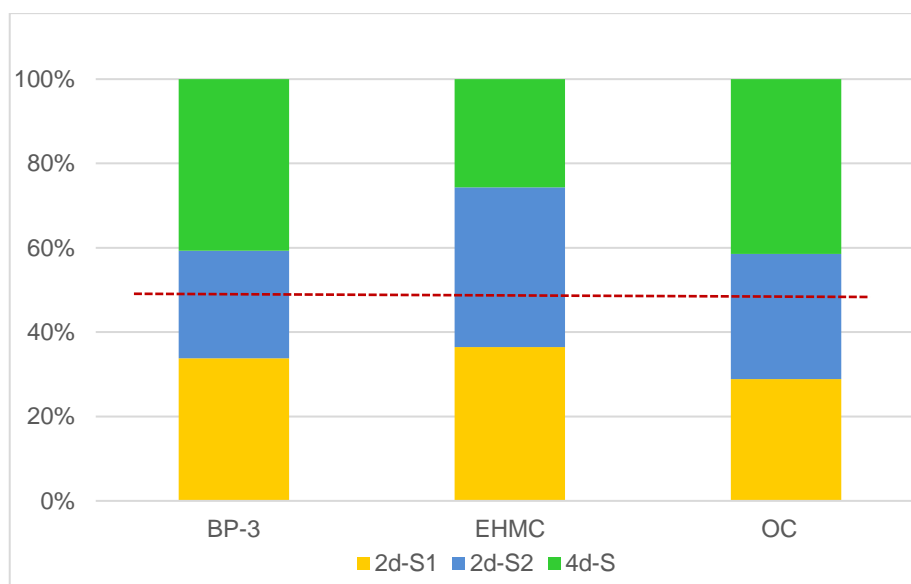
Fig. 3.13 Analyte amounts accumulated during the 2-day exposures performed in series (2d-S1 in yellow and 2d-S2 in blue) in comparison with those accumulated in the parallel 4-day exposure (4d-S in green).

It was speculated that the deviation from linearity was due to degradation processes (photolysis, hydrolysis or biodegradation) on the membrane of the (E)- EHMC isomer which is present in commercial formulations [101], as well as the degradation products of the isomer (Z)- EHMC which is detectable by the used HPLC-MS method.

Nevertheless, the presence of other photodegradation and photodimerization products needs to be verified. A preliminary investigation for the identification of some products (such as 4-methoxybenzaldehyde and cyclodimers) was carried out, by including selected ions [102]. The results suggested the presence of a cyclodimer and dimer hydrolysis products, but further investigations are needed.

Regarding Type II analytes, BPA and E1 were detected but their concentrations in water were not calculated as mentioned above. For these compounds, the laboratory calibration showed a rapid achievement of equilibrium. As a consequence, PES membranes could only be employed as equilibrium samplers for these species. Moreover, the difficulty to exhaustively describe the adsorption processes makes a more in depth study necessary to use PES as equilibrium samplers [103]. In fact, the adsorption process is complex: the field concentration of the analyte, the presence of competitors to the adsorption sites and the presence of multiple types of interaction may affect the results of C_w using K_{PESw} derived in laboratory experiments for compounds with a nonlinear sorption behavior [59,103–105].

The industrial additive BPA was detected in two samples above the LOQ (2d-S2 and 4d-S) with a concentration of 9.13 ± 0.03 and 7.4 ± 0.9 ng/PES, respectively. The concentrations observed for E1 were under the LOQ (< 2.8 ng/PES). The results of the samplings expressed as ng/PES were reported in Tab. 3.9.

Tab. 3.9 Analyte concentrations obtained in the membranes exposed in Santa Margherita Ligure Harbor.

	ng/PES				
	BP-3	**EHMC**	**OC**	**E1**	**BPA**
2d-S1	3.8 ± 0.1	8.7 ± 0.2	80 ± 38	< LOQ	< LOQ
2d-S2	2.9 ± 0.1	9.0 ± 0.3	82 ± 14	< LOQ	9.13 ± 0.03
4d-S	4.5 ± 0.04	6.1 ± 0.3	114 ± 45	< LOQ	7.4 ± 0.9

The Limits of Detection (LODs) and Quantitation (LOQs) were calculated considering the signal to noise ratio of 3 and 10 respectively. The noise was evaluated on the replicates of the tested samples for each signal of the analyte corresponding to the MRM quantitative transition. The noise was considered as the averaged integration (n = 3) value of background regions close to the analyte's signal and with the same width as the analytes' peaks. The area of the signal was obtained using a standard solution at 5 µg L^{-1}. The details on the LODs and LOQs of the method are reported in Tab. 3.10.

Tab. 3.10 LODs and LOQs for the exposed PES membranes and LODs and LOQs for the SPE extractions.

	PES						SPE	
	LOD (ng/PES)	LOQ (ng/PES)	LOD_{2d} (ng L^{-1})	LOQ_{2d} (ng L^{-1})	LOD_{4d} (ng L^{-1})	LOQ_{4d} (ng L^{-1})	LOD (ng L^{-1})	LOQ (ng L^{-1})
BPA	2.2	7.3	/	/	/	/	10.5	35.0
E2	0.8	2.5	/	/	/	/	3.2	10.8
EE2	1.7	5.8	/	/	/	/	4.6	15.2
E1	0.9	2.8	/	/	/	/	1.0	3.2
TCS	0.02	0.07	0.03	0.1	0.007	0.02	0.9	3.1
BP-3	0.8	2.8	0.05	0.15	0.02	0.08	1.3	4.2
OD-PABA	0.07	0.2	0.005	0.02	0.002	0.008	0.3	1.1
EHMC	1.6	5.5	0.1	0.4	0.06	0.2	2.7	9.0
OC	6.3	20.9	0.7	2.3	0.4	1.2	1.3	4.1

Finally, the results obtained by the passive sampling were compared with those of spot sampling. 500 mL of seawater were sampled at the beginning, in the middle and at the end of the 4d-S deployment. The water was filtered to remove the suspended organic matter and passed through SPE cartridges. SPE extracts confirmed the presence of EHMC, OC and BPA. However, only BPA in one of the spot samplings (SPE-2) and OC in all the samples were above the quantitation limit level (Tab. 3.10). The average water concentration of OC obtained using spot sampling was 4 ± 1 ng L^{-1} (Tab. 3.11). This result agrees with the TWA concentration of OC estimated by passive sampling. However, it is worth noticing that the other two UV-filters BP-3 and EHMC were respectively under the LOD (LOD$_{BP-3}$ = 1.3 ng L^{-1}) and the LOQ (LOQ$_{EHMC}$ = 9.0 ng L^{-1}) in SPE extracts, while quantifiable in the PES extracts.

Tab. 3.11 Analyte concentrations obtained using spot sampling in Santa Margherita Ligure Harbor expressed in ng L^{-1}.

	BP-3	EHMC	OC	E1	BPA
SPE-1	nd	< LOQ	4 ± 1	nd	< LOQ
SPE-2	nd	< LOQ	6 ± 1	nd	39 ± 2
SPE-3	nd	< LOQ	3 ± 1	nd	< LOQ

nd: not detected.

The presence of UV filters was assessed in a beach next to Santa Margherita Ligure harbor in a previous work during June-August 2010 [106]. Despite the presumably higher concentrations due to the considered site and season, EHMC and BP-3 were often detected but not quantified, presumably because of the lower sensitivity of the overall method. This highlights the potentiality and advantages of the developed passive sampling approach.

3.4 Conclusion

The potential use of PES membranes as integrative passive samplers for nine emerging contaminants was thoroughly investigated. The sorption onto the PES material was studied both in tap water and in synthetic seawater. Two main groups were observed based on their uptake: compounds with linear accumulation for up to 4-day deployments and compounds that reach an apparent equilibrium within 10 hours. The mechanism of sorption was then investigated by means of the Principal Component Analysis, allowing to better understand the analytes' uptake behavior by simultaneously considering different physico-chemical properties. The accumulation onto the sampler was not only related to hydrophobicity, but other interactions such as H-bonding and π-stacking were involved.

During a 4-day field deployment, five analytes were detected and for three of them the TWA concentration was estimated. The high sampling rates observed for Type I analytes and the possibility to greatly increase the exposed surface area permitted to obtain very low detection limits even during short exposures. These short exposures also permit to avoid the formation of biofouling onto the sampler surface.

Although nonporous single-phase passive samplers based on partitioning between water and the polymer (such as silicon rubber and LDPE) are widely employed for hydrophobic compounds, the use of PES can extend the range of detectable analytes, by exploiting both absorption and adsorption mechanisms. However, to verify the application for more polar compounds further investigations are requested.

This study can also be useful to better understand the influence of PES membranes on the uptake in dual-phase passive samplers (POCIS, Chemcatcher and o-DGT).

Published Papers

Scapuzzi, C., MacKeown, H., Benedetti, B., Baglietto, M., Di Carro, M., Magi, E. Polyethersulfone membrane as a single-phase passive sampler: Evaluation of the sampling performance for emerging contaminants in water, Microchemical Journal, 195, 109445, 2023. https://doi.org/10.1016/j.microc.2023.109445

MacKeown, H., Benedetti, B., Scapuzzi, C., Di Carro, M., Magi, E. A Review on Polyethersulfone Membranes in Polar Organic Chemical Integrative Samplers: Preparation, Characterization and Innovation. Critical Reviews in Analytical Chemistry, 2022. https://doi.org/10.1080/10408347.2022.2131374

Chapter 4. Characterization of several polyethersulfone membranes and evaluation of their sorption properties for hydrophilic and hydrophobic emerging contaminants

4.1 Introduction

As mentioned in section 2.1.3.3, the partition coefficients between the sorbent and water (sampled media) are important for equilibrium sampling by single-phase passive samplers. In fact, they affect the accuracy in the estimation of the analyte's water concentration (C_w) [77]. Partition coefficients also provide information regarding the affinity of a potential receiving material for target compounds; thus, they are useful for the selection of the sorbent in passive sampling devices. Nonetheless, few studies have measured the partitioning coefficient of the protective layer (usually polymeric materials) in dual-phase passive samplers, although they can be employed to better understand the uptake of chemicals by the sampler [103,107,108]. Furthermore, preliminary information regarding the affinity of some analytes for the protective membrane may lead to exclude the selected material from its application in dual-phase passive samplers [103].

The polymer water partition coefficient can be determined by allowing a chemical to reach its equilibrium distribution between polymer and water. Several methods have been proposed for these determinations. Aqueous concentrations may be maintained constant using flow-through systems or dosing materials (constant C_w design) or allowed to change over time (single-dose design) [77]. In the single dose method, the spiked water is not renewed, allowing a faster achievement of the equilibrium compared to the constant C_w design. Nevertheless, aqueous phase concentrations are often very low and difficult to measure accurately. This issue is more complex when the analytes are hydrophobic compounds with low water solubility. In fact, they may sorb to the walls of the container or to the dissolved organic matter present in the water. Smedes et al. (2009) validated a co-solvent method in which the partition coefficients are measured in water-MeOH systems [109]. A linear decrease in the partition coefficient is usually observed by increasing the percentages of organic solvent allowing to extrapolate the partition coefficient in pure water

[110]. Still, higher the concentrations in the aqueous solution at the equilibrium, the more accurate the quantification.

Previously, polyethersulfone–water partition coefficients (K_{PESw}) have been obtained using the single dose method [97,103,104,108,111–113] or the constant C_w design [59,114] as part of a dual-phase device (POCIS and Chemcatchers) or as a single-phase passive sampler. A two-compartment model was also employed for the evaluation of K_{PESw} by fitting experimental data [58]. However, the reported K_{PESw} have not always been evaluated at the equilibrium, impacting on the accuracy. Moreover, no study has yet considered the differences in analyte sorption on PES membranes from different suppliers due to differences in their non-disclosed manufacturing processes. For example, some very large differences in affinity for pesticides were found between two kinds of silicone rubbers [109,115].

In the present Chapter, flat sheet PES membranes of 0.1 μm pore size typically used in POCIS applications of three different suppliers were tested. One type of membrane of 0.45 μm pore size was also studied to evaluate the influence of pore size on the sorption phenomenon. The sorption onto PES membranes of 36 ECs with different physico-chemical properties was investigated. Differences in term of analyte recovery, matrix effects and K_{PESw} were studied. Furthermore, the flat sheet membranes were characterized by ATR FT-IR, SEM and porosity evaluations, to improve the understanding on the sorption mechanisms.

4.2 Materials and methods

4.2.1 Chemicals (standards and reagents)

Ultra-pure water, Methanol (MeOH) and acetonitrile (ACN) were purchased from VWR (Radnor, PA, USA). Acetic acid (CH_3COOH, 'AA') was provided from Sigma-Aldrich (St. Louis, MO, USA). All solvents were HPLC-MS grade. Water employed for the evaluation of PES-water partition coefficients was purified by a Milli-Q system (Millipore, Watford, Hertfordshire, UK).

Analytical standard solutions were prepared dissolving or diluting in MeOH or MeOH:water 1:1 pure powders, liquid standards and certified grade solutions (all above 98% of purity) of 36 emerging contaminants purchased from different suppliers: theophylline (THEOP), carbamazepine (CRB), benzophenone-3 (BP-3), octyl dimethyl p-aminobenzoate (OD-PABA), ethyl hexyl methoxy cinnamate (EHMC), octocrylene (OC), perfluorooctanoic acid

(PFOA), acesulfame (ACS), sucralose (SCL), bisphenol A (BPA), estrone (E1), β-estradiol (E2), 17α-ethinyl estradiol (EE2), ibuprofen (IBU), gemfibrozil (GEM), clenbuterol (CLBT), hydrochlorothiazide (HCTZ), furosemide (FRSM) and triclosan (TCS) from Sigma-Aldrich (St. Louis, MO, USA); caffeine (CAFF), ketoprofen (KET), naproxen (NAP), diclofenac (DCF) from Fluka Analytical (Saint Gallen, Switzerland); salbutamol (SLBT) from Alfa Aesar (Haverhill, MA, USA); taurine (TAU), omethoate (OMT), daminozide (DMNZ), 2,4-Dichlorophenoxyacetic acid (2,4-D), chloramphenicol (CMPH), metformin (MTF), atenolol (ATN), terbutaline (TRBT), chlormequat (CMQ), nicotine (NCT), fluroxypyr (FXP) and metoprolol (MTP) from Merck (Darmstadt, Germany).

The main physico-chemical characteristics of the 36 analytes were obtained using Chemicalize (https://chemicalize.com/app/calculation) and reported in the Appendix (Tab. 1A), their chemical structures are reported in (Tab. 2A).

4.2.2 Polyethersulfone membranes

Microporous membranes of 0.1 μm pore size were obtained from Pall Italia (P01) (Buccinasco, Italy). The other two membranes of 0.1 μm pore size were obtained from commercial POCIS purchased by E&H services (Prague, Czech Republic), and manufactured by Hangzhou Anow Microfiltration Co.,Ltd (H01) (Hanghzhou, China) and Sterlitech Corporation (S01) (Washington, USA). PES membrane disk filters of 0.45 μm pore size – which is the typical pore size employed in o-DGT applications [116] – were obtained from Pall Italia (P045) (Buccinasco, Italy).

Before assembling home-made POCIS, PES membranes are usually pre-washed to avoid the presence of residual oligomers [62]. In this work, P045 and P01 membranes were washed for 24 h with ultrapure water: MeOH (80:20 v/v), then for 24 h with MeOH [75]. As H01 and S01 membranes came from commercial POCIS (generally already pre-washed prior to assembly), to mimic the procedure before deployment no additional pre-wash was carried out.

4.2.3 Membrane characterization

The morphology of PES membranes was characterized using a Field Emission Scanning Electron Microscope (FE-SEM) ZEISS SUPRA 40 VP (White Plains, NY, USA). Images of the surface and of the cross-section of dry PES membranes were obtained at different

magnifications (125x – 30,000x). The membranes were coated by a thin layer of carbon to render them conductive. The membranes investigated using this technique were H01 and P01, while the acquisition of S01 and P045 are still required.

The potential presence of different functional groups in the polymer due to possible differences in manufacturing was assessed by the Attenuated Total Reflectance Fourier Transform Infrared spectroscopy (ATR-FTIR). A Spectrum 65 FT-IR Spectrometer (PerkinElmer, Waltham, MA, USA) equipped with a KBr beamsplitter, a DTGS detector and a diamond crystal ATR accessory was used. The spectra were recorded from 4000 cm^{-1} to 600 cm^{-1}.

A gravimetric method was employed to calculate the porosity (P) of the different PES membranes [117]. Membrane sheets were cut in pieces of known area and weighted. The thickness of the sheets was measured with a micrometre. The membranes were immersed in ultrapure water for 20 h, afterwards the water on the surface was carefully removed and the membranes were weighted. Porosity was therefore calculated by the following equation (Eq. 4.1):

$$P = \frac{w_w - w_d}{A \cdot \delta \cdot d_w} \qquad\qquad Eq.\,4.1$$

Where w_w is the weight of the wet membrane, w_d the weight of the dry membrane, A the area, δ the thickness of the membrane sheet and d_w the water density (0.997 g cm^{-3}).

The contact angle of PES membranes was measured using the sessile drop method with an Attension® contact angle meter (NanoScience Instruments -Phoenix, AZ, USA).

4.2.4 Recovery and matrix effects

PES membranes of 6 cm^2 (total surface area: 1.5 cm x 2 cm) were wetted with milli-Q water and spiked with 25 µL of a 2 mg L^{-1} mix standard solution in MeOH. Once dry, the membranes were rinsed in a beaker containing 2 mL of milli-Q water, left to dry again and extracted as described in Chapter 3 (section 3.2.3). The final extracts were diluted 1:5 (sample B) obtaining a theoretical final concentration of 10 µg L^{-1} (recovery=100%).

The same procedure was carried out on blank membranes (without the spike of the standard solution before the extraction). The extracts were then diluted 1:5 and spiked to obtain a final concentration of 10 µg L^{-1} (sample A). The recovery (R%) was calculated using Eq. 3.1 (Chapter 3, section 3.2.3):

The 2 mL of milli-Q water used for rinsing were analyzed after dilution with MeOH (1:1 v/v) to observe the losses in water of the analytes not sorbed or poorly retained and to calculate the mass balances.

The matrix effect was evaluated as described in Eq. 3.2 (Chapter 3, section 3.2.3).

4.2.5 PES-water partition coefficients

The partition coefficients [L Kg^{-1}] were estimated as the ratio of the analyte's equilibrium concentration in the polymer [µg Kg^{-1}] and the analyte's equilibrium concentration in water or in the water/MeOH mixture [µg L^{-1}] (Eq. 4.2).

$$K_{PESw} = \frac{C_{PES,eq}}{C_{w,eq}} \qquad\qquad Eq.\,4.2$$

4.2.5.1 Single-dose design

The evaluation of PES-water partition coefficients is usually carried out by the single-dose design [62]. When equilibrium is attained (within 5% of deviation from equilibrium) [77], the membranes are extracted and the concentration in water evaluated.

The time to reach equilibrium (t_{eq}) is directly proportional to the water volume and inversely proportional to the polymer mass. However, for high values of K_{PESw} a careful choice of the total amount of compound spiked into the selected volume of water must be considered to avoid exhaustive extractions. Considering the poor solubility in water of some of the more hydrophobic compounds and their high K_{PESw} values [113], a concentration of 10 µg L^{-1} in 2 L of milli-Q water for all the target compounds was selected, using PES membranes of 6 cm^2. This setup (S1) for PES exposure is presented in Fig. 3.1. In each beaker one PES membrane was deployed using a steel wire; a room temperature of 25°C was maintained during the experiment to obtain more accurate partition coefficients (which are temperature dependent). Dark conditions were employed to limit the degradation of the more photosensitive compounds. The solution was agitated using magnetic stir bars and F30 magnetic stirrers (Falc Instruments, Italy). The incubation time was of 14 days; aliquots of water were withdrawn at t_0, t_{3h}, t_{17h}, t_{2d}, t_{3d}, t_{6d}, t_{10d} and t_{14d} to monitor changes in the aqueous concentrations. This experimental configuration was applied to evaluate the K_{PESw} of the four types of PES membrane. Two independent replicates were performed for each type of membrane and a spiked solution without any receiving phase exposed was subject to the

same experimental conditions to assess the potential loss of the analytes during the time of exposure (e.g., degradation and/or sorption onto magnetic stir bars/glass walls).

After the deployment, the dry PES membranes were extracted as described in section 3.2.3 and analyzed after 1:100 dilution by HPLC-MS/MS [76].

4.2.5.2 Cosolvent method

The cosolvent method was employed for the first time to evaluate K_{PESw} of P01 membranes. Along with pure water, methanol was added to water obtaining mixtures with 10%, 20%, 30% and 40% of MeOH(v/v). Afterwards, the target compounds were spiked into 20 mL of each solution to achieve two different concentration levels: 10 µg L^{-1} for BPA, the three estrogens, TCS and the four UV filters, and 100 µg L^{-1} for the other analytes. Different concentrations were selected considering the expected affinity for the receiving phase and the sensitivity of the instrumental analytical method. An incubation of 21 days was performed, and 50 µL of water were withdrawn at the beginning, in the middle and at the end of the deployment. These aliquots were diluted 1:4 with water-methanol mixtures (final solution 1:1 water/methanol, v/v).

After the exposure, the dry PES membranes were extracted as described in section 3.2.3, extracts were diluted 1:20 and analyzed by HPLC-MS/MS.

Using the S1 setup previously described, it was not possible to calculate the partition coefficient for compounds with poor affinity with PES, because of their low concentration in the membranes. For this reason, the solutions with 0% of MeOH were employed as an alternative setup (S2) to obtain reliable K_{PESw} values for P01 membranes.

4.2.6 Instrumental analysis

The same chromatographic conditions reported in section 3.2.4 were applied for the elution of the 36 analytes selected. The MS condition and the MRM transitions (qualifiers and quantifiers) of the target compounds are reported in Tab. 3A of the Appendix.

4.3 Results and discussion

4.3.1 Comparison of the different materials

4.3.1.1 SEM and porosity characterization

The morphology of the H01 and P01 membranes was investigated by SEM. The obtained images of P01 (Fig. 4.1 and 4.2) showed an asymmetrical structure: a smooth surface on one side and a rough and more porous layer on the other side. The smooth surface is used in POCIS as the layer exposed to water, this side is denser and presents a controlled size of the pores compared to the opposite side. The cross-section of P01 showed an even distribution of pores with a sponge-like morphology. Regarding H01 membranes, the outer layers were symmetrical and smooth with an uneven distribution of pore dimensions compared to P01. However, the average size of the pores on the surface of the two membranes results roughly the same (ImageJ softwaimagej.nih.gov/ij/, 1997-2018).
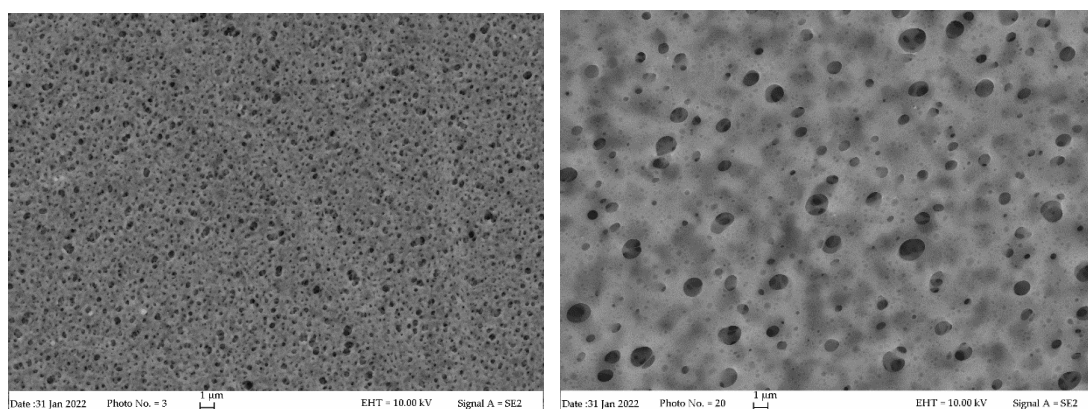

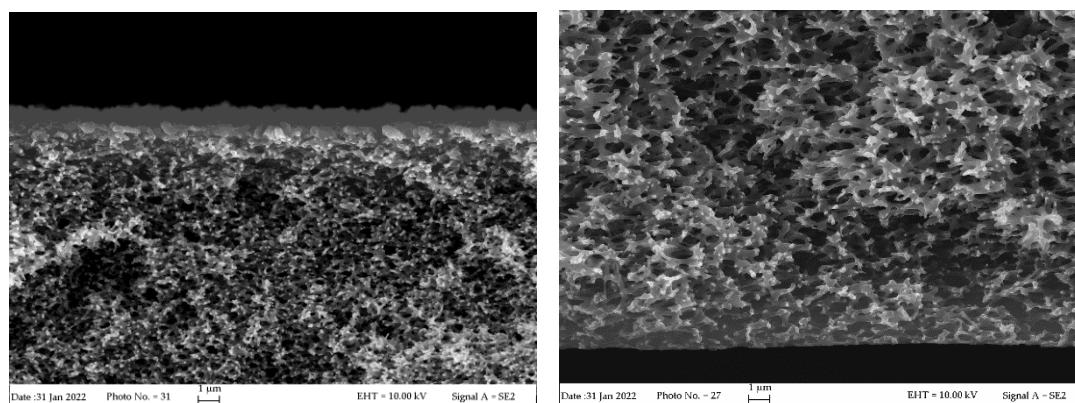Fig. 4.1 SEM images of membrane surface P01 (left) and H01 (right).

Fig. 4.2 SEM images of the cross-section of P01 (left) and H01 (right) membranes.

Based on gravimetric measurements, the porosity (free volume) estimated for the analysed membranes was: 0.82 for P01, 0.80 for H01, 0.79 for S01 and 0.78 for P045. Regarding the thickness of the membranes, H01 showed the lowest value (Tab.4.1).

Tab.4.1 Membranes parameters for porosity evaluation: area (A), thickness (δ), weight of the wet (w_w) and dry membrane (w_d) membrane, and porosity (P).

	A (cm²)	δ (μm)	w_w (mg)	w_d (mg)	P
P01	2.5	135	41.8	12.4	0.87
P045	3	145	46.4	12.4	0.78
S01	3	136	45.3	13.2	0.79
H01	2.8	115	36.6	10.8	0.80

The porosity and thickness values obtained for the H01 membrane agree with the declared information of the manufacturer (porosity of 79%, and thickness of 110 μm). No punctual information was found for the other types of membrane regarding porosity. For P01 a lower value of porosity was reported (0.7) in a previous work [19].

The hydrophilicity of PES was evaluated by the measurement of the water contact angle; a value lower than 90° was observed indicating the hydrophilic nature of the tested membrane (Fig. 4.3).

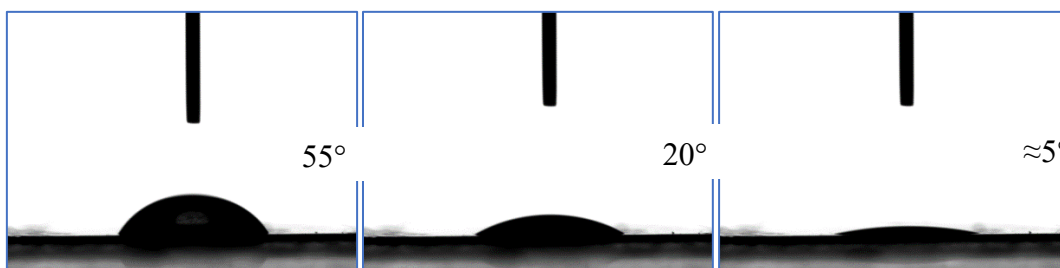Fig. 4.3: Water contact angle measurement of PES membrane (images of the water drop at t=0 s, 6 s and 12 s for P01).

4.3.1.2 Characterization (ATR)

ATR-FTIR spectra (Fig. 4.4) were acquired to obtain information regarding the functional groups on the surface of the different membranes. The peaks at 1146, 1235 and 1320 cm^{-1} can be assigned to the symmetric stretching vibrations of Ar-SO$_2$-Ar, the stretching of Ar-O-

Ar and the asymmetric stretching of Ar-SO$_2$-Ar, respectively [118]. The peak at 1297 cm^{-1} was also assigned to the stretching of S=O [118–120]. These peaks, characteristic of the chemical structure of PES, showed similar intensity for all the investigated membranes. The other main peaks were related to the aromatic moieties and alkyl chains. The signals at 3096 and 3065 cm^{-1} were produced by the aromatic C-H stretching, while those at 1576 and 1484 cm^{-1} to aromatic C=C stretching. Peaks between 900 and 675 cm^{-1} were characteristic of polynuclear aromatic C-H bending. The main difference between the spectra of the PES membranes was observed for the peak at roughly 1674 cm^{-1}. This signal is probably due to the C=O stretching of residues of tertiary amide. In fact, N,N-dimethylacetamide and N,N-dimethylformamide are the solvents usually employed for the manufacturing of PES membranes [62]. Still, this peak appears in the spectra of lab-modified PES membranes, when N,N-dimethylacetamide was employed as a solvent [121]. Furthermore, the absence of this signal in the membrane with a larger pore size (0.45 µm Pall membranes) corroborates the hypothesis of the presence of a solvent residual.
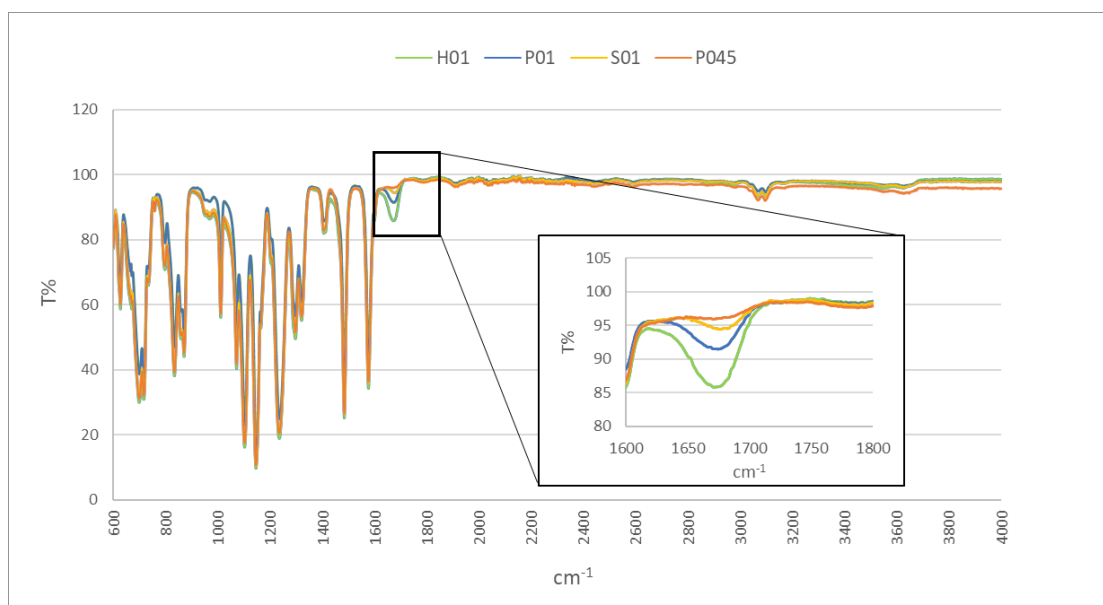

Fig. 4.4 ATR FT-IR spectra obtained for P01, S01, H01 and P045 membranes.

To conclude, the information obtained from the infrared spectroscopy did not show significant macro differences in the surface chemistry of the membranes.

4.3.2 Recovery and matrix effects

The accuracy of the method is assessed through the evaluation of the recovery and matrix effect. The evaluation of the recoveries and the loss in water can be useful also to assess preliminary the affinity of the target compounds for the sorptive material under investigation. Recoveries (Fig. 4.5 e Tab. 8A) were mostly under 50% for ACS, TAU, DMNZ, PFOA, FRSM, MTF, CMQ, OD-PABA and NCT; however, these poor R% were mostly due to the low affinity of the target compounds for the membranes or to poor stability of DMNZ that showed a problem of degradation. In fact, excluding PFOA, OD-PABA and FRSM, these analytes were quantified in the rinsing water and the mass balances (sum of the amounts of analyte in the water and in the extract compared to the spiked amount) were satisfactory (86%-141%).

Considering the membranes with the same declared pore size, the greatest differences were observed for S01. Lower R% were obtained using S01 membranes for ATN, SLBT, TRBT, OD-PABA and FXP. These analytes (excluding OD-PABA) were quantified in the rinsing water (between 33-63%). Only ACS and CAFF showed higher recoveries for S01 (71% and 90% respectively). The results of S01 obtained for OMT were excluded due to instrumental problems during the analysis. On the other hand, R% of P01 and H01 agree, although a higher loss was observed in the rinsing water of H01 for PFOA, 2,4-D and SCL. Also considering P01 and P045, lower differences were observed compared to S01. ACS, SCL, PFOA and 2,4-D showed higher R% for P01, indeed higher loss in water were observed for P045 (similar behaviour of H01).
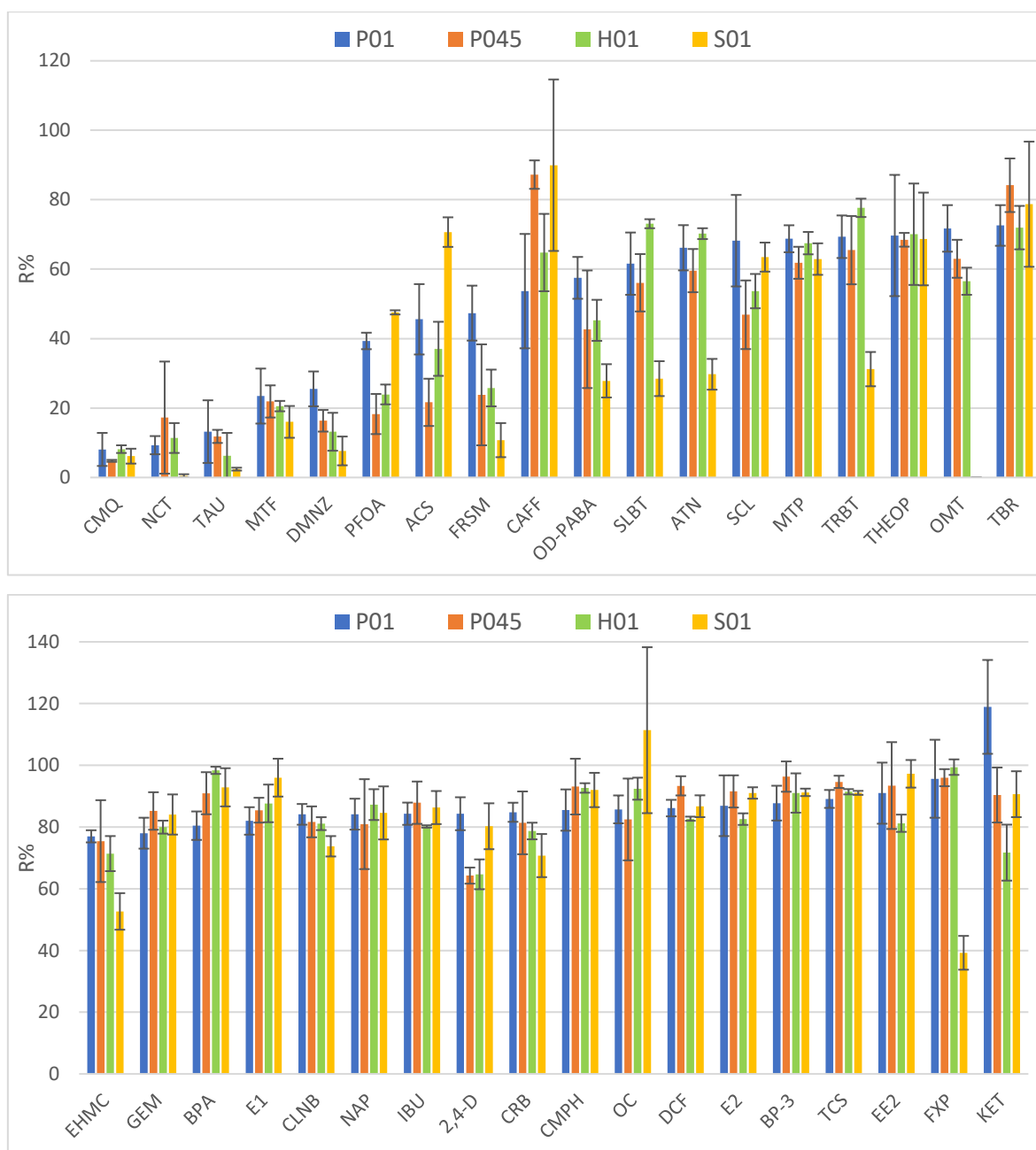
Fig. 4.5 Recoveries % (± st.dev.) obtained for the 36 target compounds.

Concerning ME% (Fig. 4.6 and Tab. 9A), a soft (80% < ME% < 120%) or moderate (50% < ME% < 150%) matrix effect was observed for most compounds at low dilutions (1:5). Still, a strong signal suppression (ME < 50%) was observed in H01 and S01 extracts for some of the more hydrophilic compounds. As reported in the Chapter 3 (section 3.3.3), also OC showed ion suppression (ME < 50%) for both P01 and S01.

Fig. 4.6 Matrix effects % obtained for the 36 target compounds. The error bars represent the confidence intervals ($\alpha = 0.01$, n=1)

4.3.3 Membrane sorption comparison

The stability of the analytes under experimental conditions was tested as described in section 4.2.5.1. Four target compounds showed a loss higher than 30% after 14 days in water: DMNZ, HCTZ, OD-PABA and EHMC. Among them, only DMNZ undergoes a complete degradation and was discarded from the list of the 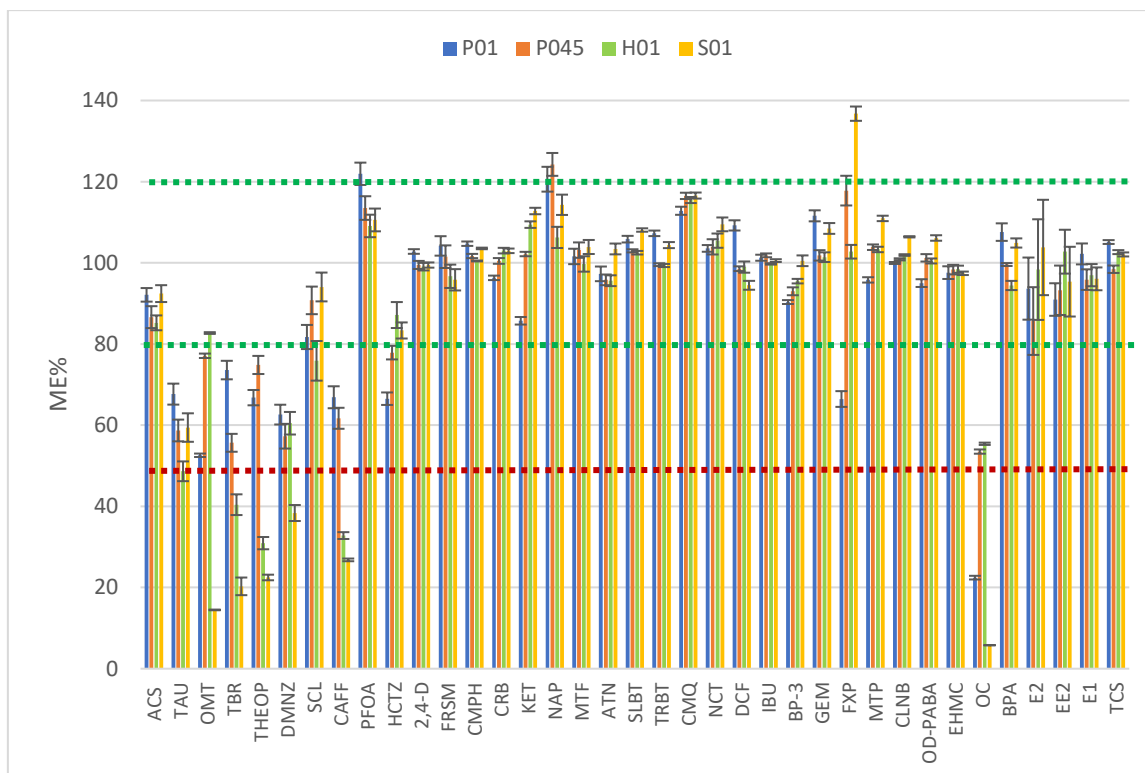studied compounds; the other three compound showed a loss of 42%, 62% and 53% (HCTZ, OD-PABA and EHMC, respectively). Satisfactory mass balance (> 70%) were obtained for all the target compounds, excluding those that showed degradation in the control: HCTZ, OD-PABA and EHMC (only for H01 and P045). Details are reported in Appendix Tab. 10A.

Using the S1 setup, the concentration in water was monitored to verify the achievement of equilibrium (Fig. 4.7). The partition coefficients could be evaluated only for 16 analytes (Fig. 4.8 e Tab. 11A) due to negligible accumulation onto the membranes for the other compounds (< 1%). The replicates for each membrane were performed independently; good repeatability was mostly obtained (relative standard deviation RSD% < 21%), with the lowest values observed using H01 membranes.
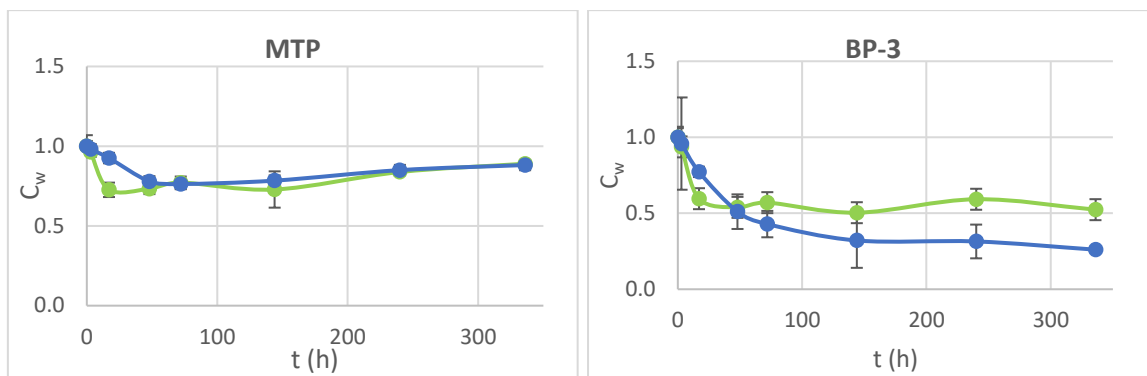
Fig. 4.7 Water concentration curves of MTP and BP-3 for H01 (green) and P01 (blue) membranes deployment. These curves were obtained to assess the achievement of the equilibrium between water and PES membranes.
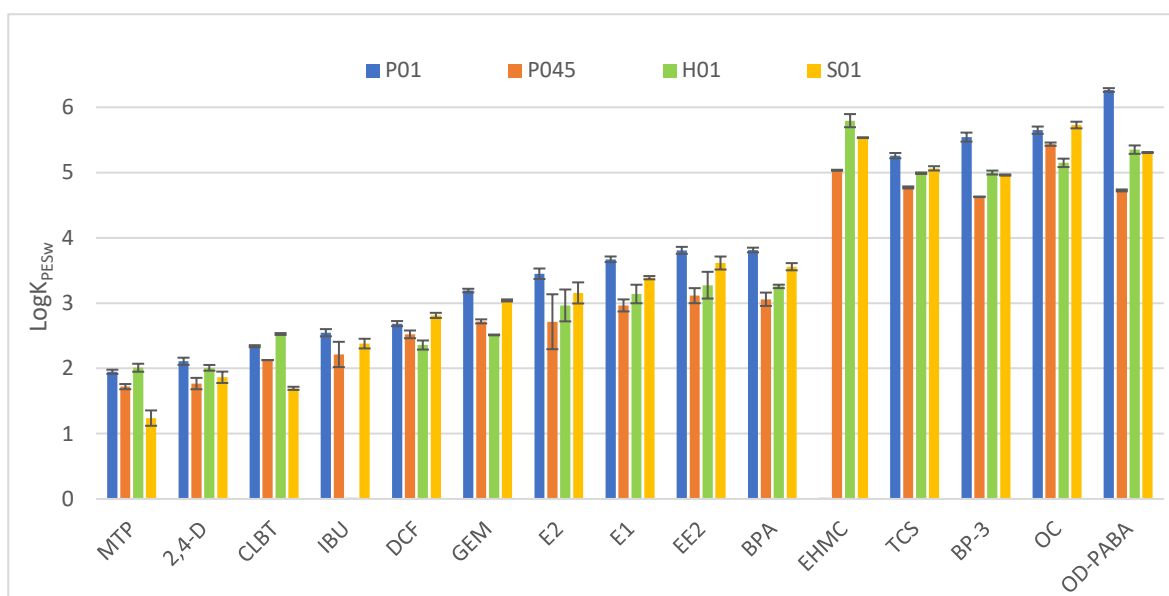
Fig. 4.8 LogK$_{PESw}$ obtained using different PES membranes: P01, P045, H01 and S01. The K$_{PESw}$ results of EHMC for P01 and IBU for H01 were not reported due to the concentration under the limit of quantification in water and in the membrane, respectively. The error bars represent the standard deviation.

HCTZ and FRSM were present in all the membrane extracts but under the limit of quantitation. SLBT was quantified only in P01, while its concentration in the other extracts was under the LOQ. TRBT was quantified both in P01 and H01 membranes. The sorption ability of the membrane follows the order P01 > S01 > H01 > P045. Considering P01 and H01 membranes, differences in the values of LogK$_{PESw}$ ≥ 0.5 were observed for CRB, BP-3, GEM, OD-PABA, OC. For P01 and S01 membranes, only BP-3, CLBT and OD-PABA showed significant differences in LogK$_{PESw}$, of 0.58, 0.71 and 0.96, respectively. The differences observed for CLBT and OD-PABA could be attributed to the experimental

variability, in particular for OD-PABA, which showed degradation due to its low stability under the experimental conditions.

In general, the differences in sorption could be ascribed to the different surface area of H01 membranes, as observed by SEM images (Fig. 4.1). Furthermore, H01 membranes presented the more intense peak at 1674 cm^{-1} associated with the presence of residues of tertiary amide that could hinder the access to some of the sorption site of the membranes.

Considering P045 and P01, a significant difference was observed for all the 16 analytes (higher than 0.5 Log units), suggesting the influence of pore size and of the surface area in sorption onto PES.

As the EHMC concentration in water was lower than the LOQ after the 14-day deployment of Pall membranes, the sorption was compared by observing the amount of analyte accumulated in the membrane; the amount accumulated was in the order P01 > S01 > H01 > P045, in the same way as for the other compounds.

4.3.4 Partition coefficients

To assess K_{PESw} of the Pall membrane of 0.1 pore size – the most employed in POCIS applications – two methods were used as reported in <u>section 4.2.5</u>: the single-dose design and the cosolvent method.

4.3.4.1 Single-dose results

Regarding the results obtained by the single-dose design, accumulation lower than 1% was observed for the more polar compounds when a large volume of water (2 L) spiked at 10 µg L^{-1} was employed. In order to obtain K_{PESw} for a greater number of compounds, the S2 setup was employed: a smaller volume of water (20 mL) and a concentration of 100 µg L^{-1} for the polar and mid-polar analytes. The concentration of UV filters, BPA, estrogens and TCS was maintained at 10 µg L^{-1}. Using these conditions, a longer exposure of 21 days was also employed. The mass balances and the stability in water are reported in Tab. 12A.

As in the first setup (S1), some of the more polar compounds, ACS, TAU, OMT, SCL, CMQ, MTF, ATN and SLBT, accumulated < 1%, while PFOA, 2,4-D, and TRBT in the range 2%-5%. Nonetheless, the evaluation of K_{PESw} was possible by S2 setup for more compounds compared to the S1 setup (22 vs. 18, 10 values with both methods).

The highest difference between the LogK_{PESw} obtained using the S1 and S2 setup was observed for NAP, roughly 1 Log unit. GEM, IBU, DCF and CRB also showed quite high

differences (0.42-0.66), however considering the standard error associated to the S2 setup, this difference can be considered negligible. On the contrary, the target compounds SLBT, TRBT, 2,4-D, MTPR and CLBT showed a difference under or equal to 0.35. Excluding 2,4-D, higher values of K_{PESw} were estimated using the S2 method. This is probably due to the longer exposure in S2 and the partial non achievement of the equilibrium in S1 (apparent equilibrium due to slow accumulation) [104].

Tab.4.2 K_{PESw} and $LogK_{PESw}$ (± standard error) obtained for P01 membranes with two different setups (S1 and S2).

	S1 setup		S2 setup	
	K_{PESw} (L Kg^{-1})	$LogK_{PESw}$ (L Kg^{-1})	K_{PESw} (L Kg^{-1})	$LogK_{PESw}$ (L Kg^{-1})
ACS	nd	nd	0.7 ± 0.1	-0.1 ± 0.2
THEOP	nd	nd	159 ± 10	2.20 ± 0.06
CAFF	nd	nd	181 ± 5	2.26 ± 0.03
PFOA	nd	nd	29 ± 1	1.46 ± 0.03
SCL	nd	nd	3 ± 1	0.5 ± 0.2
HCTZ	nd	nd	196 ± 13	2.3 ± 0.1
2,4-D	130 ± 8	2.11 ± 0.05	73 ± 2	1.86 ± 0.02
FRSM	nd	nd	147 ± 15	2.2 ± 0.1
CMPH	nd	nd	235 ± 15	2.37 ± 0.07
CRB	194 ± 8	2.29 ± 0.04	504 ± 2	2.703 ± 0.003
KET	nd	nd	1101 ± 274	3.04 ± 0.25
NAP	445 ± 30	2.2 ± 0.4	1836 ± 805	3.3 ± 0.4
MTF	nd	nd	9.1 ± 0.2	0.96 ± 0.02
ATN	nd	nd	12.4 ± 0.9	1.09 ± 0.07
SLBT	19 ± 1	1.28 ± 0.05	12.9 ± 0.6	1.11 ± 0.05
TRBT	29 ± 3	1.47 ± 0.11	31 ± 0.9	1.49 ± 0.03
NCT	nd	nd	6.1 ± 0.8	0.8 ± 0.1
DCF	558 ± 29	2.69 ± 0.04	1654 ± 928	3.2 ± 0.6
IBU	582 ± 55	2.55 ± 0.06	1484 ± 1602	3.2 ± 1.1
BP-3	349542 ± 23584	5.54 ± 0.07	nd	nd
GEM	1996 ± 73	3.19 ± 0.03	7173 ± 5511	3.9 ± 0.8
MTPR	89 ± 3	1.95 ± 0.03	134 ± 2	2.1 ± 0.01
OD-PABA	1912037 ± 62953	6.26 ± 0.03	nd	nd
CLNB	219 ± 4	2.34 ± 0.02	284 ± 19	2.5 ± 0.1
OC	449783 ± 22841	5.65 ± 0.06	nd	nd
BPA	6534 ± 231	3.81 ± 0.04	nd	nd
E2	2826 ± 225	3.45 ± 0.08	nd	nd
EE2	6473 ± 340	3.81 ± 0.05	nd	nd
E1	4713 ± 201	3.67 ± 0.04	nd	nd
TCS	218262 ± 5392	5.26 ± 0.04	nd	nd

The LogK$_{PESw}$ obtained were then correlated with the physico-chemical properties of the target compounds. To explore the nature of the data, the PCA was employed: 25 analytes were used as objects (EHMC was excluded because the K$_{PESw}$ was not calculated) and 13 physico-chemical properties as the variables describing the system. The data were subject to autoscaling prior to perform the PCA. The first two Principal Components (PCs) explain 51.3% of the total variance, in particular PC1 explains 32.4% of the variance. The loading plot shows a correlation between the variables that mainly describe hydrophobicity (e.g., Polarizability, Apolar Surface Area and the octanol-water partition coefficients at pH 5.5), and their anticorrelation along PC1 with the number of H-bonding donor and acceptor groups (Hbd and Hba) and the Total Polar Surface Area (TPSA).

From the prospective of LogK$_{PESw}$, the PC1 presents a gradient of values as shown in Fig. 4.9 by the colour scale. Thus, the main driving force of sorption seems to be hydrophobicity and hydrophobic interactions.
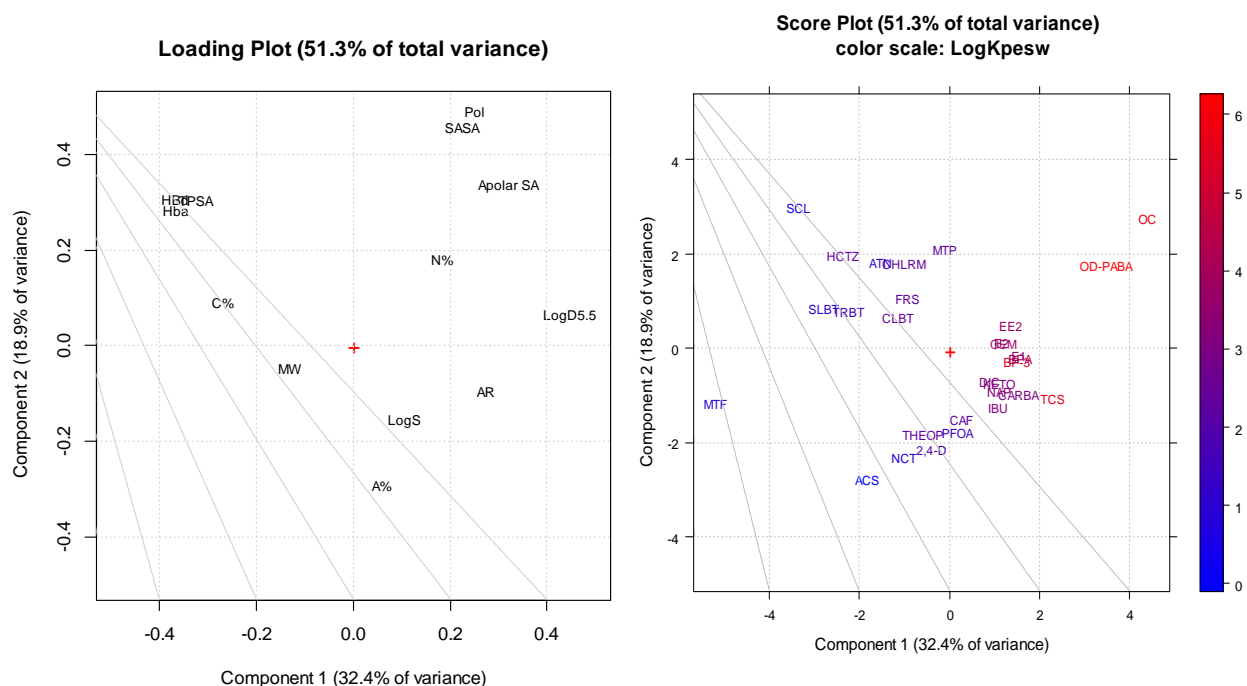
Fig. 4.9 PCA results: loading plot (left) and score plot (right). The variables considered are: LogD (pH 5.5) (LogD5.5), Molecular Weight (MW), Number of H-bonding donor groups (Hbd), Number of H-bonding acceptor groups (Hba), Topological Polar Surface Area (TPSA), Number of Aromatic Rings (AR), Polarizability (Pol), Solvent Accessible Surface Area (SASA), Apolar Surface Area (Apolar SA), Solubility (LogS), percentage of neutral analyte pH = 5.5 (N%), percentage of anionic analyte pH = 5.5 (A%), percentage of cationic analyte pH = 5.5 (C%). The colour vector in the score plot presents the values of LogK$_{PESw}$ associated to the objects.

This observation was then investigated comparing the relationship between the LogD (pH = 5.5) and the $LogK_{PESw}$, obtaining an acceptable linear correlation ($R^2 = 0.728$). This correlation was then compared with the correlation between the scores of PC1 and $LogK_{PESw}$. No improvements were observed considering the correlation coefficients ($R^2 = 0.725$) but a slightly different equation (Fig. 4.10).
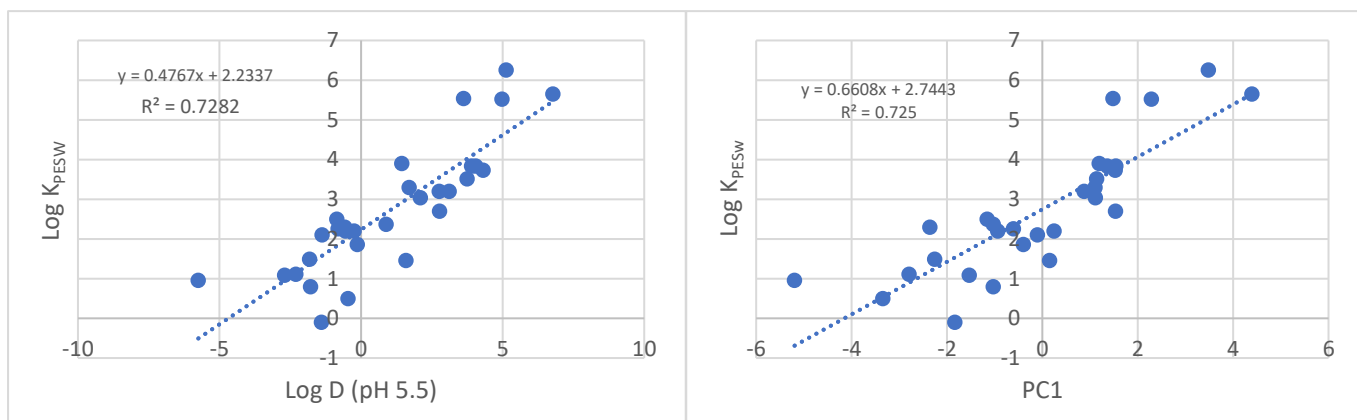
Fig. 4.10 Linear correlation between the K_{PESw} obtained for 25 target compounds and the octanol-water partition coefficients at pH 5.5 (left) or PC1 (right).

In order to better interpret the influence of the variables, the Varimax rotation was performed. The results of the loadings and the scores of Varimax highlighted the influence of both the LogD and the number of aromatic rings on the affinity for PES. In particular, the influence of these variables on the partition coefficients is described by Factor 1. Whereas Factor 2 permitted to discriminate those objects with low affinity for PES mainly due to their affinity for water (due to the presence of aromatic donor/acceptor groups).

Fig. 4.11 Varimax rotation results: loading plot (left) and score plot (right).

4.3.4.2 Cosolvent method

In this work the cosolvent method was employed for the first time to evaluate K_{PESw}. This design is usually employed for hydrophobic compounds to evaluate polymer-water partition coefficients in SR. Different percentages of an organic solvent are added to the aqueous phase in order to increase the compounds' solubility in water or to avoid their sorption on the walls of 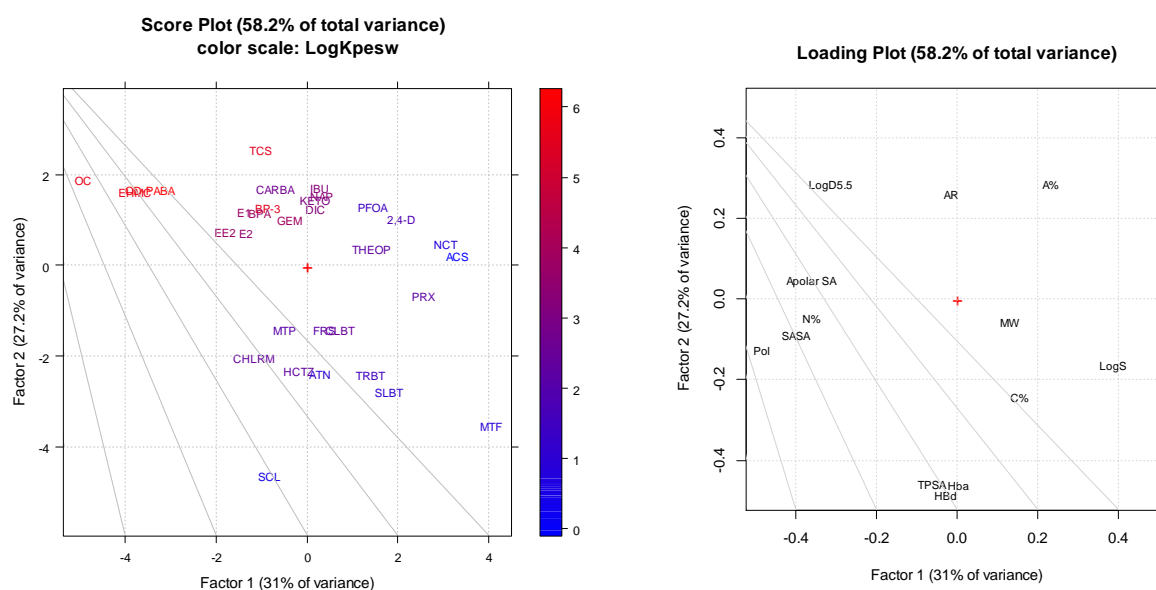the container and on the dissolved organic matter [89]. As a consequence, the higher the organic fraction present in the mixture, the lower the partition-coefficients obtained. Still, the highest equilibrium concentrations in water permit a more accurate quantification. However, the analytes investigated in this Chapter cover a wide range of $LogK_{ow}$.

Acceptable average mass balances were observed for the target compounds for the cosolvent experiment (77%-121%); the only exception was KET, with an averaged mass balance of 64%, which can be explained by the 40% of loss in the blank beaker (stability test). The 4 UV filters and TCS were not considered because of their exhaustive sorption onto PES due to the small volume employed and their high sorption affinity for the polymer, even in the presence of MeOH.

The K_{PESw} obtained at different % of MeOH in the mixture were plotted and linear correlation was observed for 11 compounds (Fig. 4.12). The analytes showing this linear

profile were E2, EE2, E1, BPA, THEOP, PFOA, HCTZ, CRB, CLBT, MTFR, CMPH and MTPR, which presented regression coefficients ranging from 0.817 to 0.998. In particular, the group including 2,4-D, FRSM, DCF, KET, IBU, GEM and NAP showed a linear decrease in K_{PESw} with increasing % MeOH only between 20% - 40% MeOH. On the contrary, MTF presented the opposite behavior: the K_{PESw} values increased by increasing the % of MeOH. This compound is the most polar of the target group (LogD = - 5.59) and lowering the polarity of water by adding crescent molar fractions of MeOH could promote the sorption onto the PES membrane.
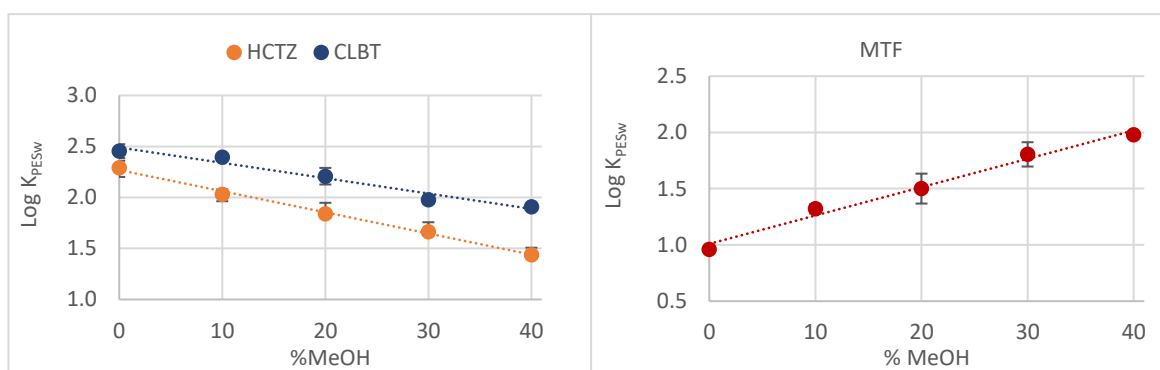
Fig. 4.12 Examples of linear regression of $LogK_{PESw}$ and the % of MeOH added in the water solutions of the analytes.

Finally, a group of three analytes did not show significant differences as function of the MeOH molar fraction in the mixture (Fig. 4.13). This smaller group included ATL, SLBT and TRBT, which presented random changes in $LogK_{PESw}$ by varying the % of MeOH in the mixture, lower than 0.2 Log unit. TRBT showed a slight increase with a good correlation, but the slope of the curve resulted negligible.
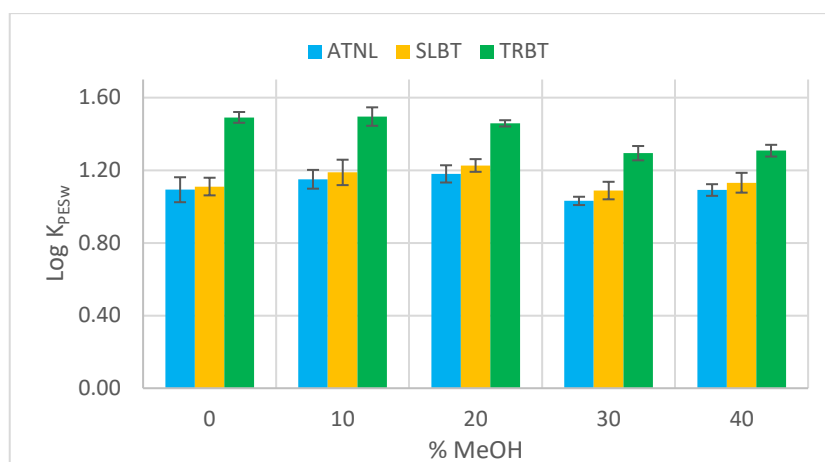
Fig. 4.13 Influence of the % of MeOH in the mixture on the sorption of ATNL, SLBT and TRBT. The values of LogK$_{PESw}$ were not influenced by the presence of an organic solvent.

4.3.5 Comparison to the literature

Three previous works have attempted to develop Poly-Parameter Linear Free Energy Relationships (pp-LFER) for K$_{PESw}$ fitting or prediction [74,103,104]. In these models the Abraham's descriptors were employed [122]: excess molar refractivity (describing part of Van der Waals force), the polarizability, the hydrogen bond acidity/donating capacity, the hydrogen bond basicity/accepting capacity and the McGowan molar volume (molecule's size). The first two models developed presented poor fit [74,104], while the latest one presented a good description of the data [103]. Improvements in fitting were obtained using a larger dataset (125 compounds vs. 21 and 90). Nevertheless, a moderate predictability was showed and for this reason the model was suggested only as screening tool.

One of the reasons for the not satisfactory results can be ascribed to the weak accuracy of some of the K$_{PESw}$ employed. In fact, several produced partition coefficients were only apparent because the achievement of the equilibrium was not verified, or in the worst case the equilibrium has clearly not been reached.

Based on the PCA results (Fig. 4.9 section 4.3.4.1), several K$_{PESw}$ data were correlated to their distribution coefficient. 77 K$_{PESw}$ present in the literature and obtained using PES sheets of 0.1 µm pore size both in single-phase [61,97,103,104] and dual-phase [59] configurations were considered together with the data presented in this work. The aim was to observe the correlations between K$_{PESw}$ values and the LogD of the chemicals (at the pH of the experimental conditions). The resulting linear regression (Fig. 4.14) showed a moderate correlation (R^2 = 0.59) and a similar relationship to the one reported above (Fig. 4.10).
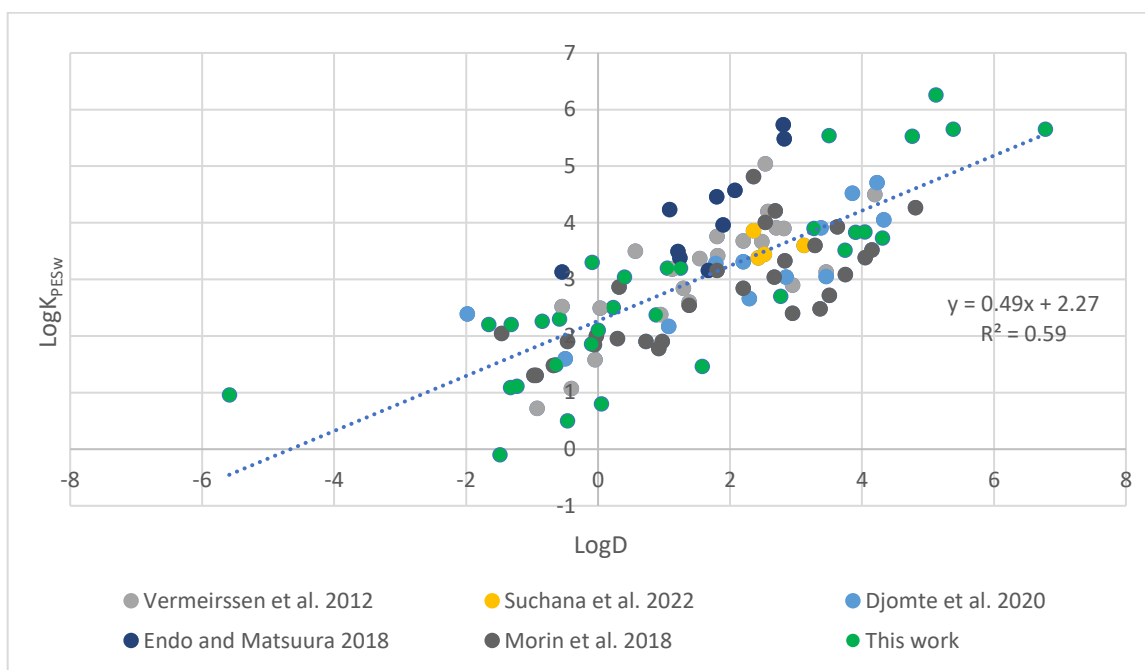
Fig. 4.14 Linear regression obtained plotting 77 $LogK_{PESw}$ present in the literature and the P01 value obtained in this work (green dots) against the LogD of the compound (pH 7 and pH 5.5, respectively). A total of 91 compounds were considered.

In addition, the K_{PESw} herein obtained were compared to those reported in previous studies, for the same compounds, for different PES membranes. The literature values were employed even when the equilibrium was not verified [59,61,108,111,112]. In Fig. 4.15 the results of this work were plotted against K_{PESw} found in the literature. The K_{PESw} were mainly included between the dotted lines representing a difference of 0.5 Log units. Most of the values outside this range correspond to the data obtained by Kaserzon et al. (2014) with membranes of larger pore size (0.45 µm and 0.2 µm) [111]. Considering the partition coefficients obtained using P045 (possibility to compare only HCTZ, 2,4-D and TCS), only TCS showed differences lower than 0.5 Log units while the gap for HCTZ and 2,4-D was even higher.
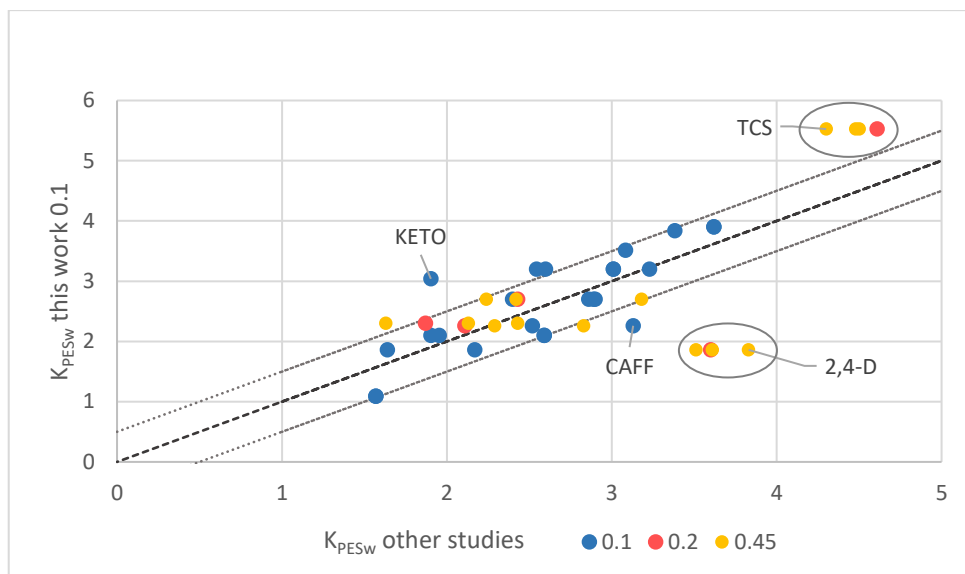
Fig. 4.15 Graph of the LogK$_{PESw}$ reported in literature for PES membranes (x-axis) and those obtained in this work for P01 membranes (y-axis) considering the compounds in common. The yellow and the pink circles highlight PES membranes of 0.45 µm and 0.2 µm pore size. The dotted lines marked the range where both compared values differ by less than a factor of 0.5.

Prieto et al. (2012) reported K$_{PESw}$ for several compounds using PES tubes for sorptive microextraction [63]. These partition coefficients were estimated in the presence of 20% of MeOH and expressed in [L L^{-1}]. Therefore, the K$_{PESw}$ of the analytes in common (E2, CAFF, TCS, OD-PABA and OC) were analysed. In particular, the partition coefficients of CAFF and E2 were compared considering the values obtained using the cosolvent method in the presence of 20% MeOH. The results differ by 0.1 Log units for CAFF and 0.53 for E2. On the other hand, the results of OD-PABA, OC and TCS could be compared only with those obtained using the S1 setup, in the absence of MeOH. As expected, the values reported in the present work were higher than 1.4 Log units. As mentioned before, in the presence of an organic solvent the partition coefficients between the polymer and the mixture were lower than in the presence of the sole water.

4.4 Conclusions

The affinity for PES membranes of 36 target compounds characterized by a broad range of physico-chemical properties was investigated. The PES-water partition coefficients of the analytes were assessed using two different methods: the single-dose design and the cosolvent method. Both methodologies presented different advantages and could be useful to limit some of the problems related to the evaluation of partition coefficients. The impact of PES

manufacturing on analyte's sorption was also studied using membranes of the same declared pore size (0.1 µm), purchased from three different producers. The results obtained showed significant differences in sorption, underlining the importance of evaluating the affinity of the selected PES protective membrane in dual-phase passive samplers to avoid inaccuracy in the estimation of pollutant's water concentrations. The influence of pore size on the accumulation was also analyzed comparing K_{PESw} of membranes with pores of 0.1 and 0.45 µm, showing a greater capacity of PES with the lowest pore dimension.

Considering the results obtained for the most employed PES membrane in passive sampling (P01), a correlation between the K_{PESw} and the physico-chemical properties of the analytes was evaluated using the Principal Component Analysis. However, the results indicated hydrophobicity as the main driving force of compounds' affinity for PES. Nonetheless, considering a reduced range of polarities, some exception related to the chemical structure can be highlighted as stated in Chapter 3 [113].

Chapter 5. PES membranes in dual-phase passive samplers: impact of the environmental conditions on field deployments

5.1 Introduction

The sorption of target contaminants onto the protective PES membranes in dual-phase passive samplers, such as POCIS, could complicate the uptake process and affect the evaluation of the TWA concentrations, in particular, when the extent of a lag phase is comparable to the deployment time or when the analytes are completely retained by the diffusive layer.

To manage these issues different strategies are employed. The simplest one is to assess the sorption of the target compounds on the protective layer during the sampler development [22,123–125]. Otherwise, after the deployment of the passive samplers the two phases (membrane and sorbent) are extracted separately and the evaluation is carried out independently, considering only the compartment with the highest sorption, when possible [61,126,127]. Other works suggest a separate extraction followed by a combined assessment of the uptake [60,97] or employ a combined extraction and assessment [23,128]. Considering the last two options, some drawbacks need to be highlighted. On the one hand, when combining the results of the two phases a gain in sensitivity is obtained. On the other hand, changes in the environmental conditions may influence the accumulation and redistribution between the phases, affecting the overall sampling rates. Furthermore, deployments in complex media and the presence of fouling can affect the matrix effects and the recoveries of the method [35,112]. It is worth noticing that both matrix effects and recoveries are often not considered/evaluated but have significative implications considering combined extractions.

In this Chapter, the impact of different environmental conditions on the sorption in POCIS devices was investigated considering the separate extraction of the PES membrane and the HLB sorbent. The samplers were deployed in Genoa harbour in three different locations and different seasons, in Santa Margherita Ligure marine waters in two different offshore sites and in Antarctica, both in coastal waters and in the effluent of the WWTP of the Italian Research Station (Mario Zucchelli).

5.2 Materials and Methods

5.2.1 Chemicals (standards and reagents)

Standards of benzophenone-3 (BP-3), bisphenol-A (BPA), estrone (E1), β-estradiol (E2), 17α-ethinyl estradiol (EE2), ethyl hexyl methoxy cinnamate (EHMC), octyl dimethyl p-aminobenzoate (OD-PABA), octocrylene (OC) and triclosan (TCS) were obtained from Sigma-Aldrich (Milan, Italy). All standards were of high purity grade (> 98%).

HPLC grade methanol (MeOH), dichloromethane (DCM), isopropanol (IPA), acetonitrile (ACN) and acetic acid were obtained from Merck (Darmstadt, Germany). Water was purified by a Milli-Q system (Millipore, Watford, Hertfordshire, UK).

5.2.2 Deployments

5.2.2.1 Genoa harbor

Pre-assembled commercial POCIS purchased from E&H services (Prague, Czech Republic) were exposed in Genoa Harbor during summer 2021 and autumn 2021 for approximately 3 weeks. In addition, in autumn PES membranes purchased from Pall Italia (Buccinasco, Italy) were exposed as single-phase passive samplers in parallel to the POCIS deployment.

POCIS had a surface area of 45.8 cm^2 (two membranes per POCIS with only one membrane side exposed) and 220 mg of HLB sorbent. In particular, the PES membranes used in these devices were from Hangzhou Anow Microfiltration Co., Ltd (Hangzhou, China). This type of membrane presented an average pore size of 0.1 μm and a 115 μm thickness (section 4.2.2). On the contrary, membranes obtained from Pall Italia had 0.1 μm of pore size and a 135 μm thickness. Single-phase PES had a total surface area of 45.8 cm^2 considering only one disk and both sides exposed.

The summer deployment was performed in duplicate at two different sites: one next to the Neptune galleon (44.4104, 8.92491 – samples G1 and G2) and the other one close to the Biosphere of Genoa Aquarium (44.4097, 8.92548 – samples B1 and B2). These deployments were performed from the 26th of July to the 16th of August 2021 and from the 4th to the 24th of August 2021, respectively. In autumn (16th November – 6th December 2021), the POCIS exposure was performed at the *Isola delle Chiatte* (44.40994, 8.92215 – samples C1 and

C2). Meanwhile, PES membranes were deployed as single-phase passive samplers (44.40994, 8.92215 – samples S1 and S2). A stainless-steel cage with a zinc anode (corrosion inhibitor) was employed to protect the devices.
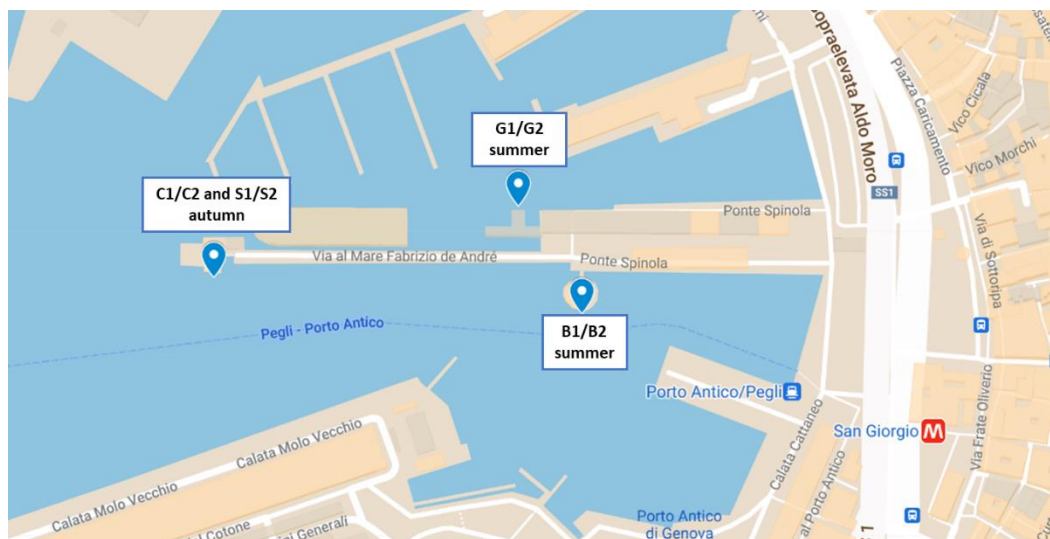
Fig. 5.1 Maps of Genoa Harbour presenting the three sampling sites: Galleon (G), Biosphere (B) and *Isola delle Chiatte* (C and S) and the corresponding samples.

5.2.2.2 S. Margherita Ligure

Pre-assembled commercial POCIS purchased from E&H services (Prague, Czech Republic) were exposed at two offshore areas in Santa Margherita Ligure (Genoa, Italy). The deployment was performed using a stainless-steel cage with a zinc anode in correspondence of two buoys M1 (44.18875, 9.13400, 3 m) and M2 (44.17800, 9.13768, 3 m). The M1 buoy was closer to the coast and the depth was around 50.2 m, while M2 buoy was further off the coast with a depth of 82.5 m. Different samplings were performed at the M1 buoy: a first sampling of three weeks from the 20th of July 2021 to the 12th of August 2021 (3 POCIS exposed) and a second one of two weeks from the 12th of August 2021 to the 26th of August 2021 (2 POCIS exposed). In parallel, to assess the linearity of the uptake, a single POCIS was deployed for five weeks (the duplicate was not performed due to the loss of the membrane, destroyed by the waves). The sampling carried out at M2 buoy consisted in a 3-week exposure of a pair of POCIS devices from the 20th of July to the 12th of August 2021.

5.2.2.3 Antarctica

As part of MATISSE project (Emerging contaminants in the Ross Sea: occurrence, sources and ecotoxicological risks, PNRA18_00216 - B2), during the 37th Italian Expedition in Antarctica, several commercial POCIS from E&H services (Prague, Czech Republic) were employed for a first monitoring of ECs release from the WWTP of Mario Zucchelli Station (MZS) and the surrounding marine waters (Road Bay).

MZS is a seasonal Italian research base in Antarctica, operational during the austral summer, from October to February. It is located on the coast of Terra Nova Bay in the Ross Sea (74°42' S and 164°07' E, altitude 15 m), where the largest marine protected area in the world was created in 2017.

For WWTP effluent assessment, the water flow was deviated in a small stainless-steel tank (Fig. 5.2A) where the POCIS were exposed (parallel to the water flux). Two POCIS protected by stainless-steel grids were deployed for two weeks, then replaced for a total of six consecutive sampling periods. Spot sampling of water was performed at the beginning, in the middle and at the end of each POCIS deployment.

Two sampling of three weeks were carried out in Road Bay, using a stainless-steel cage containing two POCIS (Fig. 5.2B). The samplings were performed in the presence and in the absence of the ice pack: from the 4th to the 25th of November 2021 (first sampling) and from the 15th of January to the 2nd of February 2022 (second sampling). The deployment was performed 136 m away from the WWTP discharge point at 3 m (November) or 5 m (January) of depth (74.69607 S, 164.12037 E, seabed: 15 m). Spot sampling of water was performed at the beginning, in the middle and at the end of each POCIS deployment. The data of the sorbent extracts and of spot sampling are reported elsewhere in details [129].
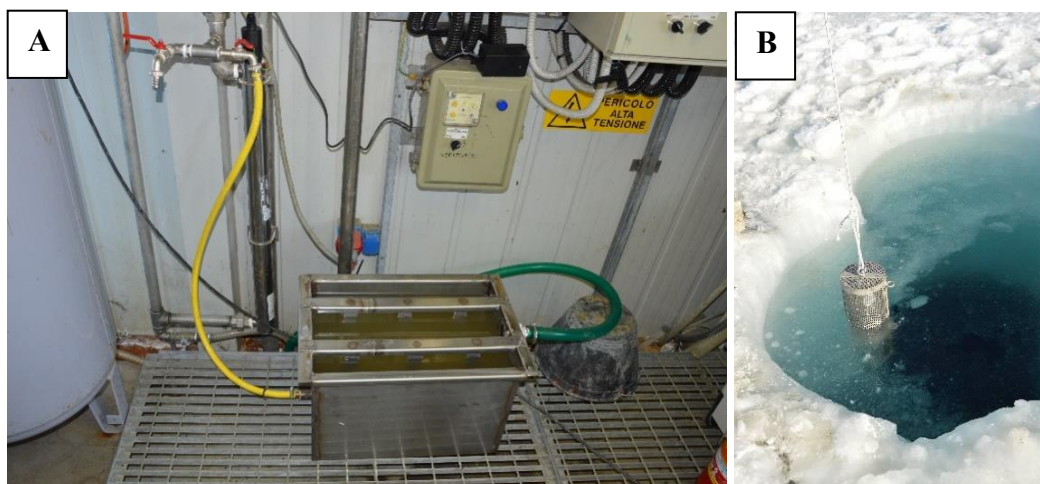
Fig. 5.2 (A) Representation of POCIS deployment in WWTP effluent and (B) Road Bay deployment during November 2021.

5.2.3 Sample processing

After the exposure, POCIS were disassembled and the HLB phase was transferred into empty SPE cartridges using ultrapure water. The sorbent was then extracted using an optimized procedure consisting in a sequential extraction with 20 mL of MeOH followed by 5 mL of a 80:20 (v/v) DCM:IPA solution [76]. Afterwards, PES membranes were carefully cleaned using a spatula to mechanically remove the biofouling and washed with abundant ultrapure water to further remove fouling, particulate matter and salts. The same cleaning procedure was employed for single-phase PES membranes. The PES membranes were then transferred into 22-mL vials and extracted as described in Chapter 3 (section 3.2.3) with MeOH. The final extracts were analyzed by HPLC-MS/MS after dilution (details reported in Chapter 3 section 3.2.4). In particular, the extracts of PES exposed in seawater and in Genoa harbor were diluted 10 times, while the extract of the WWTP effluent of Mario Zucchelli station 400 times.

5.3 Result and discussion

5.3.1 Genoa harbor deployment

The harbor waters are characterized by high fouling (especially during summer) and low turbulence. This environment promoted the growth of biofouling onto PES membranes. Algae, calcareous tubeworms and small crustaceans were observed on the samples when retrieved in August, while less fouling was present in December.

The matrix effect was evaluated for each extract; soft or moderate ME% was mainly observed. A clear difference was assessed considering the two different seasons (Fig. 5.3). In fact, samples at the same dilution (1:10) presented higher suppression in summer. A high ME% was obtained for OC, BPA and E2 for extracts of the summer campaign. However, OC showed ME% < 50% for both seasons, confirming the drawback stated in Chapter 3.
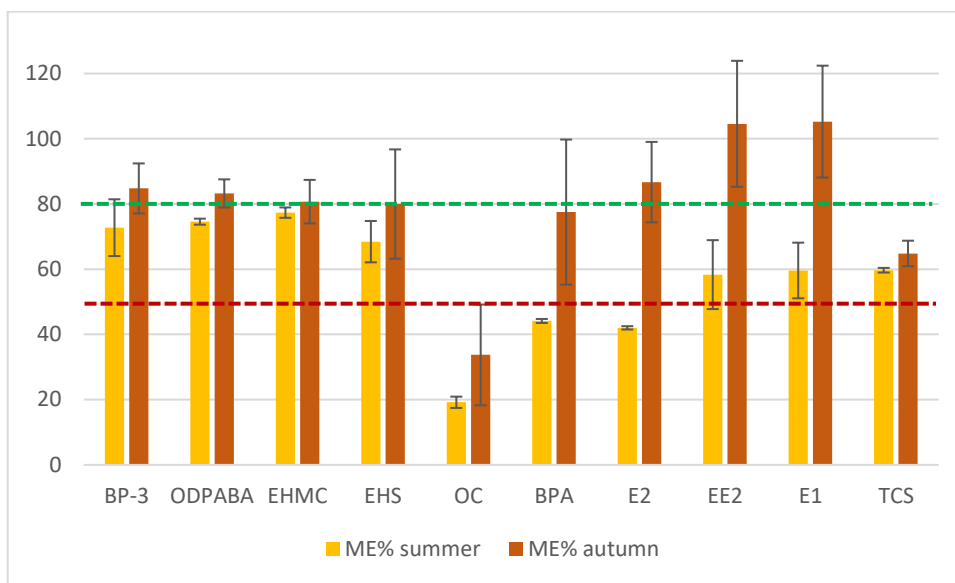
Fig. 5.3 Averaged ME% of the extracts diluted 1:10 obtained during summer exposure (yellow bars – Galleon and Biosphere) and autumn deployment (orange bars – *Isola delle Chiatte*).

Sample duplicates presented quite good RSD% (0.7-28%), excluding those of the Biosphere site (> 30%).

Since PES membranes had the same exposed surface area (45.8 cm^2), the presence of contaminants and their different concentrations were compared in Tab. 5.1 considering the total amount of compounds accumulated in the sample (ng/PES).

TCS, BP-3 and OC were detected in all samples and quantified in most of them. The highest concentrations were observed for EHMC and OC but, considering the different uptake kinetics observed in section 3.3.6, the environmental concentration could be higher for others compound such as BPA. Furthermore, due to the long deployments and the lack of information on the uptake linearity, the evaluation of the analyte's concentration in water using the lab-derived sampling rates should not be performed.

The three samplings with POCIS showed similar concentrations in the PES membranes for BPA. However, the compound was not detected in PES employed as single-phase passive samplers.

Surprisingly, the concentrations of EHMC and OC were higher in the autumn deployment. These data might be related to the thinner biofouling layer on the membranes during the colder season. More details can be obtained comparing the amount accumulated in the protective layer of POCIS with the HLB sorbent.

Tab. 5.1 Concentration (ng/PES) of the target compounds obtained averaging results of the sampler duplicates exposed in the sampling sites Galleon (G), Biosphere (B), Chiatte (C) and Chiatte for single-phase PES samplers (S).

site	BPA	E2	EE2	E1	TCS	BP-3	OD-PABA	EHMC	EHS	OC
					ng/PES					
G	17 ± 2	nd	nd	nd	< LOQ	13 ± 1	nd	nd	nd	< LOQ
B	24 ± 2	nd	nd	nd	4.5*	6 ± 2	nd	< LOQ	nd	33 ± 18
C	16 ± 4	nd	nd	4.1 ± 0.4	5.3 ± 0.6	4 ± 1	nd	27 ± 5	nd	102 ± 1
S	nd	nd	nd	nd	< LOQ	nd	nd	11 ± 1	nd	86 ± 12

*Referred only to the B1 sample

nd: not detected.

Although the same surface area was exposed, a different total volume of the sampler was employed considering POCIS membranes and single-phase PES. This can explain the lower concentration obtained in S1 and S2 samplings (Tab. 5.1). For this reason, the results were also presented as ng of analyte per g of sampler. In this way, the concentration of OC, the compound with the greatest sampling rate (Tab. 3.7), resulted higher for S1-S2 compared to C1-C2.
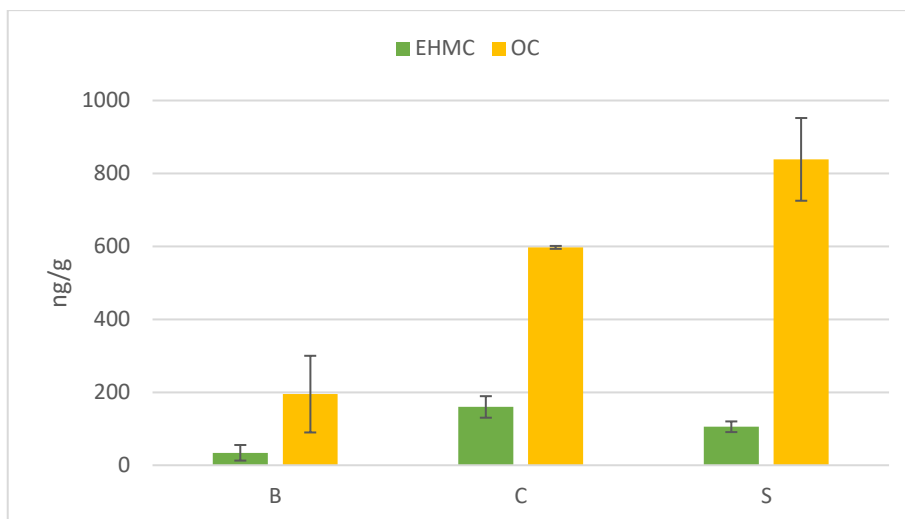
Fig. 5.4 Results obtained after extraction of POCIS membranes (B and C) and single-phase PES membranes (S) for the UV filters EHMC (green) and OC (yellow); the concentrations are expressed as ng of analyte per g of membrane.

The PES results were also compared to the concentration of the target compound in the HLB sorbent (expressed as ng of analyte per g of sorbent/membrane). Based on previous results, it was expected that the analytes accumulated mainly in the PES membrane [75]. Nevertheless, during summer the more hydrophobic UV filters (OD-PABA, EHMC and OC) were principally or completely accumulated in the POCIS sorbent. In particular, EHMC and OC were absent in the membrane for samples G1 and G2, while present for B1 and B2. This result can be due to the different exposure sites. In fact, the G1 and G2 samples were taken in an area of the harbour with more stagnant water, as can be observed by the map (Fig. 5.1), thus more fouled. Regarding OD-PABA, the results obtained in the HLB might have been affected by contamination. In fact, this UV filters was usually not detected in the samples due to its fast photodegradation in water [130]. The UV filter BP-3 was instead present in higher quantity in the PES. Still, TCS was only detected in the PES membrane even if in small amounts, as reported in Tab. 5.1 (result not reported in the Fig. 5.5). This different behaviour may be explained considering the result described in Chapter 3. In fact, as observed in the PCA (Fig. 3.11), a different interaction mechanism was expected for BP-3 and TCS: the driving force of sorption was not only hydrophobicity but also the presence of aromatic rings (especially in presence of electron-withdrawing groups) that favour the sorption on the PES polymer. Furthermore, the interactions may occur both with the polymer or directly with the biofilm on the membrane [16]. As a consequence, the presence of fouling

has a different influence on the uptake in POCIS, considering the different sorption mechanism.

The additive BPA showed small differences among the samplings, concerning the distribution between the two phases. Finally, the estrogen E1 was detected in the POCIS sorbent during the summer and in both sorbent and membranes in autumn.
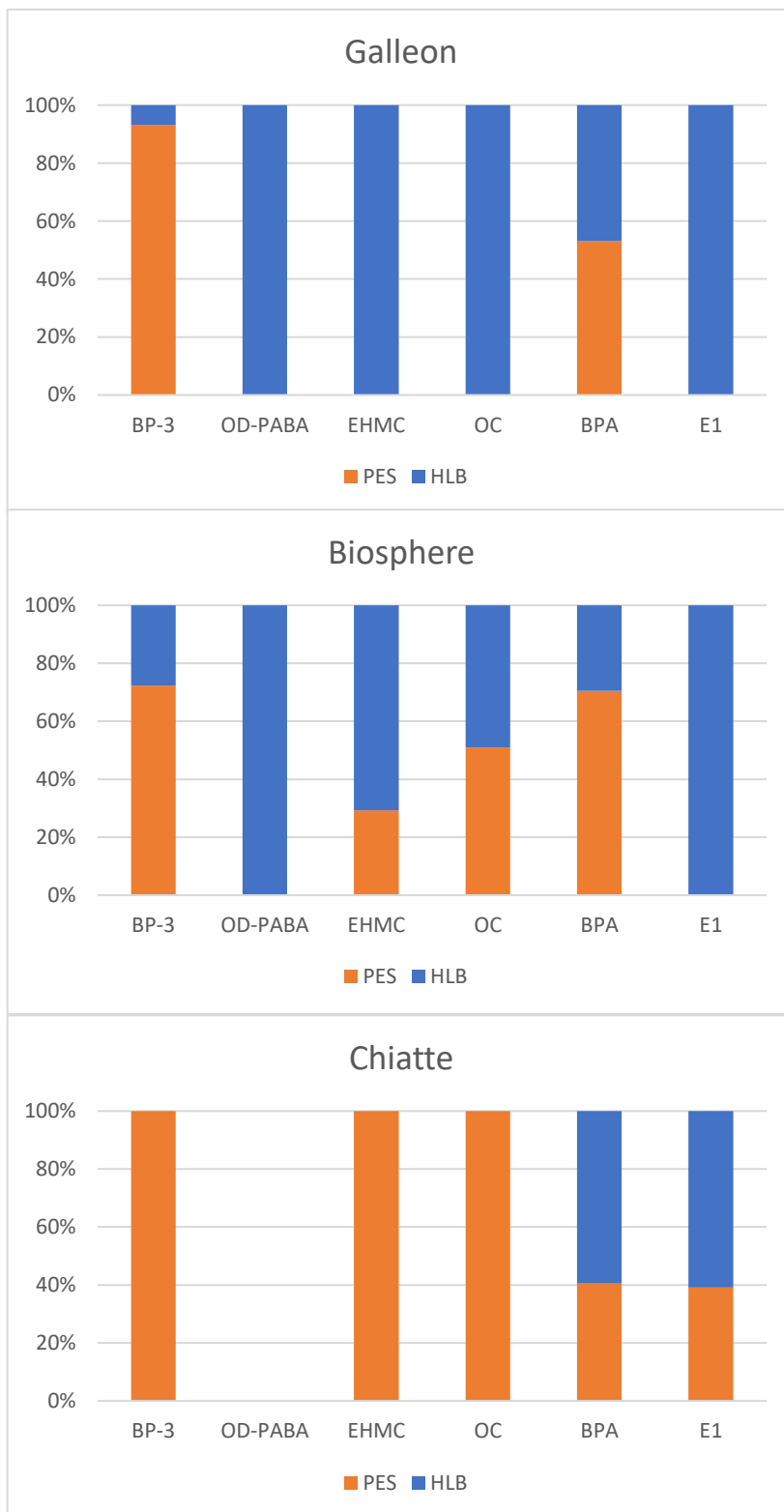
Fig. 5.5 Partitioning in the POCIS samplers (PES in orange and HLB phase in blue) of the target compounds.

5.3.2 Offshore deployment (Santa Margherita Ligure)

The application of POCIS is particularly useful in offshore waters. These sites are difficult to reach, thus obtaining numerous grab samples for an intensive and frequent monitoring is not feasible. Moreover, the expected very low concentrations of ECs require large volumes of water if using the traditional sample treatments.

During the first deployment at the M1 buoy, two of the four POCIS were destroyed by the waves generated by a very rough sea (M1-X1 and M1-X2). Three of them were retrieved (only one containing the HLB sorbent, M1-A) and processed. The data obtained showed the presence of four UV filters: BP-3, EHMC, EHS and OC. The highest concentrations were reported for EHS (402-440 ng/PES), followed by OC (89-157 ng/PES), EHMC (24-31 ng/PES) and BP-3 (11-13 ng/PES). RSDs% < 30% were observed despite the differences due to the loss of the receiving phase in two of the POCIS analysed. The same trend of concentrations was observed in the HLB sorbent of M1-A: OC > EHMC > BP-3. The analyte EHS was not detected in the sorbent, maybe because a different chromatographic method was employed, with poor sensitivity for this compound.

Regarding the same deployment, the samples obtained after two weeks of exposure were analysed. The repeatability was good (excluding EHS) with RSD% between 3-9%. Only UV filters were detected in the membrane also in this case. The data showed a drop of concentration for EHS (11 and 66 ng/PES), while the other analytes presented similar values: OC (134-140 ng/PES) > EHMC (20-23 ng/PES) > BP-3 (5 ng/PES).

Finally, using the result obtained for the 5-week sampling (M1-5W), the linearity of the uptake was assessed.
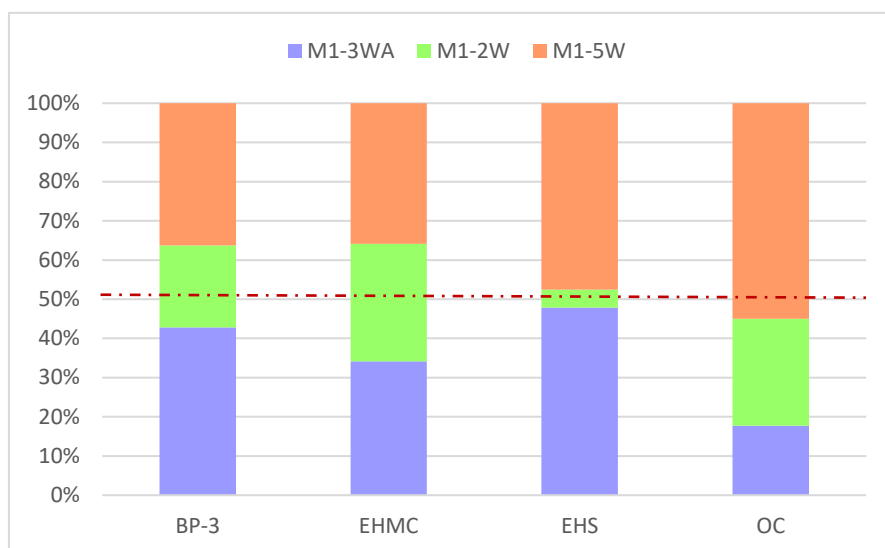
Fig. 5.6 Evaluation of the uptake linearity of the sampling for PES membranes of the POCIS exposed at M1 buoy. The results obtained for 3-week exposure (blue) were compared to the averaged concentration of the samples M1-2WA and M1-2WB of the 2-week exposure (green) and the 5-week deployment of the device M1-5W (orange).

As shown in Fig. 5.6, the accumulation resulted integrative during the 5 weeks and the concentration of the target compounds in water was provided considering the lab-derived sampling rates in SSW (Tab. 3.7). The use of a high agitation speed during the calibrations for the sampling rate evaluation, and the consequent thin WBL, agree with the turbulent flow of offshore seawater. Nonetheless, some redistribution between the PES membranes and the HLB sorbent could have occurred leading to inaccurate analyte concentrations in water. Unfortunately, the evaluation of the presence of the target analytes in the sorbent was not carried out due to problems of contamination of the extracts.

Tab. 5.2 Water concentrations estimated for the detected analytes in M1 buoy deployments.

	ng L^{-1}			
	BP-3	**EHMC**	**EHS**	**OC**
M1-3WA	0.112 ± 0.001	0.32 ± 0.02	nd	1.858 ± 0.008
M1-2W	0.083 ± 0.008	0.416 ± 0.009	nd	4.28 ± 0.04
Averaged 3W-2W	0.097 ± 0.004	0.37 ± 0.01	**nd**	3.07 ± 0.02
M1-5W	0.06 ± 0.01	0.20 ± 0.01	nd	3.4 ± 0.4

nc: not calculated due to the absence of Rs for seawater.

Literature data of the studied UV filters were reported for offshore seawaters only by one study [131]. Some works reported concentrations for coastal waters close to beaches or water discharges; values can reach hundreds of µg L^{-1}[132–136] in particular when the data were collected during the peaks of recreational activity. In fact, a great impact of bathing activity

on UV filter concentrations was established [133]. The herein reported concentrations were lower than those reported in the cited studies, reflecting the dispersion and consequent dilution of the chemicals in seawater. Although EHMC was reported as the most frequently used UV filters for sunscreen products [137], it was not the most detected compound. This could be related to the higher stability of OC [101,130,138] or in a change of product formulations, since the cited work dates back to 2002.

Concerning the duplicates of POCIS exposed in the M2 buoy, concentrations similar to M1 were observed. The highest results were reported for OC (154-201 ng/PES), while EHS was detected only in one of the PES membranes at 116 ng/PES. Finally, EHMC was quantified at 15-16 ng/PES and BP-3 at 4-6 ng/PES. In Fig. 5.7 a summary of the results obtained in the offshore samplings is reported.
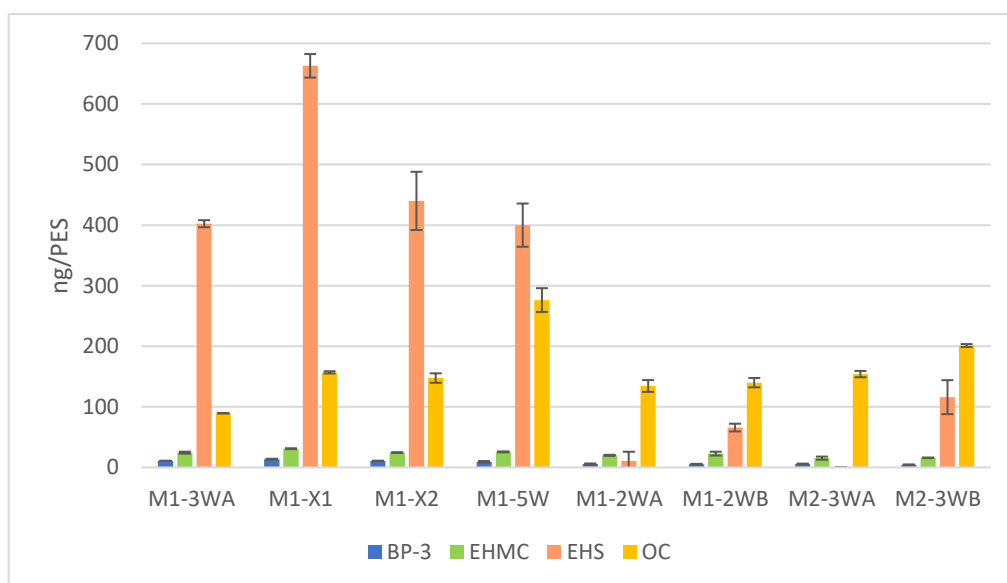
Fig. 5.7 Summary of the results obtained during the samplings performed in the offshore areas in Santa Margherita Ligure (ng/PES ± std.err.).

5.3.3 Mario Zucchelli Station: Antarctica

A high dilution (1:400) of the PES extract was necessary considering the expected concentrations in the WWTP effluent and the heavy impacted matrix. Therefore, the high dilution factor also allowed to obtain a soft matrix effect in all the samples (81% < ME < 119%).

The repeatability (RSD%) of the duplicates resulted good, between 0.2 - 23% (the only exception was BP-3 for one of the samplings: 57%).

The results of WWTP presented higher levels of concentration compared to the previous results in seawater, thus the results were expressed as µg/PES. BP-3 was detected in all the samples with the higher concentrations (2.41 – 4.96 µg/PES). The UV filter OC was also detected in all the samples and was present in the range 1.03 – 2.54 µg/PES. Although at lower concentrations, TCS and EHMC were detected in 100% of the PES membrane extracts. However, EHMC was under the quantitation limits in the last three deployments. Finally, BPA was detected in each sample but always under the LOQ.

Considering the extracts of the HLB sorbent, the target compounds BPA, BP-3, and TCS were detected. The concentrations of BP-3 and TCS (ng/g) were much higher in the PES membranes with a ratio of $3.1 < C_{PES}/C_{HLB} < 8.3$ and $5.8 < C_{PES}/C_{HLB} < 9.1$, respectively. On the contrary, the more hydrophobic UV filters OC and EHMC were detected only in the membranes. Despite the complex matrix, the sorption was not influenced as in Genoa harbour.

Regarding the sampling of seawater in Road Bay, only BP-3 was detected in PES membranes during the second deployment when the ice pack had melted. No evidence of its presence in the HLB was found. Nevertheless, both BP-3 and OC were detected in some spot samplings. This might be ascribed to the different kinetics of sorption in cold water. In fact, the temperature of seawater is typically between -2 °C and +2 °C [139]. The assessment of sampling rates has never been performed in such conditions, although a previous study showed limited differences in the R_s changing the temperature from 25 °C to 5 °C [140]. However, the evaluation was carried out only for 8 compounds (not the target compounds of this Chapter) and at different salinity conditions. Longer deployments and an in-situ calibration are required to reveal the impact of the Antarctic marine waters on the accumulation of the analytes.

5.4 Conclusions

The presented results highlighted the impact of the environmental conditions on passive sampling. The methodology employed here, involving separate extraction of sorbent and membranes, permitted to observe the impact of temperature, fouling and sediments on the uptake on PES membranes as well as the distribution between the protective layer and the internal receiving phase.

As stated in the introduction, employing the combined assessment strategy can lead to erroneous evaluation of the TWA concentration in real water, especially when the sampling rates are estimated in laboratory calibrations. The application of these combined strategies (extraction or assessment) would be useful only under environmental conditions where clean waters are studied.

Published Papers

Benedetti, B.; Baglietto, M.; MacKeown, H.; Scapuzzi, C.; Di Carro, M.; Magi, E. An optimized processing method for polar organic chemical integrative samplers deployed in seawater: Toward a maximization of the analysis accuracy for trace emerging contaminants. J. Chromatogr. A 2022, 1677, 463309. https://doi.org/10.1016/j.chroma.2022.463309

Scapuzzi, C.; Benedetti, B.; Di Carro, M.; Chiesa, E.; Pussini, N.; Magi, E. Passive Sampling of Organic Contaminants as a Novel Approach to Monitor Seawater Quality in Aquarium Ocean Tanks. Appl. Sci. 2022, 12, 2951. https://doi.org/10.3390/app12062951

Chapter 6. Evaluation of the sorption ability of biobased polymeric films and comparison with PES membranes

6.1 Introduction

In his book *The Imperative of Responsibility – In Search of an Ethics for the Technological Age* (1979) the philosopher Hans Jonas formulated the principle "Act so that the effects of your action are compatible with the permanence of genuine human life". Jonas' imperative met the definition of sustainable development formulated in the World Commission on Environment and Development's 1987 Brundtland report *Our Common Future*: "development that meets the needs of the present without compromising the ability of future generations to meet their own needs". In this raising awareness of human impact on the environment, the concept of Green Chemistry first and of Green Analytical Chemistry, after, emerged. In 1998, the 12 principles of Green Chemistry were introduced [141]. These principles were mainly focused on synthetic chemistry. Afterwards, Gałuszka et al. proposed the 12 principles of Green Analytical Chemistry (GAC) in order to adapt the principles postulated by Anastas and Warner to analytical chemistry [142]:

1. Direct analytical techniques should be applied to avoid sample treatment.
2. Minimal sample size and minimal number of samples are goals.
3. In situ measurements should be performed.
4. Integration of analytical processes and operations saves energy and reduces the use of reagents.
5. Automated and miniaturized methods should be selected.
6. Derivatization should be avoided.
7. Generation of a large volume of analytical waste should be avoided and proper management of analytical waste should be provided.
8. Multi-analyte or multi-parameter methods are preferred versus methods using one analyte at a time.
9. The use of energy should be minimized.
10. Reagents obtained from renewable source should be preferred.
11. Toxic reagents should be eliminated or replaced.

12. The safety of the operator should be increased.

Nevertheless, the effort to obtain greener procedures should not be at the expense of the analytical method. Therefore, the concept of White Analytical Chemistry (WAC) was introduced precisely to balance the greenness of the method and its usefulness and performance [143]. Both GAC and WAC support the use of reagents and materials which are biodegradable and obtainable from renewable sources.

Polylactic acid (PLA) is a biobased and compostable plastic. Briefly, PLA is produced starting from the fermentation of sugars which produce lactic acid. Afterwards, the lactic acid is treated to produce lactide which is submitted to a ring-opening polymerization to form PLA [144]. The polymer could be employed to produce porous layers and could also undergo functionalization or could be blended with ductile polymers such as polycaprolactone (PCL) [145,146]. These bioplastics have been proposed as a better alternative to fossil fuel plastics. Although some evidence of adverse effects were reported [147–149].

In this chapter, the sorptive performance of PLA/PCL membranes pure or functionalized with amino groups were compared to those reported in the previous chapters for PES membranes. The biobased PLA/PCL porous films (GAC principle number 10) were tested in order to assess their use as sorptive phase in passive sampling applications (GAC principle number 3).

6.2 Materials and methods

6.2.1 Chemicals (standards and reagents)

Ultra-pure water, isopropanol and Methanol (MeOH) were purchased from VWR (Radnor, PA, USA). All solvents were HPLC-MS grade. Ultrapure water was obtained by a Milli-Q system (Millipore, Watford, Hertfordshire, UK).

Analytical standard solutions were prepared dissolving or diluting in MeOH or MeOH:water 1:1 pure powders, liquid standards and certified grade solutions (all above 98% of purity) of 25 emerging contaminants purchased from different suppliers: theophylline (THEOP), carbamazepine (CRB), benzophenone-3 (BP-3), octyl dimethyl p-aminobenzoate (OD-PABA), ethyl hexyl methoxy cinnamate (EHMC), octocrylene (OC), perfluorooctanoic acid (PFOA), acesulfame (ACS), sucralose (SCL), bisphenol A (BPA), estrone (E1), β-estradiol

(E2), 17α-ethinyl estradiol (EE2), ibuprofen (IBU), gemfibrozil (GEM), clenbuterol (CLBT), mefenamic acid (MEF), hydrochlorothiazide (HCTZ), furosemide (FRSM) and triclosan (TCS) from Sigma-Aldrich (St. Louis, MO, USA); caffeine (CAFF), ketoprofen (KET), naproxen (NAP), diclofenac (DCF) from Fluka Analytical (Saint Gallen, Switzerland); salbutamol (SLBT) from Alfa Aesar (Haverhill, MA, USA).

Salts employed in the preparation of a simple version of Synthetic SeaWater (SSW) were sodium chloride (NaCl, $\geq$ 99%) from Sigma Aldrich (Milan, Italy), sodium sulfate (Na$_2$SO$_4$, 99%) and potassium chloride (KCl, 99.5%) from Carlo Erba Reagenti (Rodano, MI, Italy). SSW was prepared by adding NaCl, KCl and Na$_2$SO$_4$ to tap water at a concentration of 22.64 g L^{-1}, 0.78 g L^{-1} and 4.15 g L^{-1} respectively. A buffer solution was prepared using sodium hydroxide (> 98%) from Sigma Aldrich (Milan, Italy) and ammonium acetate (> 98%) from Merck (Darmstadt, Germany): 0.044 g L^{-1} and 1.928 g L^{-1}, respectively.

6.2.2 PLA/PCL porous film

The preparation of porous film of PLA/PCL was performed as described elsewhere thanks to a collaboration with the section of industrial chemistry at the University of Genoa [150,151]. Briefly, PLA/PCL solutions were prepared by dissolving the polymers in DMF at 80 °C to obtain a concentration of 10% (w/v). The ratio of PLA/PCL employed was 95/5. Afterwards, the porous films were prepared by casting the solutions onto a glass plate placed in coagulation baths at 25 °C. The films obtained were soaked in water and dried for 24 h at room temperature and then in a vacuum oven at 30 °C.

Some of the films produced were subject to aminolysis to assess if the presence of amino groups enhances the sorption of acidic compounds compared to pure PLA/PCL membranes. The films were cut in pieces of 3 cm x 1.5 cm, and pre-wetted in 5 mL of isopropanol. Afterwards, the films were transferred in a solution in isopropanol of ethylenediamine at 10% (v/v). At the end of the aminolysis, the films were removed and washed with isopropanol [151].

6.2.3 PLA/PCL recovery and matrix effect

As a first test, recovery and matrix effect were evaluated as described in Chapter 3 (section 3.2.3). However, the procedure employed for the aminolyzed PLA/PCL was slightly modified due to their different mechanical properties compared to PES membranes.

The membranes of aminolyzed PLA/PCL were washed in isopropanol for 30 min to remove residual species of manufacturing and left to dry. Then, they were soaked in ultrapure water for 1 h and spiked with a solution in MeOH containing the target analytes at 500 μg L^{-1} (or pure MeOH for the non-spiked blank membrane) and left to dry again. The spiked films were rinsed with ultrapure water in order to remove the non-sorbed analytes, left to dry for almost 1 h and finally extracted. The extraction procedure involved two steps where the membranes were immersed in vials containing 5 mL of MeOH and gently shaken on a horizontal shaker (pb International, Italy) for 30 min at 130 rpm. The extracts were then reduced to dryness on a rotary evaporator (Rotavapor® R-100, BUCHI, Switzerland) and reconstituted in 1 mL of methanol. Before the analysis, the solutions were filtered through a PTFE 0.2 μm filter. The theorical final concentration was of 5 μg L^{-1}.

6.2.4 PLA/PCL sorption ability of ECs

A preliminary evaluation of the sorption ability of the polymeric PLA/PCL films pure or aminolyzed was performed in ultrapure water. Two rectangular sheets of 1 cm x 2 cm were fixed onto a brass grid and immersed in 1.6 L of ultrapure water solution of the target compounds at 10 μg L^{-1}. After 4 days of exposure under stirring conditions (stirring rate of 1000 rpm) at room temperature, the membranes of PLA/PCL were removed, rinsed in ultrapure water to remove any remaining droplets of the solution of exposure and extracted as described above. The extracts were diluted in ultrapure water:MeOH 50:50 (v/v) and analyzed by HPLC-MS/MS (see Chapter 4 for details on the instrumental analysis). The evaluation of the achievement of the equilibrium was observed monitoring the concentrations of the analytes in water during the polymeric film deployment. A further experiment in ultrapure water was performed using non-functionalized PLA/PCL films of 4.5 cm^2 of area and a smaller volume of water (800 mL).

The sorption ability of the porous films was further evaluated using ultrapure water solution at pH 7.5 and SSW solution. The same procedure described for ultrapure water was employed, the only difference regarded the dimension of the sheets (3 cm x 1.5 cm) and the volume of water employed for the exposure (800 mL). For the details on the preparation of the buffer solutions at pH 7.5 and of SSW see Chapter 3.

6.3 Results and discussion

6.3.1 Recovery and Matrix effect

As described (in detail) in the previous chapters, the first step in the evaluation of a new material for sample preparation strategy consists in the evaluation of recovery (Eq. 3.1) and matrix effect (Eq. 3.2). In fact, recovery gives a first insight on the potential affinity of the new material for the target compounds, while matrix effect permits to assess the presence and effect of interferents released from the polymer. This last issue is of great importance considering the application in complex matrices for the detection of trace contaminants. Furthermore, the evaluation of ME permits to develop extraction protocols that limit the coextraction of interferences [152].

The matrix effect (ME) was mainly soft (80% < ME < 120%). Few compounds showed a moderate ME, whereas only DCF presented a ME > 150% (strong signal enhancement). No significant differences were observed between pure PLA/PCL films or aminolyzed films.

The ME% obtained for OC with the biobased polymer (99%) was definitely better compared to the value obtained with PES membranes (22%). This result suggests a possible release of interferents from PES membranes.

Recoveries were mainly in the range 80-120%. The compounds with the lowest values were CAFF, PRX and SCL. Compared to the R% obtained using PES membranes with 0.1 μm of pore size purchased from Pall Italia, higher recoveries were obtained for ACS and PFOA (Fig. 6.1).
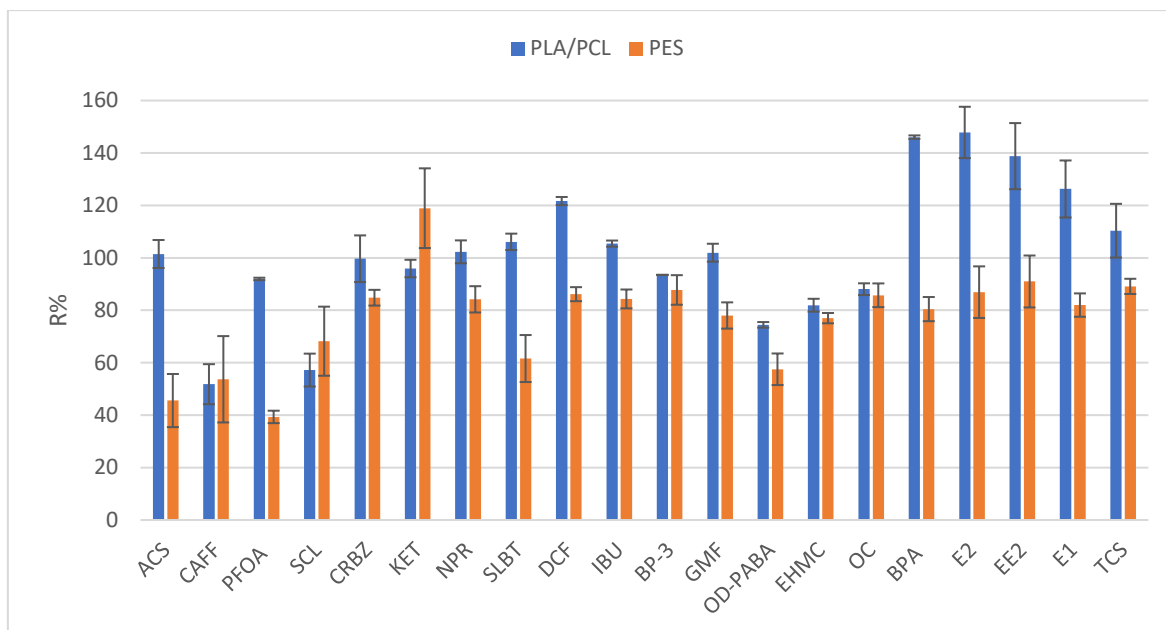
Fig. 6.1 Graphical representation of the recovery (R%) obtained for 20 target compounds using PLA/PCL film subject to aminolysis and PES. The error bars represent the standard deviations.

6.3.2 Sorption ability of biobased polymeric films

The affinity of the pure or aminolyzed PLA/PCL films for the 25 target compounds was evaluated as described in section 6.2.4 and compared to the results obtained using PES membranes. Compared to microporous PES membranes, the lab-synthetized PLA/PCL films presented similar porosity (90%) but greater pore size, resulting in a lower total surface area (Fig. 6.2).
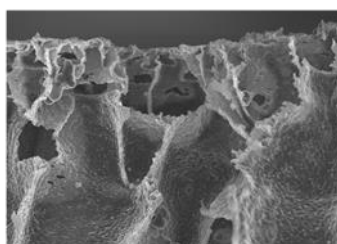
Fig. 6.2 FE-SEM analysis of PLA/PCL porous film.

Considering the concentrations in water during the 4-day exposure, the equilibrium was reached for all the investigated analytes [150]. For UV-filters, the extraction from the solution can be considered roughly exhaustive, also considering the partial degradation of OD-PABA and EHMC [113].

The preliminary experiment did not show an improvement in the sorption of the target compounds using the aminolyzed film. A difference in sorption was expected, in particular for the acidic drugs. However, the functionalization was not enough to observe an improvement in the sorption ability of the PLA/PCL polymeric film. A second experiment in ultrapure water was carried out using non-functionalized PLA/PCL membranes. These results were compared with those obtained using PES membranes and a higher sorption ability was observed using PES.

Due to the poor sorption affinity of the more polar compounds for both types of membranes under investigation, the following results present only a comparison with the analytes studied with PES in Chapter 3: estrogens (E2, EE2 and E1), TCS, BPA and 4 UV filters (BP-3, OD-PABA, EHMC and OC). The sorption was studied in ultrapure water at pH 7.5 and in SSW. The results are summarized in Fig. 6.3. To compare results obtained with PES and PLA/PCL membranes exposed to different amount of target compounds (same concentration but different total volume of water), the analyte concentrations in the polymer (μg kg^{-1}) were normalized for the total amount of compound in water (μg). The greater sorption ability of PES was confirmed also in this case: the higher surface area of the commercial PES membranes, due to the lower dimensions of the pores and the presence of different functional groups in the structure such as aromatic rings and sulphone groups, probably plays a key role in the uptake.
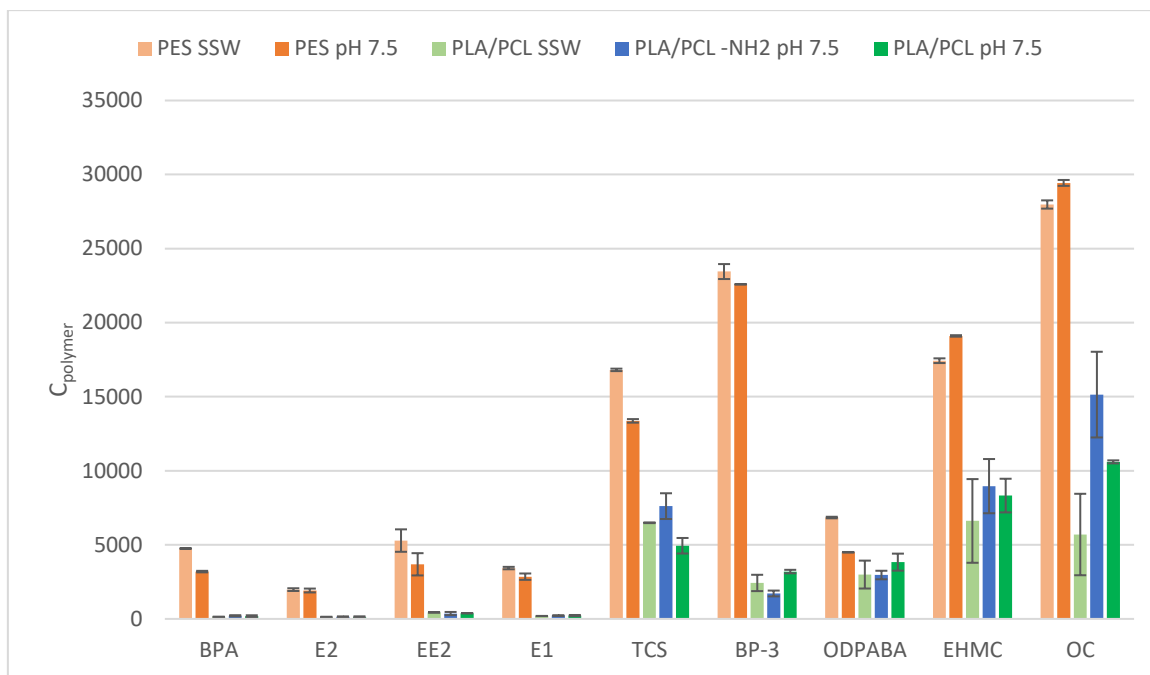
Fig. 6.3 Comparison of the concentration of the target compounds in the studied polymeric films: PES membrane of 0.1 µm of pore size, PLA/PCL non-functionalized and PLA/PCL-NH2 functionalized with amino groups. The concentrations reported ($C_{polymer}$) were obtained normalizing the analyte's concentration in the film ($\mu g\ kg^{-1}$) for the total amount of the analyte (μg) presented at t_0 in the solution.

6.4 Conclusions

This short chapter presented a summary of the results obtained using a biobased copolymer (PLA/PCL) as sorptive material for ECs with a broad range of polarities and different physico-chemical properties. The sorption was assessed using PLA/PCL porous film and film of PLA/PCL subject to aminolyzation in order to improve the sorption of acidic analytes thanks to the presence of aminogroups on the surface of the polymer. Nevertheless, the enhancement of the sorption capacity of the biobased polymers was not observed in presence of these amino functions. Furthermore, no improvements in the sorption were observed also compared to the commercial PES membranes. The higher surface area of PES and possibility to establish different interactions with the target compounds (not only hydrophobic but also π- π and O- π) make the performance of the PES commercial membranes more suitable as receiving phase, compared to PLA/PCL. In addition, the PLA/PCL films presented poorer mechanical properties compared to PES; this aspect is very important considering the manipulation and the deployment of the sampling material.

Chapter 7. Nitramines detection using passive sampling: preliminary results.

Instead of a burning bush, we face a burning planet.
Secretary-General UN COP27 (Sharm el-Sheikh)

7.1 Introduction

Since the Industrial Revolution, anthropogenic carbon dioxide (CO_2) emissions have impacted the carbon biogeochemical cycle introducing an acyclic factor, influencing its natural equilibrium. As of 1958, the monthly mean concentrations of this greenhouse gas in the atmosphere at Mauna Loa Observatory (Hawaii, USA) have been constantly increasing (Fig.7.1).

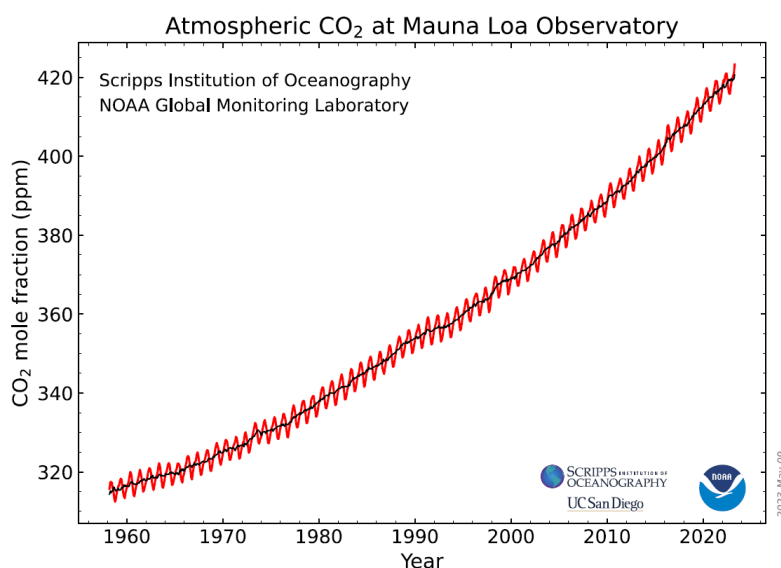Fig. 7.1 Monthly mean CO_2 measured at Mauna Loa Observatory (Hawaii, USA). The red line represents the monthly mean concentration of CO2, the black line represents the concentration corrected for the average seasonal cycle [153].

In 2022, 36.8 Gt of energy-related CO_2 were emitted. In fact, the main emissions of greenhouse gases are ascribable to the energy sector (73.2%) as showed in Fig. 7.2

[154,155]. Furthermore, the principal sink of CO_2 greenhouse gas is the atmosphere (45%) followed by land (32%) and oceans (24%).

Greenhouse gas emissions by sector, World

Greenhouse gas emissions[1] are measured in tonnes of carbon dioxide-equivalents[2] over a 100-year timescale.
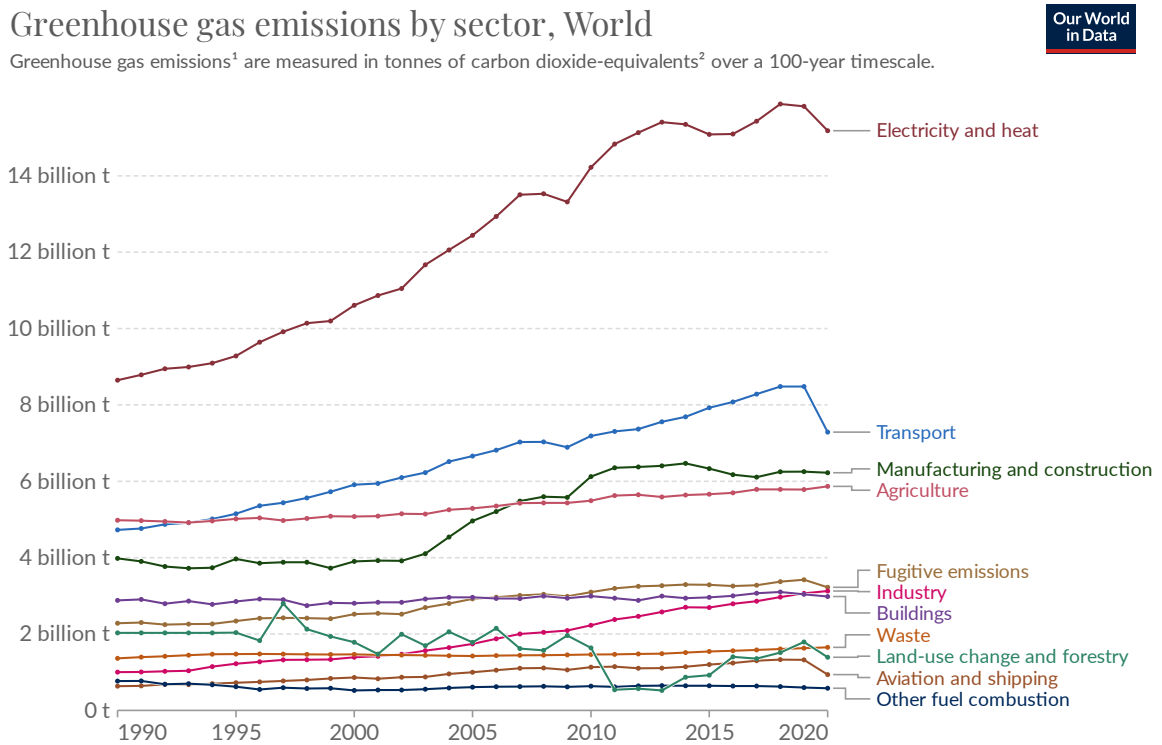
Fig. 7.2 Greenhouse gas emissions by sector measured in in tonnes of CO_2-equivalents [155].

In 2015, the UN Climate Change Conference (COP21) held in Paris led to the Paris Agreement, an international treaty on climate change. The main goal of this treaty is to limit the increase of the global average temperature to 1.5 °C (Paris Agreement 2015). In order to achieve this objective, reduction of emissions and compensation between emission and removal of greenhouse gases must be dealt with. In this context, the European Commission has introduced the European Green Deal, which contains guidelines to achieve the objective of climate neutrality by 2050 [156].

Among strategies to limit global warming, CO_2 removal technologies may play a key role. In the last twenty years, there has been a growing interest in Carbon Capture Utilization and Storage (CCUS) [157] and in 2021 approximately 40 Mt of CO_2 per year was estimated as the carbon capture capacity of the operating CCUS by the International Energy Agency.

Unlike Direct Air Capture (DAC) systems which capture CO_2 from distributed and mobile sources, CCUS capture CO_2 from stationary anthropogenic emissions [158]. In this field, three different types of CCUS have been developed: pre-combustion, oxyfuel combustion and post-combustion [159]. Nowadays, the most suitable methodology is represented by Post-Combustion Carbon Capture (PCCC), in particular those based on physical or chemical absorption. The leading technology of PCCC is based on chemical absorption with aqueous amine solvents. Briefly, the flue gas – gas produced by combustion plants – is conducted into the absorber column where a counter-current stream of amine solution is present. In this step CO_2 is chemically absorbed by reacting with the amines present in the solution, forming carbamates (with primary or secondary amines) or bicarbonates (using tertiary or hindered amines) [160,161]. The enriched solvent (containing CO_2) is then regenerated in the stripper and recycled (lean solvent). In this step a pure CO_2 stream is produced, then it is transported in the storage reservoirs.

The carbon capture process can lead to the formation of by-products. In particular, the production of nitrosamine and nitramines (Fig. 7.3) are of concern due to their mutagenic or carcinogenic potential [162]. Specifically, two different pathways of nitrosamine and nitramine formation are possible. Nitrosamines and nitramines can be produced directly in the carbon capture plant. In this situation amines undergo oxidative degradation in the presence of potential oxidants such as O_2, SOx and NOx in the flue gas. Afterwards, these by-products are emitted into the environment through solid waste, atmospheric emissions or wastewater [163]. The production of these by-products also occurs in the atmosphere as a consequence of the emission of amines from PCCC. These amines are subjected to photo-oxidation in the presence of radicals (mainly OH$^{\bullet}$) and nitrosating/nitrating agents (NO and NO_2) [164]. Afterwards, wet depositions (rain and fog) can transport these compounds to terrestrial and aquatic matrices. Once in the aquatic matrix, nitrosamines and nitramines are persistent due their limited photodegradation [165].

Fig. 7.3 Nitrosamine (left) and nitramine (right) structure.

Regulation for nitrosamines and nitramines has not yet been proposed, although some threshold values have been suggested. The Norwegian Institute of Public Health has proposed 4 ng L^{-1} as combined threshold for nitrosamines and nitramines. Other values are reported only for specific nitrosamines. In Germany, control levels for N-nitrosodimethylamine (NDMA) are 10 ng L^{-1}. The California Department of Public Health assigned a limit of 3 ng L^{-1} as a Public Health Goal for NDMA in drinking water [166], while in New Jersey a 0.7 ng L^{-1} limit has been set for NDMA and a 5 ng L^{-1} for N-Nitrosodi-n-propylamine (NDPA) in groundwater [167]. The Environmental Protection Agency (EPA) in 2016 fixed reference levels for several nitrosamine in the range 0.4-30 ng L^{-1} [167].

Although, few studies on the toxicity of nitramines are available [168–171], the mutagenic potential of some nitramines have been demonstrated [168,172]. Moreover, even if the mutagenic potential of nitramines is lower compared to nitrosamine analogues [172], their higher stability in water could pose a health risk. Furthermore, nitramines are mobile chemicals due to their hydrophilicity, these characteristics make their remotion from the environment hard. As a consequence, the monitoring of specific nitramines in water media, in particular drinking water reservoir nearby PCCC, requires a fundamental evaluation to prevent possible adverse effect on population's health.

Nevertheless, the hydrophilicity of nitramines and the low concentration levels in the aquatic environment make the detection of these compounds an issue. In this context, the use of passive sampling can help providing a continuous monitoring, the preconcentration of the analytes directly in situ and the TWA concentration of the target compounds in the water media. However, passive sampling also presents some challenges; first of all, the selection of receiving phases with sufficient adsorption capacity for these polar substances. Another important issue is related to the limited possibility to use PRCs with the samplers usually employed for polar compounds and the need to evaluate in situ sampling rates.

The aim of this work carried out at the Norwegian Institute for Water Research (NIVA, Oslo, Norway) was to test the sorption ability of several commercial sorbent towards two nitramines, N-nitroethanolamine (EtOHNA) and 1-Nitropiperazine (NIPZ), in order to develop a hydrogel passive sampler able to detect their presence in freshwater at ultra trace level (ng L^{-1}) [173].

7.2 Materials and Methods

7.2.1 Chemicals (standards and reagents)

All the solvents and the reagents were of HPLC or HPLC-MS grade. Methanol (MeOH) was purchased from Rathburn (Walkerburn, Scotland), dichloromethane (DCM) and acetonitrile (ACN) from Sigma-Aldrich (St. Louis, MO, USA), acetic acid from Fluka Analytical (Saint Gallen, Switzerland), sodium hydroxide (NaOH) and ammonium formate Merck, Sigma-Aldrich. Ultra-pure water was obtained from a Millipore Q-Gard system equipped with a Millipak 0.22 μm filter (Millipore, Watford, Hertfordshire, UK).

Agarose powder of biotechnology grade was purchased from AMRESCO (Solon, OH, USA).

The standards of N-nitroethanolamine (EtOHNA) and 1-Nitropiperazine (NIPZ) were purchased from Chemsupport. All the standards are >98% purity. Physico-chemical properties and the structure of the analytes are reported in Tab. 7.1.

Tab. 7.1 Structure and physico-chemical properties of the two target compounds. MW is the molecular weight, HBD/HBA the number of hydrogen bonding donor/acceptor atoms, TPSA the polar surface area, LogP the logarithm of the partition coefficient at pH 7. Source: http://www.chemicalize.com

	MW (g/mol)	HBD/HBA	TPSA Polarizability	Solubility water pH 7 25°C (g/L)	Vapor pressure (Torr)	LogP	pKa	Main species (%)
EtOHNA	106.08	2/4	78.1 Å² 8.26 Å^3	1000	$1.22\ 10^{-3}$	-1.24	9.38	Neutral pH 6.2 = 99,93% Neutral pH 8 = 95.96%
NIPZ	131.13	1/4	61.1 Å² 11.96 Å^3	236	$6.68\ 10^{-4}$	-2.56	8.7	Cationic pH 6.2 = 99.69% Cationic pH 8 = 83.47%

Stock solutions of EtOHNA and NIPZ were prepared using ultra-pure water at 5000 and 2000 mg L^{-1}, respectively. A standard mix containing both the analytes was prepared at 50 mg L^{-1} in ultra-pure water. Working solutions were prepared at different concentrations by subsequent dilution of the standard mix.

The standards and the standard solutions were stored at +4 °C.

7.2.2 Instrumental analysis

Concentrations of NIPZ and EtOHNA were determined by ultra performance liquid chromatography triple quadrupole mass spectrometry (UPLC-MS) using an Acquity™ UPLC and a Xevo™ TQ-S mass spectrometer (Waters). The mass spectrometer was operated in negative electrospray ionisation mode for EtOHNA and positive mode for NIPZ using multiple reaction monitoring (Tab. 7.2). Chromatographic separation was performed using an Atlantis™ T3 3 µm 2.1 x 100 mm column (Waters). The mobile phase consisted of two eluants, (A) 5.2 mM ammonium acetate in ultra-pure water and (B) MeOH:ACN (1:3 v/v) using a binary gradient schedule totalling 6 min and a flow rate of 0.5 mL/min. The gradient of (A) was 100% for 1 min, 95% by 3 min, 5% by 3.5 min, 100% by 4 min and held

until 6 min. The desolvation temperature was maintained at 400 °C, with a capillary voltage of 1.50 kV and cone voltage 23 V.

Ta. 7.2: Nitroamines analysed,their corresponding retention time and associated precursor and product ions.

Compound	Retention time (min)	Precursor ion (m/z)	Product ion (m/z)	Cone (V)	Collision (V)
EtOHNA	0.67	105.0	43.0	25	12
			46.0	25	15
NIPZ	2.19-2.30	132.0	86.1	25	8

7.2.3 Stability

The stability of the solution under storage conditions was tested by comparing the results obtained analysing the same calibration curve (10-200 ng L^{-1}) after 25 days of storage in the fridge (+4 °C). The possible analytes' degradation during the evaporation step was also evaluated; 5 mL of a 100 ng mL^{-1} standard solution of nitramines in MeOH was subjected to evaporation using a nitrogen gas (N$_2$) thermostated at 45 °C for almost 2 hours, then reconstituted in 5 mL of ultra-pure water. The test was performed in triplicate. Finally, 1 mL of the final aqueous solution was analysed by UPLC-MS/MS.

7.2.4 Preliminary sorbent assessment

Eight different commercial sorbents were tested to assess the most suitable receiving phase for nitramine PSDs. Their main physico-chemical properties and suppliers' details are reported in Table 7.3.

Tab. 7.3 Properties and suppliers of the selected sorbents.

	Oasis HLB	Strata X	ENV+	ABN	Oasis MCX	Isolute SAX	EPA 521	ENVI Carb
Amount per cartridge (mg)	200	500	1000	150	150	powder	2000	powder
Surface Area (m²/g)	814	800	1000	400	788	nd	nd	100
Part. Diameter (µm)	53.6	33	116	40	28.4	50	nd	nd
Pore volume (cm³/g)	1.31	nd	nd		82	nd	nd	nonporous
Pore Diameter (Å)	82	85	nd	40	1.29	60	nd	

nd. Data not disclosed.

SPE cartridges were prepared with the same amount of sorbent 150 ± 3 mg. Triplicates of the sorption test and a blank were carried out for each sorbent.

The sorbents were pre-washed with 3 mL of MeOH to remove possible interferents, then rinsed with 5 mL of ultrapure water. A solution containing EtOHNA and NIPZ both at 200 ng mL^{-1} was employed to evaluate the sorption ability of the selected receiving phases. 5 mL of the NAs solution was passed through the cartridges using a flow rate of 1-2 mL min^{-1}. After the extraction, the sorbents were dried under vacuum for 45/50 min and frozen. To preliminarily evaluate the sorption, 1 mL of the filtered "flow-through" loaded waters were analysed by direct injection. Afterwards, the sorbents with the major sorption abilities for both the analytes were extracted using several solvents.

Fig. 7.4 Cartridges employed for the evaluation of their sorption ability towards nitramines.

7.2.5 Evaluation of the extraction recoveries

The cartridges of the preliminary test containing ENV+, EPA 251 and ENVI Carb sorbents were extracted using 5 mL of MeOH followed by 5 mL of DCM, while the MCX cartridges were extracted using 5 mL of MeOH at pH 10 (the pH was modified using a solution of NaOH 5 mM). The use of a MeOH basified solution was necessary to change the charge state of the analytes (from positively charged to neutral) and thus to disrupt electrostatic interactions.

The extraction procedure is the following:

1. Thaw the cartridges (1 h)

2. Add 5 mL of the solvent

3. Elute with a flow rate of 1 mL min^{-1}

4. Dry the cartridge under vacuum

Afterwards, the extracts were dried using a N$_2$ evaporation system at 45 °C, and then reconstituted in 5 mL of ultrapure water.

A second test was performed using newly prepared ENV+ and ENVI Carb cartridges to assess recoveries using other solvents. Where, 5 mL of each solvent were added in series as

follows: ACN, MeOH and MeOH with 10% of acetic acid. In this second experiment, the cartridges were eluted right after the filtration of the spiked water.

7.2.6 Agarose hydrogel preparation

The diffusive agarose hydrogels layers were prepared by adding 0.75 g of agarose to 50 mL of ultra-pure water. The solution was heated (around 100 °C) and gently mixed until the complete dissolution of the agarose powder (Fig. 7.5).
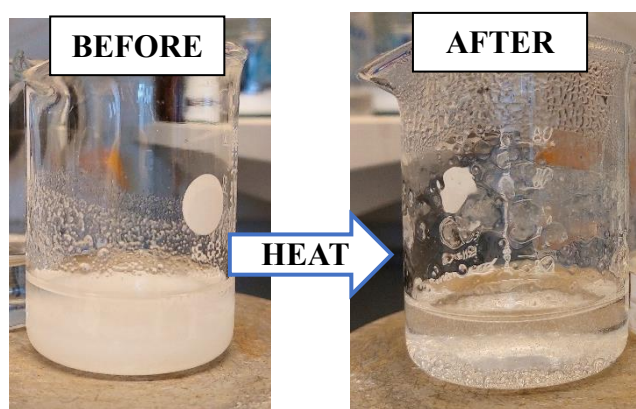

Fig. 7.5 Agarose solution at the beginning and at the end of its preparation.

The 50 mL solution was then poured into a cell plate of 6.2 cm of diameter containing four silicone spacer of 0.1 cm of thickness. The solution was pressed with a smaller cell plate to obtain a hydrogel thickness of 0.1 cm. The cell plates were warmed at 40°C during the solution preparation to reduce the speed of solidification of the hydrogel. Finally, the solution was cooled down at room temperature until it held its own shape and cut using a DGT device to obtain circles of 2.5 cm of diameter.

A slightly modified procedure was employed for the sorption hydrogel layer. The 0.75 g of the agarose powder were added to 25 mL of ultra-pure water and heated until the complete dissolution of the powder. Once the agarose almost dissolved, 25 mL of water were warmed and then added to 2 g of sorbent (ENVI Carb or MCX or a mixture 50:50 w/w of both). The sorbent was added separately to the water to avoid the formation of foam by adding directly the sorbent to the agarose solution. The sorbent and the agarose solutions were then mixed and poured into the cell plate following the procedure previously described. The obtained layers are presented in Fig. 7.6.
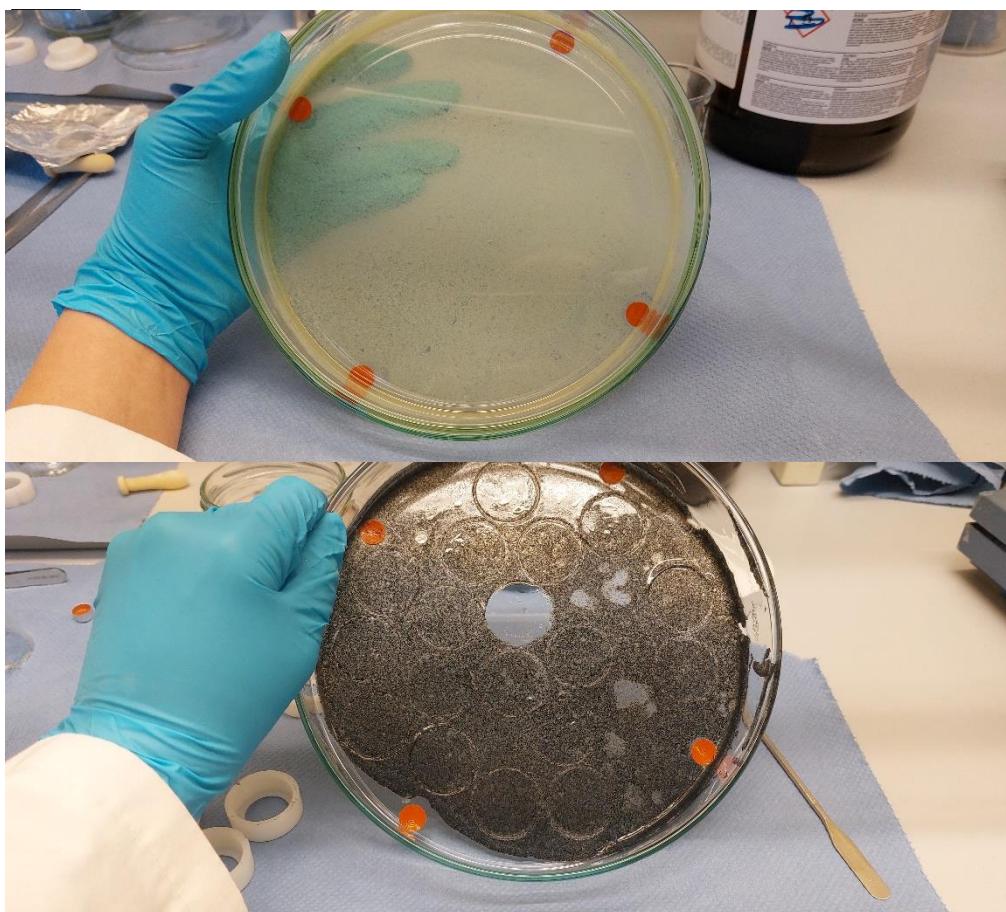
Fig. 7.6 Examples of hydrogels containing the MCX sorbent (A), and a mixture 50:50 (w/w) of MCX and ENVI Carb (B).

7.3 Results and Discussion

7.3.1 Stability

The degradation of the target compounds during the storage and the evaporation of MeOH extracts, the more stressful step of the extraction procedure, was evaluated in order to address some possible loss of the analytes during sample preparation. The results were expressed as the percentage of the area's ratio of the older standard solutions and of the freshly prepared standard solutions.

After 25 days of storage in the fridge at +4 °C, the concentration of the NIPZ standard solution had decreased by approximately 30%, across the calibration standard range (10-200 ng L^{-1}). Whereas the stability of EtOHNA is around 90%, thus negligible degradation had taken place.

To assess the possible loss of analytes during the evaporation step, the peak areas obtained for the 100 ng mL^{-1} solution of nitramines reconstituted in water after extraction were compared to the area of an aqueous standard solution not subjected to evaporation. The results showed that both EtOHNA and NIPZ were stable during the evaporation step: 96% ± 2 and 92% ± 4, respectively. These results confirmed those obtained previously by Sørensen et al. (2015) in similar conditions.

7.3.2 Commercial sorbents

The receiving phases were selected considering their use in aqueous matrices and their ability to interact with polar compounds. Furthermore, some phases with the same expected sorption mechanism but from different suppliers were tested to observe possible differences due to different functionalization, porosity or surface area. The selection rationale was described below.

Oasis HLB and Strata-X sorbents interact with target compounds not only through hydrophobic interactions, but they also possess aromatic rings and polar groups (containing N and O atoms, H-bonding acceptors) able to interact with the chemicals through H-bonding, dipole-dipole and π-π interactions. In particular, the target nitramines may interact with these sorbents by H-bonding, dipole-dipole and hydrophobic interactions. Regarding ABN and ENV+, they possess several hydroxyl groups in their DVB structure attached to alkyl moiety and to aromatic rings, respectively. These groups act as H-bonding donors and acceptors, favouring the sorption through the H-bonding acceptor groups of NAs. Apart from reversed phases, sorbents acting in mixed-mode were selected. In particular, the Oasis MCX sorbent allows interactions with basic compounds thanks to the presence of sulfonic acidic groups. This phase was expected to strongly interact with NIPZ, the sole analyte which presents an amino group mainly positively charged at neutral pH (Tab. 7.1). The Isolute-SAX sorbent, a strong anion-exchanger, was employed since it was tested for nitramines in a previous work [168]. Finally, adsorption-based sorbents were tested. Two different carbonaceous stationary phases were used: the coconut charcoal sorbent suggested in the EPA 521 methods for nitrosamines detection in water, and the Supelco ENVI-Carb.

The results of the first test were obtained considering only the analytes' concentration in the water phase before and after the extraction (Fig. 7.7). In general, the sorption of NIPZ was higher than EtOHNA for all the sorbents, excluding ENVI-Carb which showed sorption > 95% for both analytes.

In particular, the concentrations of NIPZ after extraction were <13% of the initial concentration for all the sorbents tested, excluding Isolute-SAX (60%). The lower sorption observed on an anionic exchanger is likely due to the electrostatic repulsion of the positive-charged amine group of NIPZ and the quaternary amine presented in the sorbent, while an excellent retention capacity was observed with MCX, as expected. Regarding EtOHNA, the carbonaceous sorbent ENVI-Carb appear the most suitable. However, good retention was also observed with ENV+ and the EPA 521 cartridges. Although ENV+ and ABN are quite similar, the highest surface area (see Tab. 7.3) can lead to higher sorption ability. On the other hand, the weak acidity of the hydrogen in the hydroxyl group of ENV+ may not influence the sorption [174].
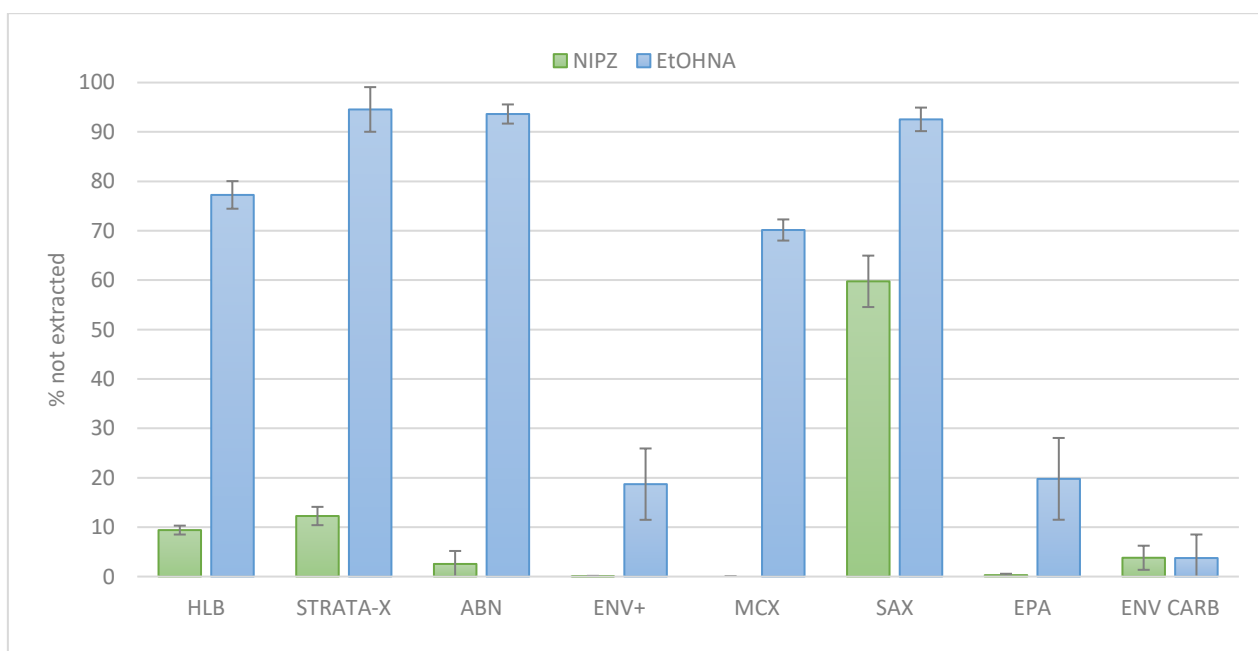
Fig. 7.7 Results obtained for the SPE test, expressed as the ratio (%) between the analyte's concentration in the spiked water after and before the filtration through the cartridges.

The lower retention of EtOHNA could be due to its higher solubility in water and TPSA, as well as the lower polarizability and MW compared to NIPZ.

7.3.3 Extraction procedure

The three types of SPE cartridges that showed the highest retention ability were extracted with 5 mL of MeOH. The extraction was evaluated in terms of recovery and matrix effects.

Regarding the recoveries, the extraction procedure with MeOH provides poor recoveries. Considering the amount of the analytes initially spiked in water and the amount not retained during the extraction step (see previous section), the recovery of EtOHNA for ENV+, EPA 521 and ENVI-Carb were 25%, 10% and 25% respectively. Concentrations of NIPZ were not found in extracts, despite the high concentrations added to the cartridges. This result has also been observed by [168]. A good matrix effect (no significant enhancement or suppression of the signal) was observed for both the analytes for all the cartridges (70-110%). Due to the low recoveries observed, cartridges were further extracted using an additional 5 mL of DCM. Nevertheless, this solvent did not improve extraction recoveries.

To further assess the extraction recoveries, new ENV+ and ENVI Carb cartridges were prepared as described above. Three different solvents were tested in series to see if recoveries for NIPZ could be improved: ACN, MeOH and MeOH with the addition of 10% of acetic acid. However, NIPZ was still not recovered. An improvement in the recoveries of EtOHNA (64% ± 4) was observed using MeOH after the passage of 5 mL of ACN suggesting that ACN is not suitable to extract the analyte but a larger volume of MeOH (more than 5 mL) may be required to obtain higher recoveries.

Considering hydrophobic interactions as the reasons for the negligible recoveries for NIPZ, the MCX cartridges were employed. In this case, the sorption occurs not only through hydrophobic interactions but also by means of electrostatic interactions between positively charged amino group of NIPZ and negatively charged sulfonic groups of the sorbent. In this case, the extraction was performed using 5 mL of MeOH at pH 10. Despite some issues due to the presence of air in the sorbent and the low volume of MeOH employed, a significant improvement in NIPZ recovery was observed: 25% ± 2.

As the purpose of the work was to develop a hydrogel passive sampler with a different extraction procedure, no other attempts to improve the SPE recoveries were carried out.

7.4 Conclusion

The detection of nitramines in water bodies such as drinking water reservoirs is of utmost importance considering the potential impact on human health of these compounds. Concerns regarding their entry in surface waters resulting from post-combustion carbon capture systems were raised in the last years in parallel to the propagation of these plants. Nevertheless, the polar nature of nitramines and their low concentration levels in the water

environment make the detection challenging. For this reason, the use of passive sampling techniques may be useful to improve the analytical methodology for their detection. The first steps in the development of a hydrogel passive samplers for nitramines were presented considering EtOHNA and NIPZ as model compounds. Two receiving phases out of the eight tested resulted promising, since the best results in term of retention and subsequent desorption were obtained: ENVI-Carb and MCX. The desorption of NIPZ resulted particularly demanding due to its strong interactions with the sorbents and only using a cation-exchange sorbent the elution of this analyte was feasible. The selected sorbents were then employed as single phases or as mixture (50:50 w/w) for the preparation of hydrogels that will be used as binding gels in passive sampling devices. The sorption performance of the binding gels will be evaluated using different aqueous matrices and a different extraction procedure involving a large amount of solvent and a longer extraction time will be tested for the improvement of the recoveries of the method.

Conclusions

The PhD work presented in this thesis aimed to assess applicability of different passive sampling techniques for the detection of emerging contaminants in aqueous matrices. The challenge was to employ this sampling strategy in complex environments such as seawater or to detect hydrophilic chemicals at low concentration levels.

The first part of the work regarded the use of polyethersulfone membranes as single-phase passive sampler. The accumulation of ten target compound was deeply investigated in several water matrices, to understand the influence of different parameters such as pH, salinity and flow rate on the uptake. Furthermore, a multivariate approach (Principal Component Analysis) permitted to explore the interactions involved in sorption, highlighting the influence of some physico-chemical characteristics of the analytes. The employment of this device in a field application confirmed the good performance of polyethersulfone for the detection of hydrophobic and mid-polar contaminants.

Due to the good sorption ability of PES membranes and the issues related to their use as protective membranes in dual-phase passive samplers, the study was then focused on understanding the sorption mechanisms for compounds with a broader variety of physico-chemical properties. The Principal Component Analysis was employed also in this part of the work, displaying hydrophobicity as the main driving force involved.

Moreover, a survey of the sorption affinity of the most employed commercial polyethersulfone membranes as protective layers in dual-phase passive samplers was performed. The results showed a different behaviour depending on the suppliers and the manufacturing process. This aspect is especially compelling considering the blurred use of different PES membranes in passive sampling devices and the absence of detailed information on them, especially in commercial samplers.

To conclude the study on PES membranes, the assessment of the partitioning between the protective membrane and the receiving phase was investigated in several field applications of the POCIS. Different distribution between the two layers was observed, suggesting the importance of keeping the extraction methodology for the sorbent and the protective membrane separate, to obtain reliable data for the analyte water concentrations.

Besides, a preliminary evaluation of the sorption ability of a biobased PLA/PCL polymeric film was carried out and the results were compared to those obtained using polyethersulfone. The comparison highlighted a definitely better performance of the commercial polyethersulfone in term of sorption and mechanical properties. Much more experimental effort is needed to find suitable biodegradable substitutes of classical polymeric membranes.

The last part of the PhD project, regarding the selection of receiving phases for the development of a hydrogel passive sampler for the detection of nitramines from freshwater, showed the challenges in the development of passive sampling devices for persistent and mobile polar chemicals in water present at very low concentrations. However, the development of passive samplers able to detect these compounds, actually not subject to reglations, is fundamental to assess their presence in the aquatic environment in the prospective of monitoring programs and ecotoxicological evaluations.

To conclude, this thesis pointed out the importance of the comprehension of the mechanism and the kinetics of sorption in passive sampling techniques. Furthermore, this work highlighted the effect of the selection of proper materials for the development of passive sampling devices for specific target compounds and the significance in the use of proper passive samplers on the evaluation of the concentration of the target contaminants in water matrices. Analogously, the analytes must be carefully selected to avoid the improper evaluation of their uptake on the devices employed for the sampling.

Publications

Scapuzzi, C.; Benedetti, B.; Di Carro, M.; Chiesa, E.; Pussini, N.; Magi, E. Passive Sampling of Organic Contaminants as a Novel Approach to Monitor Seawater Quality in Aquarium Ocean Tanks. Appl. Sci. 2022, 12, 2951. https://doi.org/10.3390/app12062951

Benedetti, B.; Baglietto, M.; MacKeown, H.; Scapuzzi, C.; Di Carro, M.; Magi, E. An optimized processing method for polar organic chemical integrative samplers deployed in seawater: Toward a maximization of the analysis accuracy for trace emerging contaminants. J. Chromatogr. A 2022, 1677, 463309. https://doi.org/10.1016/j.chroma.2022.463309

MacKeown, H., Benedetti, B., Scapuzzi, C., Di Carro, M., Magi, E. A Review on Polyethersulfone Membranes in Polar Organic Chemical Integrative Samplers: Preparation, Characterization and Innovation. Critical Reviews in Analytical Chemistry, 2022. https://doi.org/10.1080/10408347.2022.2131374

Benedetti, B., Di Carro, M., Scapuzzi, C., Magi, E. Solvent-Free Determination of Selected Polycyclic Aromatic Hydrocarbons in Plant Material Used for Food Supplements Preparation: Optimization of a Solid Phase Microextraction Method. Molecules, 28(16), 5937, 2023. https://doi.org/10.3390/molecules28165937

Scapuzzi, C., MacKeown, H., Benedetti, B., Baglietto, M., Di Carro, M., Magi, E. Polyethersulfone membrane as a single-phase passive sampler: Evaluation of the sampling performance for emerging contaminants in water, Microchemical Journal, 195, 109445, 2023. https://doi.org/10.1016/j.microc.2023.109445

References

[1]   Environmental Quality Standards (EQS) for Priority Substances: Annex I, Part A, Directive 2008/105/EC, 24 December 2008, amended by Directive 2013/39/EU, 24 August 2013, European Chemicals Agency (ECHA) (n.d.). https://echa.europa.eu/it/environmental-quality-standards?p_p_id=eucleflegislationlist_WAR_euclefportlet&p_p_lifecycle=0 (accessed December 13, 2023).

[2]   S. Sauvé, M. Desrosiers, A review of what is an emerging contaminant, Chemistry Central Journal 8 (2014) 15. https://doi.org/10.1186/1752-153X-8-15.

[3]   R. Kumar, M. Qureshi, D.K. Vishwakarma, N. Al-Ansari, A. Kuriqi, A. Elbeltagi, A. Saraswat, A review on emerging water contaminants and the application of sustainable removal technologies, Case Studies in Chemical and Environmental Engineering 6 (2022) 100219. https://doi.org/10.1016/j.cscee.2022.100219.

[4]   K. Kümmerer, 3.04 - Emerging Contaminants, in: P. Wilderer (Ed.), Treatise on Water Science, Elsevier, Oxford, 2011: pp. 69–87. https://doi.org/10.1016/B978-0-444-53199-5.00052-X.

[5]   I. Muñoz, J.C. López-Doval, N. De Castro-Català, M. Kuzmanovic, A. Ginebreda, S. Sabater, Effects of Emerging Contaminants on Biodiversity, Community Structure, and Adaptation of River Biota, in: M. Petrovic, S. Sabater, A. Elosegi, D. Barceló (Eds.), Emerging Contaminants in River Ecosystems: Occurrence and Effects Under Multiple Stress Conditions, Springer International Publishing, Cham, 2016: pp. 79–119. https://doi.org/10.1007/698_2015_5013.

[6]   R. Álvarez-Ruiz, Y. Picó, Analysis of emerging and related pollutants in aquatic biota, Trends in Environmental Analytical Chemistry 25 (2020) e00082. https://doi.org/10.1016/j.teac.2020.e00082.

[7]   T. aus der Beek, F.-A. Weber, A. Bergmann, S. Hickmann, I. Ebert, A. Hein, A. Küster, Pharmaceuticals in the environment—Global occurrences and perspectives, Environmental Toxicology and Chemistry 35 (2016) 823–835. https://doi.org/10.1002/etc.3339.

[8]   Y. Chen, Z. Guo, X. Wang, C. Qiu, Sample preparation, Journal of Chromatography A 1184 (2008) 191–219. https://doi.org/10.1016/j.chroma.2007.10.026.

[9]   J. Pawliszyn*, Sample Preparation: Quo Vadis?, ACS Publications (2003). https://doi.org/10.1021/ac034094h.

[10]   J.S. Câmara, R. Perestrelo, C.V. Berenguer, C.F.P. Andrade, T.M. Gomes, B. Olayanju, A. Kabir, C. M. R. Rocha, J.A. Teixeira, J.A.M. Pereira, Green Extraction Techniques as Advanced Sample Preparation Approaches in Biological, Food, and Environmental Matrices: A Review, Molecules 27 (2022) 2953. https://doi.org/10.3390/molecules27092953.

[11]   C.L. Arthur, Janusz. Pawliszyn, Solid phase microextraction with thermal desorption using fused silica optical fibers, Analitical Chemistry 62 (1990) 2145–2148. https://doi.org/10.1021/ac00218a019.

[12]   N. Riboni, F. Fornari, F. Bianchi, M. Careri, Recent Advances in In Vivo SPME Sampling, Separations 7 (2020) 6. https://doi.org/10.3390/separations7010006.

[13]   N.H. Godage, E. Gionfriddo, A critical outlook on recent developments and applications of matrix compatible coatings for solid phase microextraction, Trends in Analytical Chemistry 111 (2019) 220–228. https://doi.org/10.1016/j.trac.2018.12.019.

[14] B. Benedetti, M. Di Carro, C. Scapuzzi, E. Magi, Solvent-Free Determination of Selected Polycyclic Aromatic Hydrocarbons in Plant Material Used for Food Supplements Preparation: Optimization of a Solid Phase Microextraction Method, Molecules 28 (2023) 5937. https://doi.org/10.3390/molecules28165937.

[15] C.S. Gordon, J.T. Lowe, Carbon-monoxide detector, US1644014A, 1927. https://patents.google.com/patent/US1644014A/en (accessed December 4, 2023).

[16] J.N. Huckins, J.D. Petty, K. Booij, Monitors of organic chemicals in the environment: semipermeable membrane devices, Springer, New York, 2006.

[17] J.N. Huckins, M.W. Tubergen, G.K. Manuweera, Semipermeable membrane devices containing model lipid: A new approach to monitoring the bioavaiiability of lipophilic contaminants and estimating their bioconcentration potential, Chemosphere 20 (1990) 533–552. https://doi.org/10.1016/0045-6535(90)90110-F.

[18] A. Charriau, S. Lissalde, G. Poulier, N. Mazzella, R. Buzier, G. Guibaud, Overview of the Chemcatcher® for the passive sampling of various pollutants in aquatic environments Part A: Principles, calibration, preparation and analysis of the sampler, Talanta 148 (2016) 556–571. https://doi.org/10.1016/j.talanta.2015.06.064.

[19] D.A. Alvarez, J.D. Petty, J.N. Huckins, T.L. Jones-Lepp, D.T. Getting, J.P. Goddard, S.E. Manahan, Development of a passive, in situ, integrative sampler for hydrophilic organic contaminants in aquatic environments, Environmental Toxicology and Chemistry 23 (2004) 1640–1648. https://doi.org/10.1897/03-603.

[20] W. Davison, H. Zhang, In situ speciation measurements of trace components in natural waters using thin-film gels, Nature 367 (1994) 546–548. https://doi.org/10.1038/367546a0.

[21] C.-E. Chen, H. Zhang, K.C. Jones, A novel passive water sampler for in situ sampling of antibiotics, Journal of Environmental Monitoring 14 (2012) 1523–1530. https://doi.org/10.1039/C2EM30091E.

[22] B. Bonnaud, N. Mazzella, P. Boutet, A. Daval, C. Miège, Calibration comparison between two passive samplers -o-DGT and POCIS- for 109 hydrophilic emerging and priority organic compounds, Science of The Total Environment 869 (2023) 161720. https://doi.org/10.1016/j.scitotenv.2023.161720.

[23] J.K. Challis, K.M. Stroski, K.H. Luong, M.L. Hanson, C.S. Wong, Field Evaluation and in Situ Stress Testing of the Organic-Diffusive Gradients in Thin-Films Passive Sampler, Environmental Science and Technology 52 (2018) 12573–12582. https://doi.org/10.1021/acs.est.8b03622.

[24] G.A. Mills, A. Gravell, B. Vrana, C. Harman, H. Budzinski, N. Mazzella, T. Ocelka, Measurement of environmental pollutants using passive sampling devices – an updated commentary on the current state of the art, Environmental Science: Processes and Impacts 16 (2014) 369–373. https://doi.org/10.1039/C3EM00585B.

[25] H. MacKeown, B. Benedetti, M. Di Carro, E. Magi, The study of polar emerging contaminants in seawater by passive sampling: A review, Chemosphere 299 (2022) 134448. https://doi.org/10.1016/j.chemosphere.2022.134448.

[26] X. Gong, K. Li, C. Wu, L. Wang, H. Sun, Passive sampling for monitoring polar organic pollutants in water by three typical samplers, Trends in Environmental Analytical Chemistry 17 (2018) 23–33. https://doi.org/10.1016/j.teac.2018.01.002.

[27] J.N. Huckins, J.D. Petty, J.A. Lebo, F.V. Almeida, K. Booij, D.A. Alvarez, W.L. Cranor, R.C. Clark, B.B. Mogensen, Development of the Permeability/Performance Reference Compound Approach for In Situ Calibration of Semipermeable Membrane Devices, Environmental Science and Technology 36 (2002) 85–91. https://doi.org/10.1021/es010991w.

[28] A.C. Taylor, G.R. Fones, B. Vrana, G.A. Mills, Applications for Passive Sampling of Hydrophobic Organic Contaminants in Water—A Review, Critical Reviews in

Analytical Chemistry 51 (2021) 20–54.
https://doi.org/10.1080/10408347.2019.1675043.

[29] B. Chepchirchir, Occurrence and fate of endocrine disrupting chemicals and other hydrophobic organic compounds in a tropical river in Kenya, Technical University Bergakademie Freiberg, 2017.

[30] K. Booij, Passive Sampler Exchange Kinetics in Large and Small Water Volumes Under Mixed Rate Control by Sorbent and Water Boundary Layer, Environmental Toxicology and Chemistry 40 (2021) 1241–1254. https://doi.org/10.1002/etc.4989.

[31] A.P. Tcaciuc, J.N. Apell, P.M. Gschwend, Modeling the transport of organic chemicals between polyethylene passive samplers and water in finite and infinite bath conditions, Environmental Toxicology and Chemistry 34 (2015) 2739–2749. https://doi.org/10.1002/etc.3128.

[32] K. Booij, B. Vrana, J.N. Huckins, Chapter 7 Theory, modelling and calibration of passive samplers used in water monitoring, Comprehensive Analytical Chemistry 48 (2007) 141–169. https://doi.org/10.1016/S0166-526X(06)48007-7.

[33] C. Miège, N. Mazzella, I. Allan, V. Dulio, F. Smedes, C. Tixier, E. Vermeirssen, J. Brant, S. O'Toole, H. Budzinski, J.-P. Ghestem, P.-F. Staub, S. Lardy-Fontan, J.-L. Gonzalez, M. Coquery, B. Vrana, Position paper on passive sampling techniques for the monitoring of contaminants in the aquatic environment – Achievements to date and perspectives, Trends in Environmental Analytical Chemistry 8 (2015) 20–26. https://doi.org/10.1016/j.teac.2015.07.001.

[34] K. Booij, H.E. Hofmans, C.V. Fischer, E.M. Van Weerlee, Temperature-dependent uptake rates of nonpolar organic compounds by semipermeable membrane devices and low-density polyethylene membranes, Environmental Science and Technology 37 (2003) 361–366. https://doi.org/10.1021/es025739i.

[35] Y. Jeong, A. Schäffer, K. Smith, A comparison of equilibrium and kinetic passive sampling for the monitoring of aquatic organic contaminants in German rivers, Water Research 145 (2018) 248–258. https://doi.org/10.1016/j.watres.2018.08.016.

[36] S.L. MacLeod, E.L. McClure, C.S. Wong, Laboratory calibration and field deployment of the Polar organic chemical integrative sampler for pharmaceuticals and personal care products in wastewater and surface water, Environmental Toxicology and Chemistry 26 (2007) 2517–2529. https://doi.org/10.1897/07-238.1.

[37] M. Di Carro, L. Bono, E. Magi, A simple recirculating flow system for the calibration of polar organic chemical integrative samplers (POCIS): Effect of flow rate on different water pollutants, Talanta 120 (2014) 30–33. https://doi.org/10.1016/j.talanta.2013.11.088.

[38] C. Harman, K.-E. Tollefsen, O. Bøyum, K. Thomas, M. Grung, Uptake rates of alkylphenols, PAHs and carbazoles in semipermeable membrane devices (SPMDs) and polar organic chemical integrative samplers (POCIS), Chemosphere 72 (2008) 1510–1516. https://doi.org/10.1016/j.chemosphere.2008.04.091.

[39] K. Booij, H.M. Sleiderink, F. Smedes, Calibrating the uptake kinetics of semipermeable membrane devices using exposure standards, Environmental Toxicology and Chemistry 17 (1998) 1236–1245. https://doi.org/10.1002/etc.5620170707.

[40] I. Carpinteiro, A. Schopfer, N. Estoppey, C. Fong, D. Grandjean, L.F. de Alencastro, Evaluation of performance reference compounds (PRCs) to monitor emerging polar contaminants by polar organic chemical integrative samplers (POCIS) in rivers, Analitical and Bioanalitical Chemistry 408 (2016) 1067–1078. https://doi.org/10.1007/s00216-015-9199-8.

[41] N. Mazzella, S. Lissalde, S. Moreira, F. Delmas, P. Mazellier, J.N. Huckins, Evaluation of the Use of Performance Reference Compounds in an Oasis-HLB

Adsorbent Based Passive Sampler for Improving Water Concentration Estimates of Polar Herbicides in Freshwater, Environmental Science and Technology 44 (2010) 1713–1719. https://doi.org/10.1021/es902256m.

[42] A. Belles, P. Pardon, H. Budzinski, Development of an adapted version of polar organic chemical integrative samplers (POCIS-Nylon), Analitical and Bioanalitical Chemistry 406 (2014) 1099–1110. https://doi.org/10.1007/s00216-013-7286-2.

[43] C. Harman, I.J. Allan, E.L.M. Vermeirssen, Calibration and use of the polar organic chemical integrative sampler—a critical review, Environmental Toxicology and Chemistry 31 (2012) 2724–2738. https://doi.org/10.1002/etc.2011.

[44] K. Booij, N.L. Maarsen, M. Theeuwen, R. van Bommel, A method to account for the effect of hydrodynamics on polar organic compound uptake by passive samplers, Environmental Toxicology and Chemistry 36 (2017) 1517–1524. https://doi.org/10.1002/etc.3700.

[45] V. Glanzmann, N. Reymond, C. Weyermann, N. Estoppey, An improved Chemcatcher-based method for the integrative passive sampling of 44 hydrophilic micropollutants in surface water – Part A: Calibration under four controlled hydrodynamic conditions, Science of The Total Environment 871 (2023) 162037. https://doi.org/10.1016/j.scitotenv.2023.162037.

[46] V. Glanzmann, K. Booij, N. Reymond, C. Weyermann, N. Estoppey, Determining the Mass Transfer Coefficient of the Water Boundary Layer at the Surface of Aquatic Integrative Passive Samplers, Environmental Science and Technology 56 (2022) 6391–6398. https://doi.org/10.1021/acs.est.1c08088.

[47] N. Gilart, F. Borrull, N. Fontanals, R.M. Marcé, Selective materials for solid-phase extraction in environmental analysis, Trends in Environmental Analytical Chemistry 1 (2014) e8–e18. https://doi.org/10.1016/j.teac.2013.11.002.

[48] A. Andrade-Eiroa, M. Canle, V. Leroy-Cancellieri, V. Cerdà, Solid-phase extraction of organic compounds: A critical review (Part I), TrAC Trends in Analytical Chemistry 80 (2016) 641–654. https://doi.org/10.1016/j.trac.2015.08.015.

[49] D. Zahn, I.J. Neuwald, T.P. Knepper, Analysis of mobile chemicals in the aquatic environment—current capabilities, limitations and future perspectives, Analitical and Bioanalitical Chemistry 412 (2020) 4763–4784. https://doi.org/10.1007/s00216-020-02520-z.

[50] L. Chen, X. Wang, W. Lu, X. Wu, J. Li, Molecular imprinting: perspectives and applications, Chemical Society Reviews 45 (2016) 2137–2211. https://doi.org/10.1039/C6CS00061D.

[51] K. Godlewska, P. Stepnowski, M. Paszkiewicz, Pollutant analysis using passive samplers: principles, sorbents, calibration and applications. A review, Environmental Chemistry Letters 19 (2021) 465–520. https://doi.org/10.1007/s10311-020-01079-6.

[52] K. Noro, S. Endo, Y. Shikano, A. Banno, Y. Yabuki, Development and Calibration of the Polar Organic Chemical Integrative Sampler (POCIS) for Neonicotinoid Pesticides, Environmental Toxicology and Chemistry 39 (2020) 1325–1333. https://doi.org/10.1002/etc.4729.

[53] P. Oliveri, C. Malegori, R. Simonetti, M. Casale, The impact of signal pre-processing on the final interpretation of analytical outcomes – A tutorial, Analytica Chimica Acta 1058 (2019) 9–17. https://doi.org/10.1016/j.aca.2018.10.055.

[54] P. Thavamani, M. Megharaj, R. Naidu, Multivariate analysis of mixed contaminants (PAHs and heavy metals) at manufactured gas plant site soils, Environmental Monitoring and Assessment 184 (2012) 3875–3885. https://doi.org/10.1007/s10661-011-2230-4.

[55] M. Forina, C. Armanino, S. Lanteri, R. Leardi, Methods of varimax rotation in factor analysis with applications in clinical and food chemistry, Journal of Chemometrics 3 (1989) 115–125. https://doi.org/10.1002/cem.1180030504.

[56] Y. Jeong, A. Schäffer, K. Smith, Equilibrium partitioning of organic compounds to OASIS HLB® as a function of compound concentration, pH, temperature and salinity, Chemosphere 174 (2017) 297–305. https://doi.org/10.1016/j.chemosphere.2017.01.116.

[57] C. Scapuzzi, B. Benedetti, M. Di Carro, E. Chiesa, N. Pussini, E. Magi, Passive Sampling of Organic Contaminants as a Novel Approach to Monitor Seawater Quality in Aquarium Ocean Tanks, Applied Sciences 12 (2022) 2951. https://doi.org/10.3390/app12062951.

[58] N. Estoppey, J. Mathieu, E. Gascon Diez, E. Sapin, O. Delémont, P. Esseiva, L.F. de Alencastro, S. Coudret, P. Folly, Monitoring of explosive residues in lake-bottom water using Polar Organic Chemical Integrative Sampler (POCIS) and chemcatcher: determination of transfer kinetics through Polyethersulfone (PES) membrane is crucial, Environmental Pollution 252 (2019) 767–776. https://doi.org/10.1016/j.envpol.2019.04.087.

[59] N.A.O. Morin, N. Mazzella, H.P.H. Arp, J. Randon, J. Camilleri, L. Wiest, M. Coquery, C. Miège, Kinetic accumulation processes and models for 43 micropollutants in "pharmaceutical" POCIS, Science of the Total Environment 615 (2018) 197–207. https://doi.org/10.1016/j.scitotenv.2017.08.311.

[60] L. Silvani, C. Riccardi, E. Eek, M.P. Papini, N.A.O. Morin, G. Cornelissen, A.M.P. Oen, S.E. Hale, Monitoring alkylphenols in water using the polar organic chemical integrative sampler (POCIS): Determining sampling rates via the extraction of PES membranes and Oasis beads, Chemosphere 184 (2017) 1362–1371. https://doi.org/10.1016/j.chemosphere.2017.06.083.

[61] E.L.M. Vermeirssen, C. Dietschweiler, B.I. Escher, J. van der Voet, J. Hollender, Transfer Kinetics of Polar Organic Compounds over Polyethersulfone Membranes in the Passive Samplers Pocis and Chemcatcher, Environmental Science and Technolology 46 (2012) 6759–6766. https://doi.org/10.1021/es3007854.

[62] H. MacKeown, B. Benedetti, C. Scapuzzi, M. Di Carro, E. Magi, A Review on Polyethersulfone Membranes in Polar Organic Chemical Integrative Samplers: Preparation, Characterization and Innovation, Critical Reviews in Analytical Chemistry (2022). https://doi.org/10.1080/10408347.2022.2131374.

[63] A. Prieto, R. Rodil, J.B. Quintana, I. Rodríguez, R. Cela, M. Möder, Evaluation of low-cost disposable polymeric materials for sorptive extraction of organic pollutants in water samples, Analytica Chimica Acta 716 (2012) 119–127. https://doi.org/10.1016/j.aca.2011.12.023.

[64] J. Casado, I. Rodríguez, M. Ramil, R. Cela, Polyethersulfone solid-phase microextraction followed by liquid chromatography quadrupole time-of-flight mass spectrometry for benzotriazoles determination in water samples, Journal of Chromatography A 1299 (2013) 40–47. https://doi.org/10.1016/j.chroma.2013.05.061.

[65] L. Blanco-Zubiaguirre, A. Delgado, O. Ros, O. Posada-Ureta, A. Vallejo, A. Prieto, M. Olivares, N. Etxebarria, Assessment of commercially available polymeric materials for sorptive microextraction of priority and emerging nonpolar organic pollutants in environmental water samples, Environmental Science and Pollution Research 21 (2014) 11867–11883. https://doi.org/10.1007/s11356-013-2481-4.

[66] J. Cavalheiro, M. Monperrus, D. Amouroux, H. Preud'Homme, A. Prieto, O. Zuloaga, In-port derivatization coupled to different extraction techniques for the

determination of alkylphenols in environmental water samples, Journal of Chromatography A 1340 (2014) 1–7. https://doi.org/10.1016/j.chroma.2014.03.013.

[67] A. Prieto, R. Rodil, J.B. Quintana, R. Cela, M. Möder, I. Rodríguez, Evaluation of polyethersulfone performance for the microextraction of polar chlorinated herbicides from environmental water samples, Talanta 122 (2014) 264–271. https://doi.org/10.1016/j.talanta.2014.01.024.

[68] O. Ros, J.K. Izaguirre, M. Olivares, C. Bizarro, M. Ortiz-Zarragoitia, M.P. Cajaraville, N. Etxebarria, A. Prieto, A. Vallejo, Determination of endocrine disrupting compounds and their metabolites in fish bile, Science of the Total Environment 536 (2015) 261–267. https://doi.org/10.1016/j.scitotenv.2015.07.074.

[69] O. Ros, A. Vallejo, L. Blanco-Zubiaguirre, M. Olivares, A. Delgado, N. Etxebarria, A. Prieto, Microextraction with polyethersulfone for bisphenol-A, alkylphenols and hormones determination in water samples by means of gas chromatography-mass spectrometry and liquid chromatography-tandem mass spectrometry analysis, Talanta 134 (2015) 247–255. https://doi.org/10.1016/j.talanta.2014.11.015.

[70] L. Mijangos, H. Ziarrusta, M. Olivares, O. Zuloaga, M. Möder, N. Etxebarria, A. Prieto, Simultaneous determination of 41 multiclass organic pollutants in environmental waters by means of polyethersulfone microextraction followed by liquid chromatography–tandem mass spectrometry, Analytical and Bioanalytical Chemistry 410 (2018) 615–632. https://doi.org/10.1007/s00216-017-0763-2.

[71] O. Posada-Ureta, M. Olivares, A. Delgado, A. Prieto, A. Vallejo, M. Irazola, A. Paschke, N. Etxebarria, Applicability of polydimethylsiloxane (PDMS) and polyethersulfone (PES) as passive samplers of more hydrophobic organic compounds in intertidal estuarine environments, Science of the Total Environment 578 (2017) 392–398. https://doi.org/10.1016/j.scitotenv.2016.10.194.

[72] O. Posada-Ureta, M. Olivares, L. Zatón, A. Delgado, A. Prieto, A. Vallejo, A. Paschke, N. Etxebarria, Uptake calibration of polymer-based passive samplers for monitoring priority and emerging organic non-polar pollutants in WWTP effluents, Analytical and Bioanalytical Chemistry 408 (2016) 3165–3175. https://doi.org/10.1007/s00216-016-9381-7.

[73] L. Mijangos, H. Ziarrusta, A. Prieto, O. Zugazua, O. Zuloaga, M. Olivares, A. Usobiaga, A. Paschke, N. Etxebarria, Evaluation of polar organic chemical integrative and hollow fibre samplers for the determination of a wide variety of organic polar compounds in seawater, Talanta 185 (2018) 469–476. https://doi.org/10.1016/j.talanta.2018.03.103.

[74] B.S. Chepchirchir, X. Zhou, A. Paschke, G. Schüürmann, Polyethersulfone as suitable passive sampler for waterborne hydrophobic organic compounds – Laboratory calibration and field test in the Sosiani river, Kenya, Science of the Total Environment 699 (2020) 134056. https://doi.org/10.1016/j.scitotenv.2019.134056.

[75] H. MacKeown, E. Magi, M. Di Carro, B. Benedetti, Unravelling the role of membrane pore size in polar organic chemical integrative samplers (POCIS) to broaden the polarity range of sampled analytes, Analytical and Bioanalytical Chemistry 414 (2022) 1963–1972. https://doi.org/10.1007/s00216-021-03832-4.

[76] B. Benedetti, M. Baglietto, H. MacKeown, C. Scapuzzi, M. Di Carro, E. Magi, An optimized processing method for polar organic chemical integrative samplers deployed in seawater: Toward a maximization of the analysis accuracy for trace emerging contaminants, Journal of Chromatography A 1677 (2022) 463309. https://doi.org/10.1016/j.chroma.2022.463309.

[77] K. Booij, F. Smedes, I.J. Allan, Guidelines for determining polymer-water and polymer-polymer partition coefficients of organic compounds, 61 (2017) 1–32. https://doi.org/10.17895/ICES.PUB.3285.

[78] R. Leardi, C. Melzi, G. Polotti, CAT (Chemometric Agile Tool), (2023). http://gruppochemiometria.it/index.php/software.

[79] F. Vanryckeghem, S. Huysman, F. Smedes, H. Van Langenhove, L. Vanhaecke, K. Demeestere, A Simple Teabag Equilibrium Passive Sampler using hydrophilic divinylbenzene sorbent for contaminants of emerging concern in the marine environment, Science of the Total Environment 777 (2021). https://doi.org/10.1016/j.scitotenv.2021.146055.

[80] N.B. Hartmann, S. Rist, J. Bodin, L.H. Jensen, S.N. Schmidt, P. Mayer, A. Meibom, A. Baun, Microplastics as vectors for environmental contaminants: Exploring sorption, desorption, and transfer to biota, Integrated Environmental Assessment and Management 13 (2017) 488–493. https://doi.org/10.1002/ieam.1904.

[81] E. Steinle-Darling, M. Zedda, M.H. Plumlee, H.F. Ridgway, M. Reinhard, Evaluating the impacts of membrane type, coating, fouling, chemical properties and water chemistry on reverse osmosis rejection of seven nitrosoalklyamines, including NDMA, Water Research 41 (2007) 3959–3967. https://doi.org/10.1016/j.watres.2007.05.034.

[82] E.L. Teuten, J.M. Saquing, D.R.U. Knappe, M.A. Barlaz, S. Jonsson, A. Björn, S.J. Rowland, R.C. Thompson, T.S. Galloway, R. Yamashita, D. Ochi, Y. Watanuki, C. Moore, P.H. Viet, T.S. Tana, M. Prudente, R. Boonyatumanond, M.P. Zakaria, K. Akkhavong, Y. Ogata, H. Hirai, S. Iwasa, K. Mizukawa, Y. Hagino, A. Imamura, M. Saha, H. Takada, Transport and release of chemicals from plastics to the environment and to wildlife, Philosophical Transactions of the Royal Society B Biological Sciences 364 (2009) 2027–2045. https://doi.org/10.1098/rstb.2008.0284.

[83] T. Hüffer, T. Hofmann, Sorption of non-polar organic compounds by micro-sized plastic particles in aqueous solution, Environmental Pollution 214 (2016) 194–201. https://doi.org/10.1016/j.envpol.2016.04.018.

[84] J.J. Pignatello, B. Xing, Mechanisms of Slow Sorption of Organic Chemicals to Natural Particles, Environmental Science and Technology 30 (1996) 1–11. https://doi.org/10.1021/es940683g.

[85] B. Xing, J.J. Pignatello, Dual-Mode Sorption of Low-Polarity Compounds in Glassy Poly(Vinyl Chloride) and Soil Organic Matter, Environmental Science and Technology 31 (1997) 792–799. https://doi.org/10.1021/es960481f.

[86] E. Rutkowska, B. Łozowicka, P. Kaczyński, Three approaches to minimize matrix effects in residue analysis of multiclass pesticides in dried complex matrices using gas chromatography tandem mass spectrometry, Food Chemistry 279 (2019) 20–29. https://doi.org/10.1016/j.foodchem.2018.11.130.

[87] R. Upadhyay, S. Singh, G. Kaur, Sorption of pharmaceuticals over microplastics' surfaces: interaction mechanisms and governing factors, Environmental Monitoring and Assessment 194 (2022) 803. https://doi.org/10.1007/s10661-022-10475-0.

[88] C. Wu, K. Zhang, X. Huang, J. Liu, Sorption of pharmaceuticals and personal care products to polyethylene debris, Environmental Science and Pollution Research 23 (2016) 8819–8826. https://doi.org/10.1007/s11356-016-6121-7.

[89] F. Smedes, Silicone–water partition coefficients determined by cosolvent method for chlorinated pesticides, musks, organo phosphates, phthalates and more, Chemosphere 210 (2018) 662–671. https://doi.org/10.1016/j.chemosphere.2018.07.054.

[90] M.G. Pintado-Herrera, P.A. Lara-Martín, E. González-Mazo, I.J. Allan, Determination of silicone rubber and low-density polyethylene diffusion and polymer/water partition coefficients for emerging contaminants, Environmental Toxicology and Chemistry 35 (2016) 2162–2172. https://doi.org/10.1002/etc.3390.

[91] R. Verhagen, E. O'Malley, F. Smedes, J.F. Mueller, S. Kaserzon, Calibration parameters for the passive sampling of organic UV filters by silicone; diffusion coefficients and silicone–water partition coefficients, Chemosphere 223 (2019) 731–737. https://doi.org/10.1016/j.chemosphere.2019.02.077.

[92] L. Brüggemann, W. Quapp, R. Wennrich, Test for non-linearity concerning linear calibrated chemical measurements, Accreditation and Quality Assurance 11 (2006) 625–631. https://doi.org/10.1007/s00769-006-0205-x.

[93] P.S. Bäuerlein, J.E. Mansell, T.L. ter Laak, P. de Voogt, Sorption Behavior of Charged and Neutral Polar Organic Compounds on Solid Phase Extraction Materials: Which Functional Group Governs Sorption?, Environmental Science and Technology 46 (2012) 954–961. https://doi.org/10.1021/es203404x.

[94] J.Y. Goh, K.S. Goh, Y.M. Yip, C.K. Ng, High salinity enhances the adsorption of 17α-ethinyl estradiol by polyethersulfone membrane: isotherm modelling and molecular simulation, International Journal of Environmental Science and Technology 19 (2022) 5195–5204. https://doi.org/10.1007/s13762-021-03468-y.

[95] C.K. Ng, C.D. Bope, A. Nalaparaju, Y. Cheng, L. Lu, R. Wang, B. Cao, Concentrating synthetic estrogen 17A-ethinylestradiol using microporous polyethersulfone hollow fiber membranes: Experimental exploration and molecular simulation, Chemical Engineering Journal 314 (2017) 80–87. https://doi.org/10.1016/j.cej.2016.12.109.

[96] C.D. Bope, A. Nalaparaju, C.K. Ng, Y. Cheng, L. Lu, Molecular simulation on the interaction of Ethinylestradiol (EE2) with polymer membranes in wastewater purification, Molecular Simulation 44 (2018) 638–647. https://doi.org/10.1080/08927022.2018.1426853.

[97] V.T. Djomte, S. Chen, C.K. Chambliss, Effects of suspended sediment on POCIS sampling rates, Chemosphere 241 (2020) 124972. https://doi.org/10.1016/j.chemosphere.2019.124972.

[98] L. Charlestra, A. Amirbahman, D.L. Courtemanch, D.A. Alvarez, H. Patterson, Estimating pesticide sampling rates by the polar organic chemical integrative sampler (POCIS) in the presence of natural organic matter and varying hydrodynamic conditions, Environmental Pollution 169 (2012) 98–104. https://doi.org/10.1016/j.envpol.2012.05.001.

[99] S. Lissalde, N. Mazzella, P. Mazellier, Polar organic chemical integrative samplers for pesticides monitoring: Impacts of field exposure conditions, Science of The Total Environment 488–489 (2014) 188–196. https://doi.org/10.1016/j.scitotenv.2014.04.069.

[100] S.F. Anis, R. Hashaikeh, N. Hilal, Microfiltration membrane processes: A review of research trends over the past decade, Journal of Water Process Engineering 32 (2019) 100941. https://doi.org/10.1016/j.jwpe.2019.100941.

[101] S. Ramos, V. Homem, A. Alves, L. Santos, Advances in analytical methods and occurrence of organic UV-filters in the environment — A review, Science of The Total Environment 526 (2015) 278–311. https://doi.org/10.1016/j.scitotenv.2015.04.055.

[102] L.A. MacManus-Spencer, M.L. Tse, J.L. Klein, A.E. Kracunas, Aqueous photolysis of the organic ultraviolet filter chemical octyl methoxycinnamate, Environmental Science and Technology 45 (2011) 3931–3937. https://doi.org/10.1021/es103682a.

[103] S. Suchana, E. Passeport, Implications of polar organic chemical integrative sampler for high membrane sorption and suitability of polyethersulfone as a single-phase sampler, Science of The Total Environment 850 (2022) 157898. https://doi.org/10.1016/j.scitotenv.2022.157898.

[104] S. Endo, Y. Matsuura, Characterizing Sorption and Permeation Properties of Membrane Filters Used for Aquatic Integrative Passive Samplers, Environmental Science and Technology 52 (2018) 2118–2125. https://doi.org/10.1021/acs.est.7b05144.

[105] V. Fauvelle, S.L. Kaserzon, N. Montero, S. Lissalde, I.J. Allan, G. Mills, N. Mazzella, J.F. Mueller, K. Booij, Dealing with Flow Effects on the Uptake of Polar Compounds by Passive Samplers, Environmental Science and Technology 51 (2017) 2536–2537. https://doi.org/10.1021/acs.est.7b00558.

[106] K.T.N. Nguyen, C. Scapolla, M. Di Carro, E. Magi, Rapid and selective determination of UV filters in seawater by liquid chromatography–tandem mass spectrometry combined with stir bar sorptive extraction, Talanta 85 (2011) 2375–2384. https://doi.org/10.1016/j.talanta.2011.07.085.

[107] D.A. Alvarez, J.N. Huckins, J.D. Petty, T. Jones-Lepp, F. Stuer-Lauridsen, D.T. Getting, J.P. Goddard, A. Gravell, Chapter 8 Tool for monitoring hydrophilic contaminants in water: polar organic chemical integrative sampler (POCIS), Comprehensive Analytical Chemistry 48 (2007) 171–197. https://doi.org/10.1016/S0166-526X(06)48008-9.

[108] Y. Jeong, A. Schäffer, K. Smith, Comparison of the sampling rates and partitioning behaviour of polar and non-polar contaminants in the polar organic chemical integrative sampler and a monophasic mixed polymer sampler for application as an equilibrium passive sampler, Science of the Total Environment 627 (2018) 905–915. https://doi.org/10.1016/j.scitotenv.2018.01.273.

[109] F. Smedes, R.W. Geertsma, T. van der Zande, K. Booij, Polymer−Water Partition Coefficients of Hydrophobic Compounds for Passive Sampling: Application of Cosolvent Models for Validation, Environmental Science and Technology 43 (2009) 7047–7054. https://doi.org/10.1021/es9009376.

[110] T. Zhu, C.T. Jafvert, D. Fu, Y. Hu, A novel method for measuring polymer-water partition coefficients, Chemosphere 138 (2015) 973–979. https://doi.org/10.1016/j.chemosphere.2014.12.040.

[111] S.L. Kaserzon, D.W. Hawker, K. Kennedy, M. Bartkow, S. Carter, K. Booij, J.F. Mueller, Characterisation and comparison of the uptake of ionizable and polar pesticides, pharmaceuticals and personal care products by POCIS and Chemcatchers, Environmental Sciences: Processes and Impacts 16 (2014) 2517–2526. https://doi.org/10.1039/c4em00392f.

[112] Y. Jeong, H. ah Kwon, H.P. Jeon, A. Schäffer, K. Smith, Quantitative evaluation of polyethersulfone and polytetrafluoroethylene membrane sorption in a polar organic chemical integrative sampler (POCIS), Environmental Pollution 266 (2020). https://doi.org/10.1016/j.envpol.2020.115224.

[113] C. Scapuzzi, H. MacKeown, B. Benedetti, M. Baglietto, M. Di Carro, E. Magi, Polyethersulfone membrane as a single-phase passive sampler: Evaluation of the sampling performance for emerging contaminants in water, Microchemical Journal 195 (2023) 109445. https://doi.org/10.1016/j.microc.2023.109445.

[114] B.S. Chepchirchir, X. Zhou, A. Paschke, G. Schüürmann, Polyethersulfone as suitable passive sampler for waterborne hydrophobic organic compounds – Laboratory calibration and field test in the Sosiani river, Kenya, Science of The Total Environment 699 (2020) 134056. https://doi.org/10.1016/j.scitotenv.2019.134056.

[115] A. Martin, C. Margoum, J. Randon, M. Coquery, Silicone rubber selection for passive sampling of pesticides in water, Talanta 160 (2016) 306–313. https://doi.org/10.1016/j.talanta.2016.07.019.

[116] R. Guibal, R. Buzier, S. Lissalde, G. Guibaud, Adaptation of diffusive gradients in thin films technique to sample organic pollutants in the environment: An overview of o-DGT passive samplers, Science of The Total Environment 693 (2019) 133537. https://doi.org/10.1016/j.scitotenv.2019.07.343.

[117] H. Rabiee, M.H.D.A. Farahani, V. Vatanpour, Preparation and characterization of emulsion poly(vinyl chloride) (EPVC)/TiO2 nanocomposite ultrafiltration membrane, Journal of Membrane Science 472 (2014) 185–193. https://doi.org/10.1016/j.memsci.2014.08.051.

[118] A. Pihlajamäki, P. Väisänen, M. Nyström, Characterization of clean and fouled polymeric ultrafiltration membranes by Fourier transform IR spectroscopy–attenuated total reflection, Colloids and Surfaces A: Physicochemical and Engineering Aspects 138 (1998) 323–333. https://doi.org/10.1016/S0927-7757(96)03883-6.

[119] A. Jalali, A. Shockravi, V. Vatanpour, M. Hajibeygi, Preparation and characterization of novel microporous ultrafiltration PES membranes using synthesized hydrophilic polysulfide-amide copolymer as an additive in the casting solution, Microporous and Mesoporous Materials 228 (2016) 1–13. https://doi.org/10.1016/j.micromeso.2016.03.024.

[120] A. Shockravi, V. Vatanpour, Z. Najjar, S. Bahadori, A. Javadi, A new high performance polyamide as an effective additive for modification of antifouling properties and morphology of asymmetric PES blend ultrafiltration membranes, Microporous and Mesoporous Materials 246 (2017) 24–36. https://doi.org/10.1016/j.micromeso.2017.03.013.

[121] V. Vatanpour, A. Shockravi, H. Zarrabi, Z. Nikjavan, A. Javadi, Fabrication and characterization of anti-fouling and anti-bacterial Ag-loaded graphene oxide/polyethersulfone mixed matrix membrane, Journal of Industrial and Engineering Chemistry 30 (2015) 342–352. https://doi.org/10.1016/j.jiec.2015.06.004.

[122] M.H. Abraham, A. Ibrahim, A.M. Zissimos, Determination of sets of solute descriptors from chromatographic measurements, Journal of Chromatography A 1037 (2004) 29–47. https://doi.org/10.1016/j.chroma.2003.12.004.

[123] M. Caban, H. Męczykowska, P. Stepnowski, Application of the PASSIL technique for the passive sampling of exemplary polar contaminants (pharmaceuticals and phenolic derivatives) from water, Talanta 155 (2016) 185–192. https://doi.org/10.1016/j.talanta.2016.04.035.

[124] B. Medon, B.G. Pautler, A. Sweett, J. Roberts, F.F. Risacher, L.A. D'Agostino, J. Conder, J.R. Gauthier, S.A. Mabury, A. Patterson, P. McIsaac, R. Mitzel, S.G. Hakimabadi, A.L.-T. Pham, A field-validated equilibrium passive sampler for the monitoring of per- and polyfluoroalkyl substances (PFAS) in sediment pore water and surface water, Environmental Science: Processes and Impacts 25 (2023) 980–995. https://doi.org/10.1039/D2EM00483F.

[125] X. Ji, J.K. Challis, M. Brinkmann, A critical review of diffusive gradients in thin films technique for measuring organic pollutants: Potential limitations, application to solid phases, and combination with bioassays, Chemosphere 287 (2022) 132352. https://doi.org/10.1016/j.chemosphere.2021.132352.

[126] J.B. Renaud, L. Sabourin, E. Topp, M.W. Sumarah, Spectral Counting Approach to Measure Selectivity of High-Resolution LC–MS Methods for Environmental Analysis, Analitical Chemistry 89 (2017) 2747–2754. https://doi.org/10.1021/acs.analchem.6b03475.

[127] V. Castro, J.B. Quintana, I. Carpinteiro, J. Cobas, N. Carro, R. Cela, R. Rodil, Combination of different chromatographic and sampling modes for high-resolution

mass spectrometric screening of organic microcontaminants in water, Anal Bioanal Chem 413 (2021) 5607–5618. https://doi.org/10.1007/s00216-021-03226-6.

[128] A. Casari, L. Tonidandel, G. Zolezzi, A. Bellin, P. Negri, A. Barbero, R. Larcher, A. Casari, L. Tonidandel, G. Zolezzi, A. Bellin, P. Negri, A. Barbero, R. Larcher, Validation of a calibration model able to estimate the concentration of pesticides in an alpine stream through passive sampling (POCIS) monitoring, Environmental Chemistry (2023). https://doi.org/10.1071/EN23052.

[129] F. Vernazza, Tecniche di campionamento passivo per lo studio di contaminanti emergenti in aree remote, Università degli Studi di Genova, 2022.

[130] R. Rodil, M. Moeder, R. Altenburger, M. Schmitt-Jansen, Photostability and phytotoxicity of selected sunscreen agents and their degradation mixtures in water, Analytical and Bioanalytical Chemistry 395 (2009) 1513–1524. https://doi.org/10.1007/s00216-009-3113-1.

[131] A. Goksøyr, K.E. Tollefsen, M. Grung, K. Løken, E. Lie, A. Zenker, K. Fent, M. Schlabach, S. Huber, Balsa Raft Crossing the Pacific Finds Low Contaminant Levels, Environmental Science and Technology 43 (2009) 4783–4790. https://doi.org/10.1021/es900154h.

[132] M.I. Cadena-Aizaga, S. Montesdeoca-Esponda, Z. Sosa-Ferrera, J.J. Santana-Rodríguez, Occurrence and environmental hazard of organic UV filters in seawater and wastewater from Gran Canaria Island (Canary Islands, Spain), Environmental Pollution 300 (2022) 118843. https://doi.org/10.1016/j.envpol.2022.118843.

[133] J. Labille, D. Slomberg, R. Catalano, S. Robert, M.-L. Apers-Tremelo, J.-L. Boudenne, T. Manasfi, O. Radakovitch, Assessing UV filter inputs into beach waters during recreational activity: A field study of three French Mediterranean beaches from consumer survey to water analysis, Science of The Total Environment 706 (2020) 136010. https://doi.org/10.1016/j.scitotenv.2019.136010.

[134] L. Guo, H. Chen, Y. Zhang, L. Bo, J. Li, Determination of Chromium Speciation in Tap Water Using Diffusive Gradients in Thin Film Technique, Chemistry Letters 43 (2014) 849–850. https://doi.org/10.1246/cl.140100.

[135] M.M.P. Tsui, H.W. Leung, T.-C. Wai, N. Yamashita, S. Taniyasu, W. Liu, P.K.S. Lam, M.B. Murphy, Occurrence, distribution and ecological risk assessment of multiple classes of UV filters in surface waters from different countries, Water Research 67 (2014) 55–65. https://doi.org/10.1016/j.watres.2014.09.013.

[136] K. Fisch, J.J. Waniek, D.E. Schulz-Bull, Occurrence of pharmaceuticals and UV-filters in riverine run-offs and waters of the German Baltic Sea, Marine Pollution Bulletin 124 (2017) 388–399. https://doi.org/10.1016/j.marpolbul.2017.07.057.

[137] S.C. Rastogi, UV filters in sunscreen products − a survey, Contact Dermatitis 46 (2002) 348–351. https://doi.org/10.1034/j.1600-0536.2002.460605.x.

[138] A. Ricci, M.N. Chrétien, L. Maretti, J.C. Scaiano, TiO2-promoted mineralization of organic sunscreens in water suspension and sodium dodecyl sulfate micelles, Photochemical and Photobiological Sciences 2 (2003) 487–492. https://doi.org/10.1039/b212815b.

[139] P. Rivaro, C. Ianni, L. Langone, C. Ori, G. Aulicino, Y. Cotroneo, M. Saggiomo, O. Mangoni, Physical and biological forcing of mesoscale variability in the carbonate system of the Ross Sea (Antarctica) during summer 2014, Journal of Marine Systems 166 (2017) 144–158. https://doi.org/10.1016/j.jmarsys.2015.11.002.

[140] E. Magi, M. Di Carro, C. Mirasole, B. Benedetti, Combining passive sampling and tandem mass spectrometry for the determination of pharmaceuticals and other emerging pollutants in drinking water, Microchemical Journal 136 (2018) 56–60. https://doi.org/10.1016/j.microc.2016.10.029.

[141] P. Anastas, J. Warner, P. Anastas, J. Warner, Green Chemistry: Theory and Practice, Oxford University Press, Oxford, New York, 2000.

[142] A. Gałuszka, Z. Migaszewski, J. Namieśnik, The 12 principles of green analytical chemistry and the SIGNIFICANCE mnemonic of green analytical practices, Trends in Analytical Chemistry 50 (2013) 78–84. https://doi.org/10.1016/j.trac.2013.04.010.

[143] P.M. Nowak, R. Wietecha-Posłuszny, J. Pawliszyn, White Analytical Chemistry: An approach to reconcile the principles of Green Analytical Chemistry and functionality, TrAC Trends in Analytical Chemistry 138 (2021) 116223. https://doi.org/10.1016/j.trac.2021.116223.

[144] A. Schwarz, Š. Ferjan, J. Kunst, Life cycle assessment of advanced grade PLA product with novel end-of-life treatment through depolymerization, Science of The Total Environment 905 (2023) 167020. https://doi.org/10.1016/j.scitotenv.2023.167020.

[145] G. Damonte, B. Barsanti, A. Pellis, G.M. Guebitz, O. Monticelli, On the effective application of star-shaped polycaprolactones with different end functionalities to improve the properties of polylactic acid blend films, European Polymer Journal 176 (2022) 111402. https://doi.org/10.1016/j.eurpolymj.2022.111402.

[146] N. More, M. Avhad, S. Utekar, A. More, Polylactic acid (PLA) membrane—significance, synthesis, and applications: a review, Polymer Bulletin 80 (2023) 1117–1153. https://doi.org/10.1007/s00289-022-04135-z.

[147] K.A. Athanasiou, G.G. Niederauer, C.M. Agrawal, Sterilization, toxicity, biocompatibility and clinical applications of polylactic acid/ polyglycolic acid copolymers, Biomaterials 17 (1996) 93–102. https://doi.org/10.1016/0142-9612(96)85754-1.

[148] T. Viel, M. Cocca, L. Manfra, D. Caramiello, G. Libralato, V. Zupo, M. Costantini, Effects of biodegradable-based microplastics in Paracentrotus lividus Lmk embryos: Morphological and gene expression analysis, Environmental Pollution 334 (2023) 122129. https://doi.org/10.1016/j.envpol.2023.122129.

[149] X. Liu, S. Ahmad, J. Ma, D. Wang, J. Tang, Comparative study on the toxic effects of secondary nanoplastics from biodegradable and conventional plastics on Streptomyces coelicolor M145, Journal of Hazardous Materials 460 (2023) 132343. https://doi.org/10.1016/j.jhazmat.2023.132343.

[150] L. Ambrosetti, Sviluppo di film porosi a base di PLA: Applicazione al pre-trattamento di campioni acquosi, Università degli Studi di Genova, 2023.

[151] G. Damonte, R. Spotorno, D. Di Fonzo, O. Monticelli, Multifunctional Porous Films Based on Polylactic Acid/Polycaprolactone Blend and Graphite Nanoplateles, ACS Appl. Polym. Mater. 4 (2022) 6521–6530. https://doi.org/10.1021/acsapm.2c00923.

[152] M.L. Williams, A.A. Olomukoro, R.V. Emmons, N.H. Goodage, E. Gionfriddo, Matrix effects demystified: Strategies for resolving challenges in analytical separations of complex samples, Journal of Separation Science (2023) 2300571. https://doi.org/10.1002/jssc.202300571.

[153] N. US Department of Commerce, Global Monitoring Laboratory - Carbon Cycle Greenhouse Gases, (n.d.). https://gml.noaa.gov/ccgg/trends/ (accessed December 5, 2023).

[154] CO2 Emissions in 2022 – Analysis, IEA (n.d.). https://www.iea.org/reports/co2-emissions-in-2022 (accessed December 5, 2023).

[155] H. Ritchie, P. Rosado, M. Roser, Emissions by sector: where do greenhouse gases come from?, Our World in Data (2023). https://ourworldindata.org/emissions-by-sector (accessed December 5, 2023).

[156] The European Green Deal, European Commission (2021).
https://commission.europa.eu/strategy-and-policy/priorities-2019-2024/european-green-deal_en (accessed December 5, 2023).

[157] M. Coccia, New directions of technologies pointing the way to a sustainable global society, Sustainable Futures 5 (2023) 100114.
https://doi.org/10.1016/j.sftr.2023.100114.

[158] M. Erans, E.S. Sanz-Pérez, D.P. Hanak, Z. Clulow, D.M. Reiner, G.A. Mutch, Direct air capture: process technology, techno-economic and socio-political challenges, Energy and Environmental Science 15 (2022) 1360–1405.
https://doi.org/10.1039/D1EE03523A.

[159] P.S. Fennell, S.J. Davis, A. Mohammed, Decarbonizing cement production, Joule 5 (2021) 1305–1311. https://doi.org/10.1016/j.joule.2021.04.011.

[160] S.D. Peu, A. Das, M.S. Hossain, M.A.M. Akanda, M.M.H. Akanda, M. Rahman, M.N. Miah, B.K. Das, A.R.M.T. Islam, M.M. Salah, A Comprehensive Review on Recent Advancements in Absorption-Based Post Combustion Carbon Capture Technologies to Obtain a Sustainable Energy Sector with Clean Environment, Sustainability 15 (2023) 5827. https://doi.org/10.3390/su15075827.

[161] A.J. Reynolds, T.V. Verheyen, S.B. Adeloju, E. Meuleman, P. Feron, Towards Commercial Scale Postcombustion Capture of CO2 with Monoethanolamine Solvent: Key Considerations for Solvent Management and Environmental Impacts, Environmental Science and Technology 46 (2012) 3643–3654.
https://doi.org/10.1021/es204051s.

[162] H.E. Buist, S. Devito, R.A. Goldbohm, R.H. Stierum, J. Venhorst, E.D. Kroese, Hazard assessment of nitrosamine and nitramine by-products of amine-based CCS: Alternative approaches, Regulatory Toxicology and Pharmacology 71 (2015) 601–623. https://doi.org/10.1016/j.yrtph.2014.01.017.

[163] X. Chen, G. Huang, C. An, Y. Yao, S. Zhao, Emerging N-nitrosamines and N-nitramines from amine-based post-combustion CO2 capture – A review, Chemical Engineering Journal 335 (2018) 921–935. https://doi.org/10.1016/j.cej.2017.11.032.

[164] C.J. Nielsen, H. Herrmann, C. Weller, Atmospheric chemistry and environmental impact of the use of amines in carbon capture and storage (CCS), Chemical Society Reviews 41 (2012) 6684–6704. https://doi.org/10.1039/C2CS35059A.

[165] L. Sørensen, K. Zahlsen, A. Hyldbakk, E.F. da Silva, A.M. Booth, Photodegradation in natural waters of nitrosamines and nitramines derived from CO2 capture plant operation, International Journal of Greenhouse Gas Control 32 (2015) 106–114.
https://doi.org/10.1016/j.ijggc.2014.11.004.

[166] Pesticide and Environmental Toxicology Branch Office of Environmental Health Hazard Assessment California Environmental Protection Agency, Public Health Goal for N-Nitrosodimethylamine in Drinking Water, 2006. chrome-extension://efaidnbmnnnibpcajpcglclefindmkaj/https://oehha.ca.gov/media/downloads/water/chemicals/phg/122206ndmaphg.pdf.

[167] Environmenal Protection Agency, Six-Year Review 3 Technical Support Document for Nitrosamines, n.d.

[168] A. Bjerke, K. Bonaunet, O.-A. Braathen, O.G. Brakstad, M. Dušinská, C. Dye, L.M.B. Fjellsbø, G. Hammerseth, B.H. Hansen, S.-H. Hansen, P. Kaur, H. Leknes, S. Manø, Z. Magdolenova, M.-B. Pedersen, E.R. Pran, S. Ravnum, M. Schlabach, Y. Stenstrøm, T. Syversen, M. Vadset, K. Zahlsen, Nitramine analysis procedure development and screening toxicity study, NILU Norwegian Institute for Air Research, 2011.

[169] C. Coutris, A.L. Macken, A.R. Collins, N. El Yamani, S.J. Brooks, Marine ecotoxicity of nitramines, transformation products of amine-based carbon capture

technology, Science of The Total Environment 527–528 (2015) 211–219. https://doi.org/10.1016/j.scitotenv.2015.04.119.

[170] L.M. Fjellsbø, A.R. Van Rompay, J. Hooyberghs, I. Nelissen, M. Dusinska, Screening for potential hazard effects from four nitramines on human eye and skin, Toxicology in Vitro 27 (2013) 1205–1210. https://doi.org/10.1016/j.tiv.2013.02.004.

[171] M. Hillebrand, S. Pflugmacher, A. Hahn, Toxicological risk assessment in CO2 capture and storage technology, International Journal of Greenhouse Gas Control 55 (2016) 118–143. https://doi.org/10.1016/j.ijggc.2016.10.014.

[172] E.D. Wagner, J. Osiol, W.A. Mitch, M.J. Plewa, Comparative in Vitro Toxicity of Nitrosamines and Nitramines Associated with Amine-based Carbon Capture and Storage, Environmental Science and Technology 48 (2014) 8203–8211. https://doi.org/10.1021/es5018009.

[173] J. Urík, B. Vrana, An improved design of a passive sampler for polar organic compounds based on diffusion in agarose hydrogel, Environmental Science and Pollution Research 26 (2019) 15273–15284. https://doi.org/10.1007/s11356-019-04843-6.

[174] J.W. Grate, Hydrogen-Bond Acidic Polymers for Chemical Vapor Sensing, Chemical Reviews 108 (2008) 726–745. https://doi.org/10.1021/cr068109y.
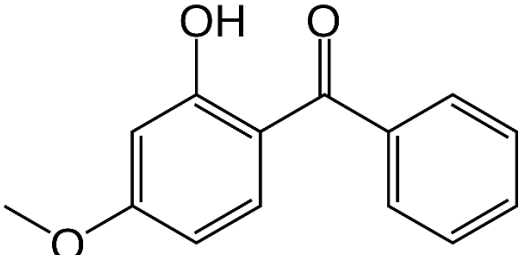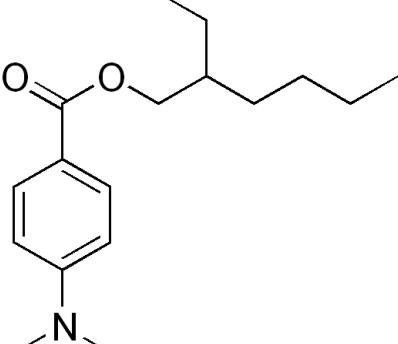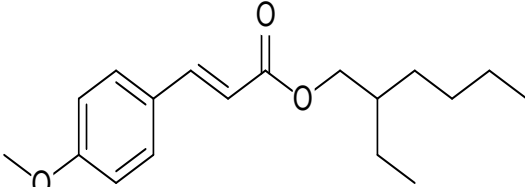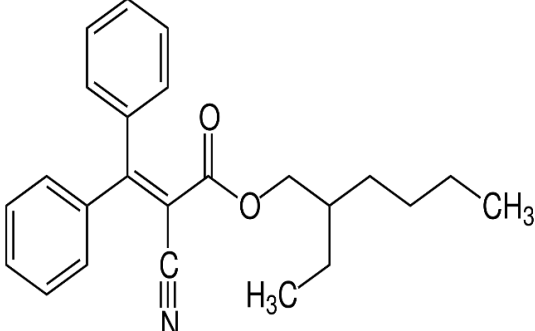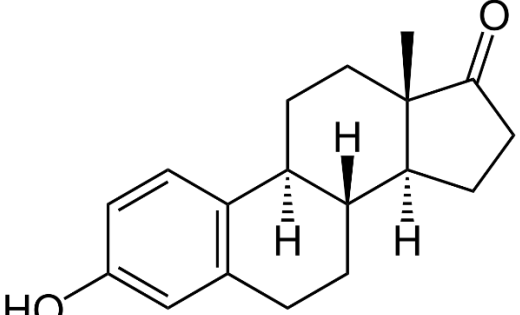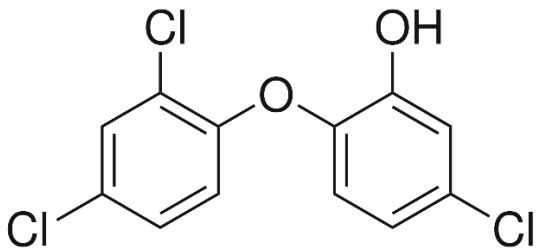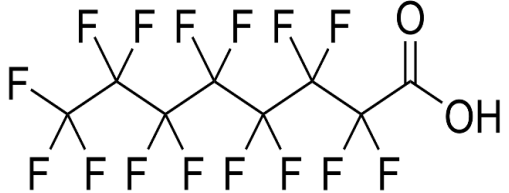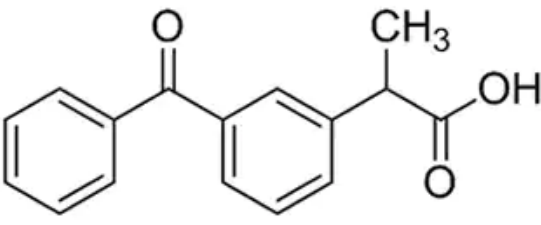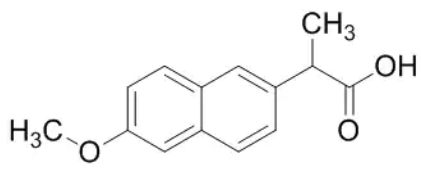
Appendix
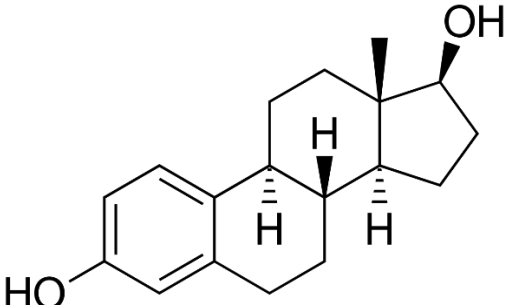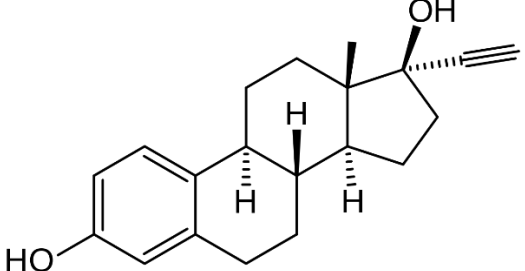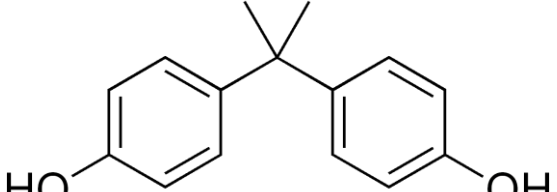
Tab. 1A Physico-chemical properties of the target compound of this studys: LogD (pH 5.5) (LogD5.5), Molecular Weight (MW), Number of H-bonding donor groups (Hbd), Number of H-bonding acceptor groups (Hba), Topological Polar Surface Area (TPSA), Number of Aromatic Rings (AR), Polarizability (Pol), Solvent Accessible Surface Area (SASA), Apolar Surface Area (Apolar SA), Solubility (LogS), percentage of neutral analyte pH = 5.5 (N%), percentage of anionic analyte pH = 5.5 (A%), percentage of cationic analyte pH = 5.5 (C%).
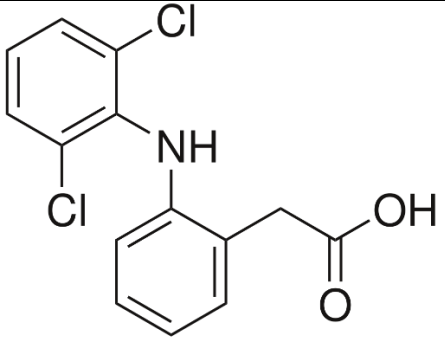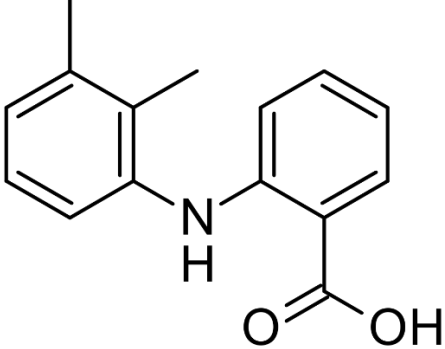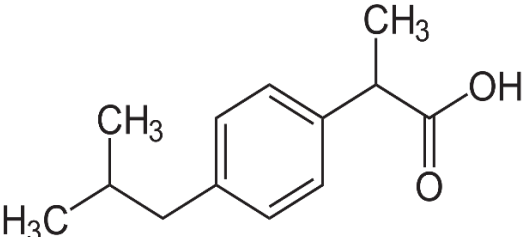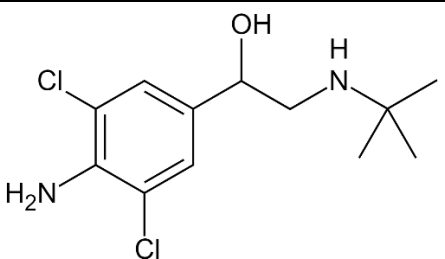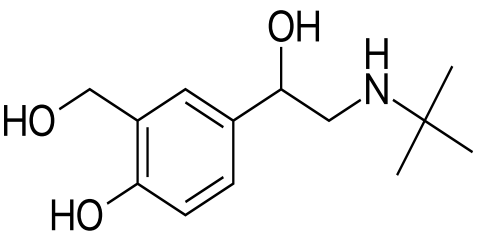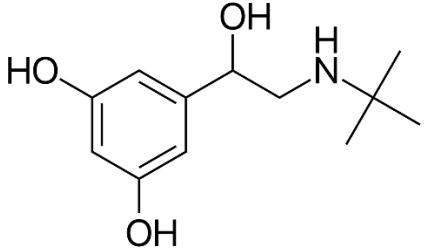
Analyte	LogD7.5	LogD5.5	MW	HBd	Hba	TPSA	AR	Pol	SASA	LogS	Apolar SA	N%	A%	C%
MTF	-5.59	-5.75	129.167	4	5	88.99	0	13	278.34	1.81	189.35	0	0	100
CMQ	-3.31	-3.31	122.62	0	0	nd	0	13.23	286.87	nd	nd	0	0	100
ATN	-1.33	-2.7	266.341	3	4	84.58	1	29.09	535.74	0.2	451.16	0	0.02	99.98
TAU	-2.62	-2.62	125.14	2	4	80.39	0	10.73	282.71	0.99	202.32	99.99	0.01	0
DMNZ	-4.23	-2.38	160.173	2	4	69.64	0	15.04	373.81	2.6	304.17	9.07	90.92	0
SLBT	-1.23	-2.31	239.315	4	4	72.72	1	26.58	463.93	1.2	391.21	0.01	0	99.99
TRBT	-0.64	-1.82	225.288	4	4	72.72	1	24.73	436.62	1.14	363.9	0.04	0	99.96
NCT	0.05	-1.78	162.236	0	2	16.13	1	19.45	340.47	1.05	324.34	0	0	100
PRX	-1.32	-1.61	180.17	1	5	68.50	2	16.46	295.31	-0.22	226.81	28.23	0	71.56
ACS	-1.49	-1.4	163.15	1	4	72.47	0	13.45	304.69	0.72	232.22	3.18	0	96.82
MTP	-0.001	-1.37	267.369	2	4	50.72	1	30.34	602.12	0.3036	551.4	0	0.02	99.98
CLBT	0.23	-0.85	277.19	3	3	58.28	1	28.42	448.13	0	389.85	0.01	0	99.99
THEOP	-0.85	-0.81	180.2	1	3	69.30	2	16.1	316.7	-0.96	247.4	99.80	0	0.20
FXP	-1.87	-0.68	255.0	2	5	85.44	1	19.4	382.9	0	297.5	0.51	99.49	0
HCTZ	-0.5855	-0.5757	297.7	3	5	118.36	1	25.3	419.9	-17,924	301.6	99.97	0.03	0
OMT	-0.55	-0.55	213.2	1	2	64.63	0	19.1	446.8	-0.7	382.2	100	0	0
CAFF	-0.55	-0.55	194.2	0	3	58.44	2	17.9	368.4	-0.44	309.9	100.00	0	0
SCL	-0.47	-0.47	397.6	5	8	128.84	0	32.7	422.5	-2.3	293.6	100.00	0	0
FRSM	-1.66	-0.24194	330.7	3	5	122.63	2	29.5	503.9	0	381.3	1	99	0
2,4-D	-0.1	-0.13	221.0	1	3	46.53	1	19.1	370.6	-0.35	324.1	0.2	99.8	0
CMPH	0.88	0.88	323.1	3	5	112.7	1	27.8	460.5	-3.21	347.8	100	0	0
GEM	3.27	1.44	250.3	1	3	46.53	1	27.9	533.4	-2.19	486.9	7.63	92.37	0
PFOA	1.58	1.59	414.1	1	2	37.30	0	16.7	440.0	-1.01	402.7	0.00	100.00	0
NAP	-0.09	1.7	230.3	1	3	46.53	2	26.4	452.5	-2.16	406.0	5.20	94.80	0
KET	0.40	2.1	254.3	1	3	54.37	2	28.0	452.3	-2.34	397.9	3.05	96.95	0
DCF	1.05	2.76	296.2	2	3	49.33	2	29.0	425.0	-2.79	375.6	0.10	96.89	0
CRB	2.77	2.77	236.3	1	1	46.33	2	27.0	370.9	-3.79	324.6	100.00	0.00	0
IBU	1.25	3.11	206.3	1	2	37.30	1	23.7	430.1	-2.81	392.8	18.36	81.64	0
BP-3	3.5	3.62	228.2	1	3	46.53	2	25.1	443.7	-3.36	397.2	78.92	21.08	0
E2	3.74	3.75	272.4	2	2	40.46	1	31.3	395.1	-3.99	354.6	99.85	0.15	0
EE2	3.9	3.9	296.4	2	2	40.46	1	33.9	411.2	-4.83	370.8	99.85	0.15	0
BPA	4.04	4.05	228.3	2	2	40.46	2	26.6	413.1	-3.18	372.6	99.48	0.52	0
E1	4.31	4.31	270.4	1	2	37.3	1	30.8	396.1	-4.18	358.8	99.85	0.15	0
TCS	4.76	4.98	289.5	1	1	29.46	2	27.0	413.4	-5.27	384.0	60.25	39.75	0
OD-PABA	5.12	5.12	277.4	0	2	29.54	1	32.5	623.2	-4.84	593.7	100	0	0

EHMC	5.38	5.38	290.4	0	2	35.53	1	33.6	639.0	-5.56	603.4	100	0	0
OC	6.78	6.78	361.5	0	2	50.09	2	42.4	646.7	-7.18	596.6	100	0	0

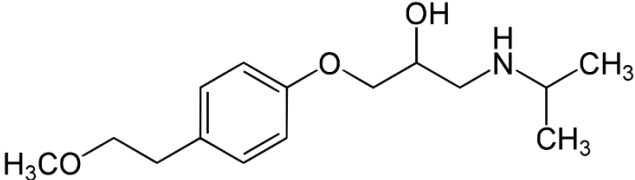Tab. 2A Acronym, class and chemical structures of the target compounds presented in Chapter 3, 4, 5 and 6.

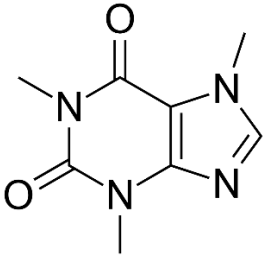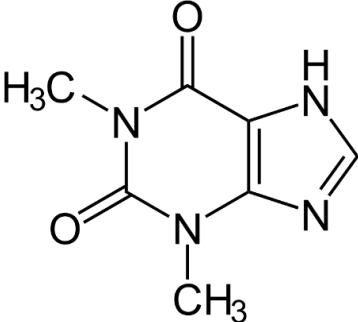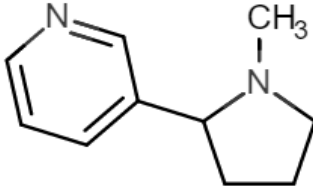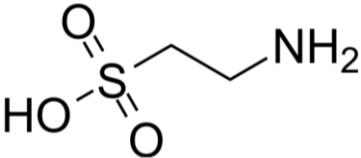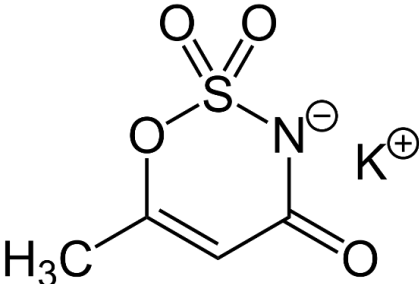| Compound	Class	Chemical structure
Benzofenone-3 (BP-3)	UV-filter	
Octyl dimethyl p-aminobenzoate (OD-PABA)	UV-filter	
Ethyl hexyl methoxy cinnamate (EHMC)	UV-filter	
Octocrylene (OC)	UV-filter	
Estrone (E1)	Estrogen	
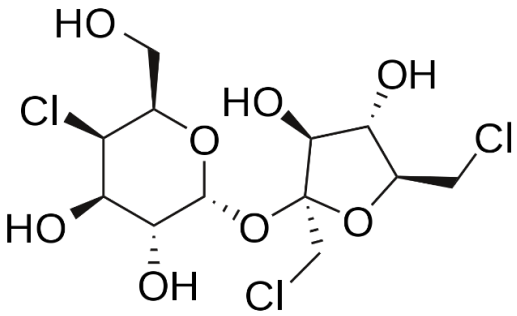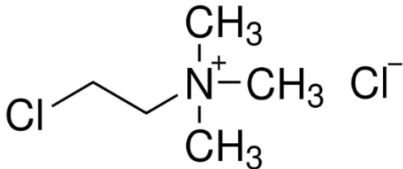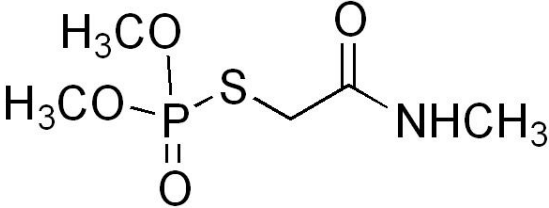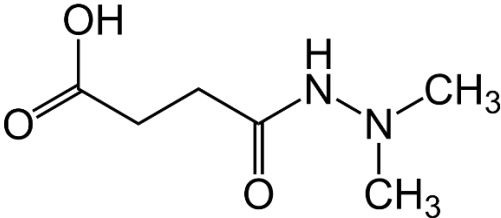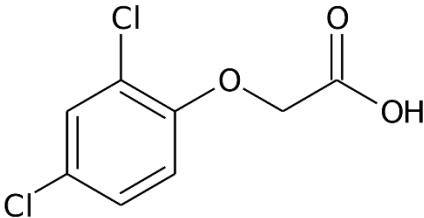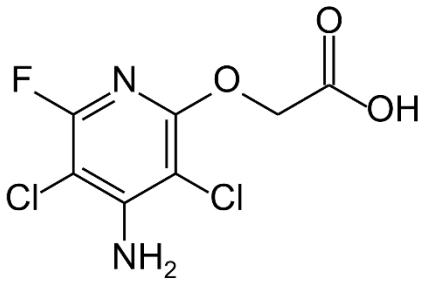
β-estradiole (E2)	Estrogen	
17α- ethinyl estradiol (EE2)	Estrogen	
Bisphenolo A (BPA)	Industrial additive	
Triclosan (TCS)	Industrial additive	
Perfluoroctanoic acid (PFOA)	Industrial additive	
Ketoprofen (KET)	pharmaceutical drug	
Naproxen (NAP)	pharmaceutical drug	

Diclofenac (DCF)	pharmaceutical drug	
Mefenamic acid (MEF)	pharmaceutical drug	
Ibuprofen (IBU)	pharmaceutical drug	
Clenbuterol (CLBT)	pharmaceutical drug	
salbutamol (SLBT)	pharmaceutical drug	
Terbutalin (TRBT)	pharmaceutical drug	

Furosemide (FRSM)	pharmaceutical drug	
Hydrochlorotiazide (HCTZ)	pharmaceutical drug	
Carbamazepine (CRB)	pharmaceutical drug	
Gemfibrozil (GEM)	pharmaceutical drug	
Metformin (MET)	Pharmaceutical drug	
Chloramphenicol (CMPH)	pharmaceutical drug	
Atenolol (ATN)	pharmaceutical drug	

Metoprolol (MTP)	pharmaceutical drug	
Caffeine (CAFF)	Stimulants	
Theophilline (THEOP)	Stimulants	
Nicotine (NCT)	Stimulants	
Taurine (TAU)	Stimulants	
Acesulfame K (ACS)	artificial sweetener	

Sucralose (SLC)	artificial sweetener	
Chlormequat (CMQ)	Pesticide	
Omethoate (OMT)	Pesticide	
Daminozide (DMNZ)	Pesticide	
2,4-Dichlorophenoxyacetic acid (2,4-D)	Pesticide	
Fluroxypyr (FXP)	Pesticide	

Tab. 3A Optimized MS parameters for the MRM transitions of the target chemicals.

Analyte	Formula	Polarity of ESI	RT (min)	Quantifier transition (m/z)		CE (V)	frag (V)	Qualifier transition (m/z)		CE (V)
ACS	$C_4H_5NO_4S$	ESI -	0.64	162	82	12	94	162	78	36
TAU	$C_2H_7NO_3S$	ESI -	0.84	124	79.9	24	96	nd	/	/
OMT	$C_5H_{12}NO_4PS$	ESI +	0.85-1	214	155	12	68	214	125	20
DMNZ	$C_6H_{12}N_2O_3$	ESI +	0.87	161.1	143.1	8	68	161.1	61.2	8
PRX	$C_7H_8N_4O_2$	ESI +	1	181	124	20	77	nd	/	/
THEOP	$C_7H_8N_4O_2$	ESI +	1	181	124	20	77	nd	/	/
CAFF	$C_8H_{10}N_4O_2$	ESI +	1	195	138	20	100	195	110	20
PFOA	$C_8HF_{15}O_2$	ESI -	1	413	369	5	40	413	169	20
SCL	$C_{12}H_{19}Cl_3O_8$	ESI -	1	455	395	4	104	457	397	4
HCTZ	$C_7H_8ClN_3O_4S_2$	ESI -	1.05	296	269	16	170	296	205	20
2,4-D	$C_8H_6Cl_2O_3$	ESI -	1.2	219	160.8	8	68	219	124.9	28
FRSM	$C_{12}H_{11}ClN_2O_5S$	ESI -	1.3	329	285	12	90	329	205	20
CMPH	$C_{11}H_{12}Cl_2N_2O_5$	ESI -	1.34	321	257	4	96	321	151.9	12
CRB	$C_{15}H_{12}N_2O$	ESI +	1.76	237	194	20	120	237	165	48
KET	$C_{16}H_{14}O_3$	ESI -	2.7-2.9	253	209	2	40	nd	/	/
NAP	$C_{14}H_{14}O_3$	ESI -	2.8-3	229	170	5	40	229	169	15
MTF	$C_4H_{11}N_5$	ESI +	3.3-3.8	130.1	68.1	40	96	130.1	60.1	12
ATN	$C_{14}H_{22}N_2O_3$	ESI +	3.4-4	267.2	145.1	28	152	267.2	56.2	36
SLBT	$C_{13}H_{21}NO_3$	ESI +	3.6-4.2	240	148	16	96	240	222	8
TRBT	$C_{12}H_{19}NO_3$	ESI +	3.7-4.4	226.1	152.1	16	96	226.1	107.1	32
CMQ	$C_5H_{13}ClN$	ESI +	3.7-4.4	122.1	59.2	20	96	122.1	58.2	36
NCT	$C_{10}H_{14}N_2$	ESI +	3.8-4.6	163.1	130.1	20	96	163.1	117.1	32
DCF	$C_{14}H_{11}Cl_2NO_2$	ESI -	4.8	294	250	5	40	294	214	20
IBU	$C_{13}H_{18}O_2$	ESI -	5	205	161	2	40	nd	/	/
BP-3	$C_{14}H_{12}O_3$	ESI +	5.4	229	151	16	116	229	105	16
GMF	$C_{15}H_{22}O_3$	ESI -	5.6-5.7	249	121	4	110	249	106	50
FXP	$C_7H_5Cl_2FN_2O_3$	ESI +	6.6-7.6	255	209	16	96	255	181	24
MTP	$C_{15}H_{25}NO_3$	ESI +	7.4-8.4	268.2	74.1	24	124	268.2	56.2	32
CLBT	$C_{12}H_{18}Cl_2N_2O$	ESI +	8.3-10.1	277	203	12	80	277	132	32

OD-PABA	$C_{17}H_{27}NO_2$	ESI +	8.9	278	151	32	116	278	166	20
EHMC	$C_{18}H_{26}O_3$	ESI +	9.06	291	161	16	60	261	179	4
EHS	$C_{15}H_{22}O_3$	ESI +	9.33	251	139	4	76	nd	/	/
OC	$C_{24}H_{27}NO_2$	ESI +	9.6-9.7	362	250	8	152	362	232	20
BPA	$C_{15}H_{16}O_2$	ESI -	2.6	227	212	12	128	227	133	24
E2	$C_{18}H_{24}O_2$	ESI -	3	271	145	40	180	271	183	40
EE2	$C_{20}H_{24}O_2$	ESI -	3.8	295	145	30	180	295	159	35
E1	$C_{18}H_{22}O_2$	ESI -	4.1	269	145	30	110	269	143	60
TCS	$C_{12}H_7Cl_3O_2$	ESI -	6.8	287	35	4	72	289	35	4

Tab. 4A Type I analytes PES uptake from tap water: Student's t-test for the evaluation of the intercept significance in the linear regression: b_0 is the intercept value, $SE(b_0)$ the standard error for the b_0 value and t_{calc} and t_{tab} the calculated and tabulated t values, respectively.

	b_0	$SE(b_0)$	t_{calc}	t_{tab} ($\alpha = 0.01$; n = 7)
TCS	0.31	0.18	1.73	
BP-3	0.17	0.34	0.51	
OD-PABA	0.19	0.20	0.95	3.71
EHMC	0.39	0.18	2.17	
OC	0.31	0.10	3.12	

Tab. 5A PES uptake of Type I analytes during tap water calibration: determination coefficient (R^2) obtained for the linear regression.

	TCS	BP-3	OD-PABA	EHMC	OC
R^2	0.960	0.950	0.970	0.987	0.987

Tab. 6A Type I analytes PES uptake from SSW: Student's t-test for the evaluation of the intercept significance in the linear regression: b_0 is the intercept value, $SE(b_0)$ the standard error for the b_0 value and t_{calc} and t_{tab} the calculated and tabulated t values, respectively.

	b_0	$SE(b_0)$	t_{calc}	t_{tab} ($\alpha = 0.01$; n = 4)
BP-3	1.2	1.7	0.68	
OD-PABA	0.09	1.3	0.07	
EHMC	0.12	1.4	0.089	5.84
OC	0.0002	1.4	0.0003	
TCS	0.15	1.27	0.12	

Tab. 7A PES uptake of Type I analytes during SSW calibration: determination coefficient (R^2) obtained for the linear regression.

	TCS	BP-3	OD-PABA	EHMC	OC
R^2	0.999	0.955	0.999	0.997	0.990

Fig. 1A Tap water uptake results of the Type I analytes: residual plot (left) and plot of experimental vs. predicted values (right) for the linear regression.
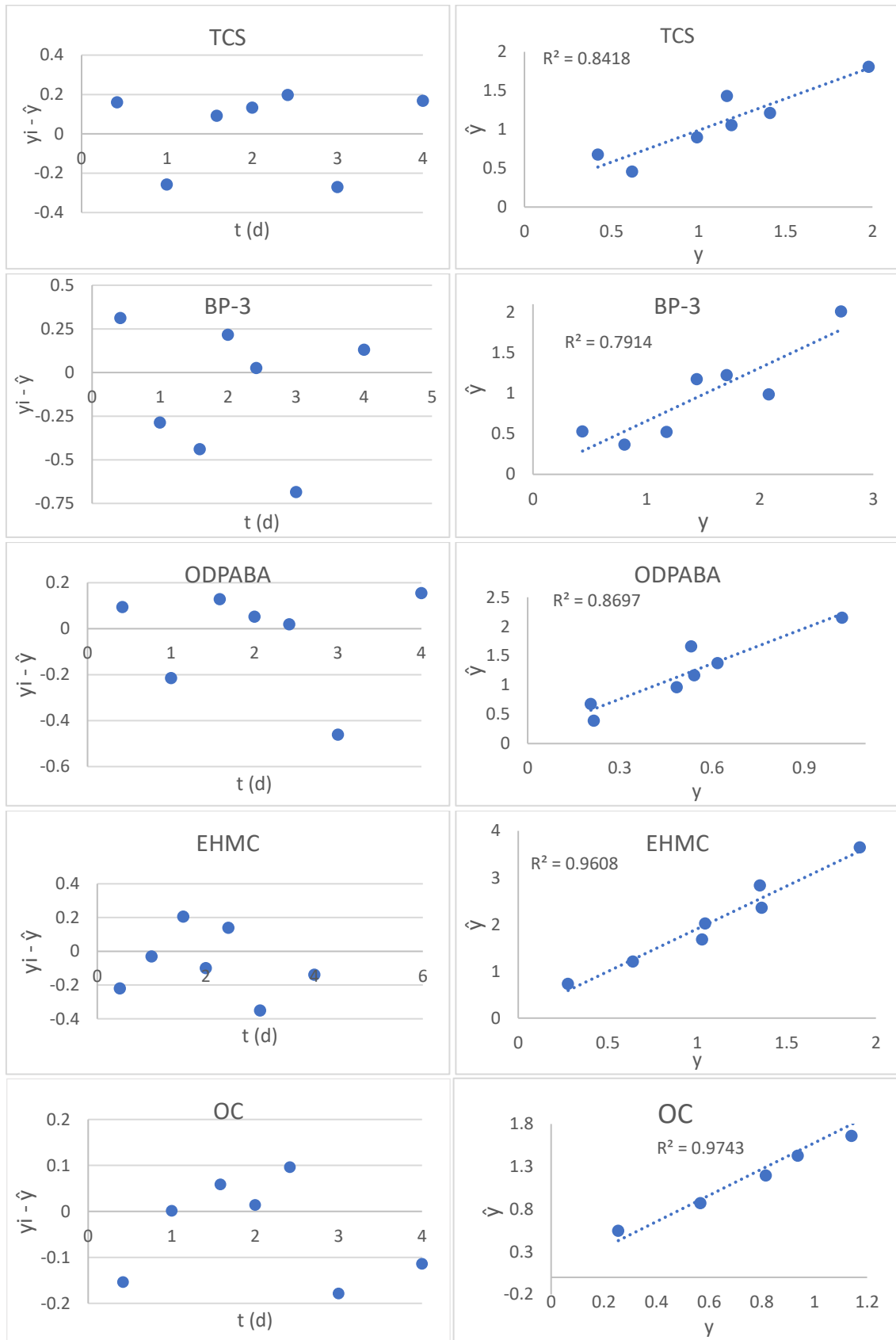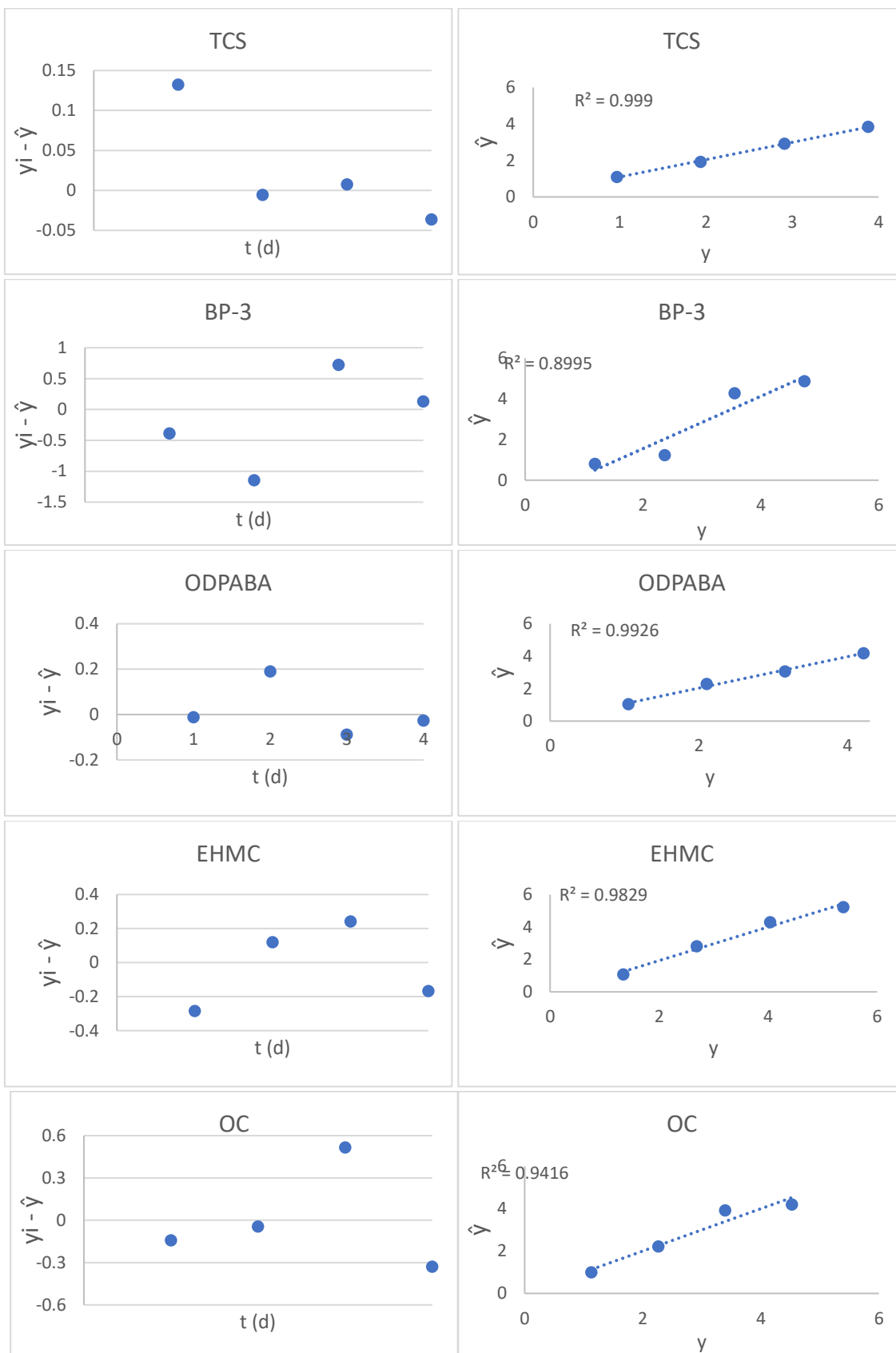
Fig. 2A SSW uptake results of the Type I analytes: residual plot (left) and plot of experimental vs. predicted values (right) for the linear regression.

Tab. 8A Recoveries (R%) obtained for the target analytes using different PES membranes (P01, P045; H01 and S01) and the corresponding % of the target compounds lost in water during the rinsing step of the membranes (W%). More details in Chapter 4.

	P01		P045		H01		S01	
	R%	*W%*	*R%*	*W%*	*R%*	*W%*	*R%*	*W%*
ACS	46 ± 10	36 ± 8	22 ± 7	69 ± 9	37 ± 8	58 ± 14	71 ± 4	19 ± 2
TAU	13 ± 9	51 ± 9	12 ± 2	69 ± 19	6 ± 7	67 ± 15	2 ± 0	83 ± 7
OMT	72 ± 7	21 ± 4	63 ± 5	32 ± 1	57 ± 4	42 ± 8	nd	nd
THEOP	70 ± 17	9 ± 2	68 ± 2	17 ± 7	70 ± 15	21 ± 5	69 ± 13	12 ± 1
DMNZ	26 ± 5	40 ± 8	16 ± 3	59 ± 14	13 ± 5	57 ± 13	8 ± 4	65 ± 11
SCL	68 ± 13	20 ± 5	47 ± 10	45 ± 7	54 ± 5	43 ± 10	63 ± 4	32 ± 2
CAFF	54 ± 16	7 ± 1	87 ± 4	9 ± 4	65 ± 11	11 ± 2	90 ± 25	5.7 ± 0.4
PFOA	39 ± 2	< 5%	18 ± 6	9.3 ± 0.3	24 ± 3	10 ± 3	48 ± 1	< 5%
HCTZ	88 ± 1	< 5%	91 ± 7	< 5%	90 ± 2	< 5%	93 ± 4	< 5%
2,4-D	84 ± 5	< 5%	64 ± 3	25 ± 2	65 ± 5	22 ± 8	80 ± 7	7 ± 2
FRSM	47 ± 8	nd	24 ± 15	< 5%	26 ± 5	< 5%	11 ± 5	< 5%
CMPH	85 ± 7	nd	93 ± 9	< 5%	93 ± 2	< 5%	92 ± 6	< 5%
CRB	85 ± 3	< 5%	81 ± 10	< 5%	79 ± 3	< 5%	71 ± 7	< 5%
KET	119 ± 15	nd	90 ± 9	nd	72 ± 9	nd	91 ± 7	nd
NAP	84 ± 5	nd	81 ± 15	< 5%	87 ± 5	< 5%	85 ± 9	< 5%
MTF	23 ± 8	34 ± 7	22 ± 5	33 ± 4	21 ± 1	32 ± 4	16 ± 5	72 ± 11
ATN	66 ± 7	17 ± 5	60 ± 6	19 ± 2	70 ± 2	13 ± 2	30 ± 4	58 ± 9
SLBT	62 ± 9	22 ± 6	56 ± 8	24 ± 3	73 ± 1	15 ± 3	28 ± 5	57 ± 7
TRBT	69 ± 6	10 ± 3	65 ± 10	10 ± 2	78 ± 3	6 ± 1	31 ± 5	40 ± 7
CMQ	8 ± 5	49 ± 11	5 ± 0	52 ± 4	8 ± 1	44 ± 8	6 ± 2	77 ± 11
NCT	9 ± 3	11 ± 3	17 ± 16	12 ± 9	11 ± 4	20 ± 3	0 ± 0	10 ± 8
DIC	86 ± 3	nd	93 ± 3	nd	83 ± 1	nd	87 ± 4	nd
IBU	84 ± 4	nd	88 ± 7	< 5%	80 ± 0	< 5%	86 ± 5	< 5%
BP-3	88 ± 6	nd	96 ± 5	nd	91 ± 6	nd	91 ± 1	nd
GEM	78 ± 5	< 5%	85 ± 6	< 5%	80 ± 2	< 5%	84 ± 7	< 5%
FXP	96 ± 13	24 ± 5	96 ± 3	28 ± 3	99 ± 3	16 ± 3	39 ± 5	59 ± 11
MTP	69 ± 4	< 5%	62 ± 5	< 5%	67 ± 3	< 5%	63 ± 5	16 ± 3
CLNB	84 ± 3	< 5%	82 ± 5	< 5%	81 ± 2	< 5%	74 ± 3	13 ± 3
OD-PABA	57 ± 6	nd	43 ± 17	nd	45 ± 6	nd	28 ± 5	nd
EHMC	77 ± 2	nd	75 ± 13	nd	71 ± 6	nd	53 ± 6	nd
OC	86 ± 5	nd	82 ± 13	nd	92 ± 4	nd	111 ± 27	nd
BPA	80 ± 5	nd	91 ± 7	nd	98 ± 1	nd	93 ± 6	nd
E2	87 ± 10	nd	92 ± 5	nd	83 ± 2	nd	91 ± 2	nd
EE2	91 ± 10	nd	93 ± 14	nd	81 ± 3	nd	97 ± 4	nd
E1	82 ± 4	nd	85 ± 4	nd	88 ± 6	nd	96 ± 6	nd
TCS	89 ± 3	nd	95 ± 2	nd	91 ± 1	nd	91 ± 1	nd

Tab. 9A Values of the matrix effect (ME%) obtained for the target analytes of Chapter 4.

	ME%			
	P01	**P045**	**H01**	**S01**
ACS	92	87	85	92
TAU	68	59	49	59
OMT	53	77	83	nd
THEOP	67	75	31	22
DMNZ	63	57	60	38
SCL	82	91	76	94
CAFF	67	62	33	27
PFOA	122	114	109	111
HCTZ	67	78	87	83
2,4-D	103	99	99	99
FRSM	104	102	97	96
CMPH	105	102	100	104
CRB	96	100	103	103
KET	86	102	109	113
NAP	121	124	106	114
MTF	102	103	100	104
ATN	97	96	96	103
SLBT	106	103	102	108
TRBT	107	100	99	104
CMQ	113	117	115	117
NCT	104	104	105	109
DIC	109	99	99	94
IBU	101	102	100	101
BP-3	90	93	95	101
GEM	112	102	101	108
FXP	66	118	103	137
MTP	96	104	103	111
CLNB	100	101	102	106
OD-PABA	95	101	100	106
EHMC	98	98	98	97
OC	22	53	55	6
BPA	108	100	94	105
E2	94	86	98	104
EE2	91	93	103	95
E1	102	96	97	96
TCS	105	98	103	102

Tab. 10A Mass balance obtained for the evaluation of K_{PESw} using different type of membranes (Chapter 4).

	Mass balance (%)			
	P01	**P045**	**H01**	**S01**
OMT	91	86	83	90
HCTZ	59	61	58	61
2,4-D	93	105	92	102
FRSM	91	105	89	101
CRB	104	108	96	96
NAP	95	93	129	97
SLBT	83	104	86	102
TRBT	77	102	81	99
DCF	95	103	79	97
IBU	82	76	68	73
BP-3	86	101	78	97
GMF	101	111	100	105
MTP	88	103	89	98
OD-PABA	48	31	30	56
EHMC	71	52	50	76
CLBT	95	103	92	100
OC	120	100	130	106

Tab. 11A Values of K_{PESw} and $LogK_{PESw}$ obtained using four type of PES membranes (P01, P045, H01 and S01). For EHMC data were reported both as K_{PESw} and as the total amount of compound accumulated into the membranes (*).

	P01		P045		H01		S01	
	K_{PESw} (L/Kg)	$LogK_{PESw}$	K_{PESw} (L/Kg)	$LogK_{PESw}$	K_{PESw} (L/Kg)	$LogK_{PESw}$	K_{PESw} (L/Kg)	$LogK_{PESw}$
2,4-D	130 ± 8	2.11 ± 0.05	59 ± 5	1.77 ± 0.09	103 ± 5	2.01 ± 0.04	81 ± 4	1.86 ± 0.09
CRB	194 ± 8	2.29 ± 0.04	14 ± 2	1.2 ± 0.1	29 ± 5	1.5 ± 0.2	63 ± 2	1.8 ± 0.03
NAPR	445 ± 30	2.2 ± 0.4	14 ± 2	1.2 ± 0.1	nd	nd	148 ± 4	2.16 ± 0.03
TRBT	29 ± 3	1.5 ± 0.1	nd	nd	nd	nd	7.6 ± 0.5	0.88 ± 0.06
DIC	558 ± 29	2.69 ± 0.04	332 ± 20	2.52 ± 0.06	257 ± 19	2.36 ± 0.07	650 ± 27	2.81 ± 0.04
IBU	582 ± 55	2.55 ± 0.06	164 ± 32	2.2 ± 0.2	nd	nd	240 ± 18	2.38 ± 0.07
BP-3	349542 ± 23584	5.54 ± 0.07	42539 ± 179	4.629 ± 0.004	100230 ± 3044	5.00 ± 0.03	91670 ± 836	4.962 ± 0.009
GEM	1996 ± 73	3.19 ± 0.03	525 ± 16	2.72 ± 0.03	372 ± 10	2.513 ± 0.006	1100 ± 17	3.041 ± 0.02
MTP	89 ± 3	1.95 ± 0.03	53 ± 2	1.72 ± 0.04	108 ± 6	2.01 ± 0.06	nd	nd
OD-PABA	1912037 ± 62953	6.26 ± 0.03	53298 ± 777	4.73 ± 0.01	226805 ± 3685	5.35 ± 0.06	202887 ± 3003	5.307 ± 0.007
EHMC	nd	nd	108467 ± 823	5.035 ± 0.008	635228 ± 46812	5.8 ± 0.1	342923 ± 2531	5.535 ± 0.006
EHMC	730694* ± 118	/	252661* ± 1918	/	456102* ± 40	/	660689* ± 83	/
CLBT	219 ± 4	2.34 ± 0.02	134 ± 0	2.127 ± 0.001	362 ± 3	2.53 ± 0.01	50 ± 1	1.69 ± 0.02
OC	449783 ± 22841	5.65 ± 0.06	272479 ± 6814	5.44 ± 0.03	150384 ± 12917	5.15 ± 0.06	535330 ± 27424	5.73 ± 0.05
BPA	6534 ± 231	3.81 ± 0.04	1146 ± 117	3.1 ± 0.1	1803 ± 47	3.26 ± 0.03	3624 ± 186	3.56 ± 0.06
E2	2826 ± 225	3.45 ± 0.08	519 ± 218	2.7 ± 0.4	942 ± 230	3 ± 0.2	1435 ± 225	3.2 ± 0.2
EE2	6473 ± 340	3.81 ± 0.05	1300 ± 150	3.1 ± 0.1	1921 ± 353	3.3 ± 0.2	4120 ± 431	3.6 ± 0.1
E1	4713 ± 201	3.67 ± 0.04	922 ± 85	2.96 ± 0.09	1382 ± 206	3.1 ± 0.1	2454 ± 62	3.39 ± 0.03
TCS	218262 ± 5392	5.26 ± 0.04	59223 ± 893	4.77 ± 0.02	98218 ± 1124	4.99 ± 0.01	116152 ± 3928	5.06 ± 0.03

* Data expressed as µg/Kg

Tab. 12A Results of the mass balance (MB%) and the stability (S%) in the water of the control beaker for KPESw evaluation using the S1 and S2 setup (Chapter 4).

	S1 setup		S2 setup	
	MB%	S %	MB%	S %
ACS	nd	106	125	120
PRX+THEOP	nd	97	142	110
OMT	91	72	90	96
DMNZ	nd	0	22	0
CAFF	nd	107	116	103
PFOA	nd	92	111	116
SCL	nd	98	101	99
HCTZ	59	59	75	69
2,4-D	93	102	108	99
FRSM	91	105	105	102
CMPH	nd	102	102	98
CRB	104	103	100	101
KET	nd	91	68	59
NAP	95	83	107	89
CMQ	nd	nd	100	92
MTF	nd	103	100	86
ATN	nd	101	97	95
SLBT	83	95	97	96
TRBT	77	99	100	96
NCT	nd	116	103	72
DIC	95	110	103	95
IBU	82	75	77	53
GEM	101	106	109	100
BP-3	86	104	120	105
MTP	88	101	104	102
OD-PABA	48	38	129	12
EHMC	71	47	141	4
CLNB	95	100	105	102
OC	120	84	66	58
BPA	90	98	132	116
E2	84	106	100	157
EE2	92	115	153	109
E1	89	94	131	136
TCS	94	98	132	107

Acknowledgments